TECHNISCHE UNIVERSITÄT MÜNCHEN

Lehrstuhl für Mikrobielle Ökologie

Molecular characterization of cereulide synthesis in emetic *Bacillus cereus*

GENIA LÜCKING

Vollständiger Abdruck der von der Fakultät Wissenschaftszentrum Weihenstephan für Ernährung, Landnutzung und Umwelt der Technischen Universität München zur Erlangung des akademischen Grades eines

Doktors der Naturwissenschaften

genehmigten Dissertation.

Vorsitzender:		Univ.-Prof. Dr. S. Scherer
Prüfer der Dissertation:	1.	Univ.-Prof. Dr. M. Ehling-Schulz (Veterinärmedizinische Universität Wien/Österreich)
	2.	Univ.-Prof. Dr. R. F. Vogel

Die Dissertation wurde am 27.01.2009 bei der Technischen Universität München eingereicht und durch die Fakultät Wissenschaftszentrum Weihenstephan für Ernährung, Landnutzung und Umwelt am 10.03.2009 angenommen.

“If you don't make mistakes, you're not working on hard enough problems.
And that's a big mistake.”

Frank Wilczek

TABLE OF CONTENTS

LIST OF FIGURES

LIST OF TABLES

SUMMARY

The emetic toxin cereulide of the foodborne pathogen *Bacillus cereus* is a heat- and acid stable depsipeptide structurally related to the antibiotic valinomycin. It is assembled by a nonribosomal peptide synthetase, encoded by the cereulide synthetase gene cluster (*ces*). In this work the expression of cereulide synthesis was analysed in detail and a first comprehensive insight into its molecular regulation was obtained. Gene inactivation mutagenesis of the emetic reference strain *B. cereus* F4810/72 revealed the effects of well known transcription factors on *ces* transcription and cereulide production. It was shown that cereulide synthesis is independent of the *B. cereus* specific virulence regulator PlcR, but belongs to the Spo0A-AbrB regulon. The transition state factor AbrB was found to bind efficiently to the main promoter region of the *ces* operon, indicating that AbrB acts as a direct repressor of cereulide production by negatively affecting *ces* transcription. However, data presented here also display that cereulide synthesis is part of a complex regulatory network involving several further transcription factors as well as environmental factors. It is expected that these results contribute to a better understanding of virulence gene expression and pathogenicity of emetic *B. cereus*.

Besides the investigation of cereulide regulation mechanisms, the 24 kb cereulide synthetase gene cluster was functionally analysed. The gene cluster is located on a pXO1-like megaplasmid, namely pBCE. Initial proteomic studies using a plasmid cured strain of *B. cereus* F4810/72 revealed a large impact of pBCE on the organism, especially on its secretome. The *ces* locus harbours besides the typical nonribosomal peptide synthetase genes, a gene encoding for a putative hydrolase (*cesH*), a 4'-phosphopantetheinyl transferase gene (*cesP*) and two genes coding for a putative ABC transporter (*cesCD*). Functional analysis of these genes showed that disruption of *cesH* or *cesP* had no effect on *ces* transcription levels or cereulide formation. In contrast, the putative ABC transporter CesCD was essential for cereulide synthesis without affecting *ces* transcription. Based on bioinformatic analysis and experimental data presented here, it is tempting to speculate that CesCD plays an important role in both toxin transport and cereulide biosynthesis.

ZUSAMMENFASSUNG

Das emetische Toxin Cereulid des Lebensmittelpathogens *Bacillus cereus* ist ein hitze- und säurestabiles Depsipeptid. Es wird nicht-ribosomal von einer Peptidsynthetase hergestellt, welche von den Cereulidsynthetase Genen (*ces*) codiert wird. In der vorliegenden Arbeit wurde die Transkription und Expression der Cereulidsynthetase näher untersucht um Aufschluss über deren molekulare Regulation zu geben. Mittels Mutagenese-Studien des emetischen Referenz-stammes *B. cereus* F4810/72 wurde die Wirkung bekannter Transkriptionsfaktoren auf die Cereulid Produktion getestet. Dabei stellte sich heraus, dass die Synthese von Cereulid nicht von dem *B. cereus* spezifischen Virulenzgen-Reglulator PlcR abhängt, sondern dem Spo0A-AbrB Regulon angehört. Es konnte gezeigt werden, dass der „transition state factor“ AbrB in der Lage ist an den Hauptpromotor des *ces* Operons zu binden und somit als direkter Repressor der *ces* Transkription fungiert. Darüber hinaus beeinflussen weitere Transkriptions- und Umweltfaktoren die Bildung von Cereulid, woraus zu schließen ist, dass die Toxinproduktion Teil eines komplexen regulatorischen Netzwerks ist. Im Rahmen dieser Arbeit konnte ein erster Einblick in dieses Netzwerk gewonnen und die ersten regulatorischen Gene identifiziert werden. Die Arbeit trägt somit zu einem besseren Verständnis der Pathogenität von emetischen *B. cereus* bei.

Ein weiterer Schwerpunkt der Arbeit war die funktionelle Charakterisierung des 24 kb großen Cereulidsynthetase Genclusters, welches auf einem pXO1-ähnlichem Plasmid namens pBCE lokalisiert ist. Initiale Proteom-Studien mit einer plasmidfreien Variante von *B. cereus* F4810/72 zeigten, dass pBCE nicht nur die Toxizität sondern das komplette Sekretom des Stammes stark beeinflusst. Neben den typischen Peptidsynthetase Genen beinhaltet der *ces* Genlokus ein Gen für eine putative Hydrolase (*cesH*), ein 4’-Phosphopantetheinyl-Transferase Gen (*cesP*) und zwei Gene, die für einen ABC Transporter codieren (*cesCD*). Eine funktionelle Analyse dieser Gene zeigte, dass die Inaktivierung von *cesH* oder *cesP* keinen Einfluss auf die *ces* Transkription sowie Cereulid Bildung hat. Der putative ABC Transporter CesCD dagegen erwies sich als essentiell für die Toxinsynthese, ohne dabei die *ces* Transkription zu beeinflussen. Weiterführende Experimente lassen darauf schließen, dass CesCD eine wichtige Rolle sowohl beim Transport von Cereulid als auch bei dessen Biosynthese spielt.

1 INTRODUCTION

1.1 Pathogenicity of the *Bacillus cereus* group

The endospore-forming, Gram-positive, motile rod *Bacillus cereus* is the name giving species of the *Bacillus cereus* group. This group presents a genetically highly homogeneous subdivision of the genus *Bacillus* and comprises six species namely *Bacillus cereus, Bacillus anthracis, Bacillus thuringiensis, Bacillus mycoides, Bacillus pseudomycoides* and *Bacillus weihenstephanensis* (Gordon *et al.*, 1973; Lechner *et al.*, 1998; Nakamura, 1998; Priest & Alexander, 1988). Based on genetic evidence it was proposed that these Bacilli present one species (Helgason *et al.*, 2000b), despite their diverse pathogenic potential. However, all members of the *Bacillus cereus* group can be distinguished by specific phenotypic features including distinct virulence factors. Noteworthy, these distinguishing determinants between the species are mainly encoded by genes located on plasmids.

B. anthracis causes the fatal human and animal disease anthrax and has become increasingly noted for its use as a biological weapon (Jernigan *et al.*, 2002). The genes encoding the main virulence factors, the anthrax toxins and the capsule, are located on the two virulence plasmids pXO1 and pXO2 (Mock & Fouet, 2001). *B. thuringiensis* is considered an insect pathogen producing parasporal crystal toxins, which are also plasmid-encoded and are commercially used as biocontrol agents (Aronson & Shai, 2001; Berry *et al.*, 2002). *Bacillus cereus* is recognized as an opportunistic pathogen, which is mainly responsible for two types of food poisoning: diarrhoea and emesis. Chromosomal encoded enterotoxins cause the diarrhoeal syndrome, while the genetic determinants responsible for the emetic type of disease are plasmid-borne. However, also non-gastrointestinal infections such as periodontitis, endocarditis, endophthalmitis and meningitis have been reported in association with *B. cereus* (Davey & Tauber, 1987; Gaur *et al.*, 2001; Helgason *et al.*, 2000a; Kotiranta *et al.*, 2000). In the diarrhoeal type of illness abdominal pain and diarrhoea appear 8-16 h after ingestion of contaminated food and usually last no longer than 24 h. The symptoms are caused by heat-labile enterotoxins, which are produced during vegetative growth of *B. cereus* in the small intestine of the host

(Granum & Lund, 1997). Hemolysin BL (Beecher *et al.*, 1995), the non-hemolytic enterotoxin (Lund & Granum, 1996) and cytotoxin K (Lund *et al.*, 2000) are the best studied enterotoxins involved in this foodborne illness. The emetic type of food poisoning is characterized by nausea and vomiting, which occurs 0.5 to 6 h after ingestion of contaminated food and can last up to 24 h. The emetic syndrome is the result of intoxication with the heat stable toxin cereulide preformed in food. Although both types of foodborne diseases caused by *B. cereus* are usually self-limiting, also severe and even fatal cases have occasionally been reported (Dierick *et al.*, 2005; Lund *et al.*, 2000; Mahler *et al.*, 1997). The species *B. mycoides* and *B. pseudomycoides* are phenotypically differentiated from other group members by their characteristic colony shape due to rhizoid growth (Di Franco *et al.*, 2002; Nakamura, 1998). The food spoilage organism *B. weihenstephanensis* is mainly characterized by its psychrotolerance (Lechner *et al.*, 1998).

1.2 Cereulide and its synthetase gene cluster

The cyclic dodecadepsipeptide cereulide is responsible for the emetic type of foodborne illness caused by *B. cereus*. Due to its resistance towards heat, low pH and proteolytic enzymes, it is, if once produced, not inactivated by processing steps like reheating food and thus of particular concern for catering and the food industry (for review see Ehling-Schulz *et al.*, 2004; Schoeni & Wong, 2005). Although the exact mechanism by which cereulide causes emesis in humans has not been clarified, several biological effects of cereulide have been described. Similar to the antibiotic valinomycin, cereulide inhibits mitochondrial activity by acting as a potassium ionophore, leading to membrane depolarization (Hoornstra *et al.*, 2003; Mikkola *et al.*, 1999). Moreover, cereulide was shown to cause vomiting in an animal model by stimulating the vagus afferent through binding to 5-HT_3 receptors of the duodenum (Agata *et al.*, 1995). Other effects that were found in connection with cereulide are cellular damage (Shinagawa *et al.*, 1996) and inhibition of natural killer cells of the immune system (Paananen *et al.*, 2002).

The chemical structure of cereulide consists of three repeats of the following amino acids: [D-*O*-Leu-D-Ala-L-*O*-Val-L-Val]$_3$ (Agata *et al.*, 1994). Due to this structure cereulide was expected and shown to be synthesized enzymatically by a

nonribosomal peptide synthetase (NRPS) (Ehling-Schulz *et al.*, 2005b). NRPSs are multifunctional enzyme complexes consisting of repetitive modules, which selectively catalyze the activation and thioester formation of one amino, α-hydroxy or carboxylic acid monomer in the peptide product (Turgay *et al.*, 1992). The order of the modules usually corresponds directly to that of the monomers in the peptide chain. In general the core of each module consists of an adenylation (A) domain for substrate activation, a peptidyl carrier (PCP) domain for covalent binding and a condensation (C) domain for peptide bound formation (for review see Finking & Marahiel, 2004). The cereulide peptide synthetase was found to be located on a pXO1-like plasmid, designated pBCE, and was identified as a 24 kb *ces* gene cluster comprising seven coding DNA sequences (Ehling-Schulz *et al.*, 2006). Figure 1 present an overview on the genetic organization of the *ces* genes, namely *cesH, cesP, cesT, cesA, cesB, cesC* and *cesD*.

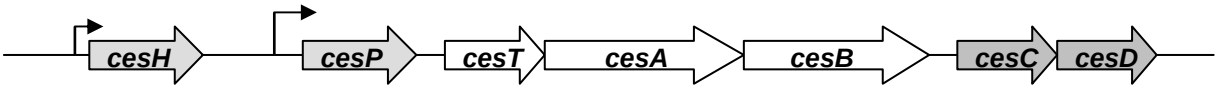

Figure 1. Genetic organization of the cereulide synthetase gene cluster located on the megaplasmid pBCE. The operon comprises a putative hydrolase (*cesH*), a 4'-phosphopantetheinyl transferase (*cesP*), a type II thioesterase (*cesT*), two NRPS modules (*cesA* and *cesB*) and a putative ABC transporter (*cesC* and *cesD*). Previous transcriptional analysis revealed that *cesH* is transcribed from its own promoter, while *cesPTABCD* are co-transcribed as a single polycistronic operon (Dommel, 2008). Identified promoter regions are marked by arrows.

The first gene, located at the 5' terminus of the *ces* locus, is *cesH* showing homology (up to 57% identity) to a hydrolase or acetlytransferase of *B. cereus* group members. The function of this putative hydrolase in respect of cereulide synthesis is so far unknown. The next gene of the *ces* cluster *(cesP)* codes for a putative 4'-phosphopantetheinyl transferase (PPTase). In general PPTases are crucial enzymes for the activation of NRPS and their genetic determinants are often found in close proximity to *nrps* genes. PPTases catalyse the transfer of a 4'-phosphopantetheine moiety of coenzyme A onto a conserved serine residue of the PCP domain, thereby converting the *apo*-carrier protein to its active *holo*-form (Lambalot *et al.*, 1996). In the *ces* locus, *cesP* probably codes for such a protein with according function. The adjacent to *cesP* located gene *cesT* codes for a putative type II thioesterase (TEII),

which are also often found in association with *nrps* genes. In contrast to the type I thioesterase, which is an integrated part of the NRPS enzyme catalysing the product release, the external TEII reactivates the NRPS by removing misprimed monomers (Schwarzer *et al.*, 2002). The importance of this regeneration function was demonstrated by gene deletion of the SrfA-TEII of *B. subtilis*, resulting in 84% reduction of the surfactin production (Schneider & Marahiel, 1998). Thus, it is possible that the type II thioesterase encoded by *cesT* plays a similarly relevant role in cereulide synthesis. The structural *nrps* genes *cesA* and *cesB* encode the modules that are responsible for the activation and incorporation of each two monomers (D-O-Leu and D-Ala for CesA and L-O-Val and L-Val for CesB*)* in the peptide chain. A novel mechanism for α-hydroxy acid incorporation was reported, since the CesA1 and CesB1 modules activate α-keto acids (instead of α-hydroxy acid or amino acids), followed by chiral reduction on the assembly line (Magarvey *et al.*, 2006). Next to the typical *nrps* genes two additional ORFs were found at the 3' terminus of the *ces* locus. While *cesC* codes for a putative ATP-binding protein, *cesD* shows homology to a permease component of an ABC transporter (Ehling-Schulz *et al.*, 2006).

1.3 Regulation of virulence gene expression

The level of virulence varies strongly among *B. cereus,* ranging from harmless strains, which are used as probiotics, to highly toxic, even lethal strains. It is likely that the diverse toxigenic potential of *B. cereus* is mainly due to strain-dependent differences in the regulation of toxin expression (Stenfors Arnesen *et al.*, 2008). In general, the expression of bacterial virulence factors is linked to various environment signals and is a tightly regulated process. The regulation of virulence gene expression is usually quite complex, since several regulatory mechanisms are often simultaneously involved and different virulence factors are coordinately controlled by single global regulators (for review see Finlay & Falkow, 1997). In *B. cereus* and *B. thuringiensis* the transcriptional activator PlcR controls most known virulence factors, including the enterotoxins Hbl, Nhe and CytK as well as degradative enzymes and surface proteins (Agaisse *et al.*, 1999; Gohar *et al.*, 2002). An extensive study of the PlcR regulon of *B. cereus* ATCC14579 identified 45 PlcR controlled proteins, of which 40 are secreted or attached to cell wall structures (Gohar *et al.*, 2008). PlcR is part of a quorum sensing system and regulates virulence gene expression in a cell-

density dependent manner by interaction with the autoinducer PapR. Only in the presence of this cell-cell signalling peptide, PlcR binds efficiently to a conserved motif, known as the PlcR-box, of the target genes and activates their expression (Declerck *et al.*, 2007; Slamti & Lereclus, 2002). However, the activity of PlcR depends not only on cell-density, but also on signals linked to the nutritional- and growth state of the cell. For example, the global sporulation regulator Spo0A was shown to repress *plcR* transcription in the stationary growth phase under sporulating conditions (Lereclus *et al.*, 2000).

Disruption of *plcR* causes a reduction but does not completely abolish virulence in *B. cereus* and *B. thuringiensis* (Callegan *et al.*, 2003; Salamitou *et al.*, 2000). Hence, additional regulatory mechanisms must be involved in virulence gene expression. Recent studies revealed that enterotoxin production also depends on the metabolic state of the cell, since its expression was found to be controlled by the anaerobic growth regulator Fnr, the redox-sensing two component system ResDE and the catabolite control protein CcpA (Duport *et al.*, 2006; van der Voort *et al.*, 2008; Zigha *et al.*, 2007). Interestingly, in *B. anthracis* PlcR is inactive due to a nonsense mutation in the *plcR* gene and, hence, toxin gene expression is independent of the PlcR regulon and involves other regulatory pathways instead (Agaisse *et al.*, 1999; Fouet & Mock, 2006; Mignot *et al.*, 2001). For example the plasmid-borne *atxA* gene was shown to encode a master regulator controlling the expression of anthrax toxins and many other genes located on pXO1, pXO2 and on the chromosome (Bourgogne *et al.*, 2003). Furthermore, CodY, a global regulator of stationary phase gene expression, was reported to influence virulence not only of *B. anthracis* but of several other Gram-positive bacteria (Sonenshein, 2005). Finally, different members of the global Spo0A regulon, like the transition state factor AbrB and the alternative sigma factor σ^H were shown to be involved in virulence gene expression of *B. anthracis* (Hadjifrangiskou *et al.*, 2007; Saile & Koehler, 2002).

1.4 The Spo0A regulon

The sporulation transcription factor Spo0A has a profound effect on global gene expression of *Bacillus* species. It influences the transcription of over 500 *Bacillus subtilis* genes, of which 121 are controlled directly by this master regulator (Fawcett

et al., 2000; Molle *et al.*, 2003a). Once activated by a complex phosphorelay including several histidine kinases (Jiang *et al.*, 2000), the response regulator Spo0A induces the onset of sporulation, but is also involved in the transcriptional regulation of various other stationary phase processes, such as protease production, competence or biofilm production (Albano *et al.*, 1987; Ferrari *et al.*, 1986; Hamon & Lazazzera, 2001). A crucial and early role of phosphorylated Spo0A is the repression of *abrB* transcription (Strauch *et al.*, 1990). AbrB acts as a transition state regulator by mainly suppressing stationary phase gene expression during the exponential growth phase. In *B. subtilis,* a wide range of AbrB-controlled genes have been identified, which are involved in the production of antibiotics, degradative enzymes, motility, sporulation, development of competence and many other metabolic and physiological processes (for review see Phillips & Strauch, 2002). One target, which is repressed by AbrB, is the *sigH* gene encoding the alternative sigma factor σ^H (Strauch, 1995). The σ^H RNA polymerase holoenzyme activates genes that are essential for post-exponential gene expression and sporulation, including *spo0A* itself (Predich *et al.*, 1992). Thus, the expression of the regulators Spo0A, AbrB and σ^H is connected in a feedback mechanism that is crucial for sporulation initiation (Figure 2).

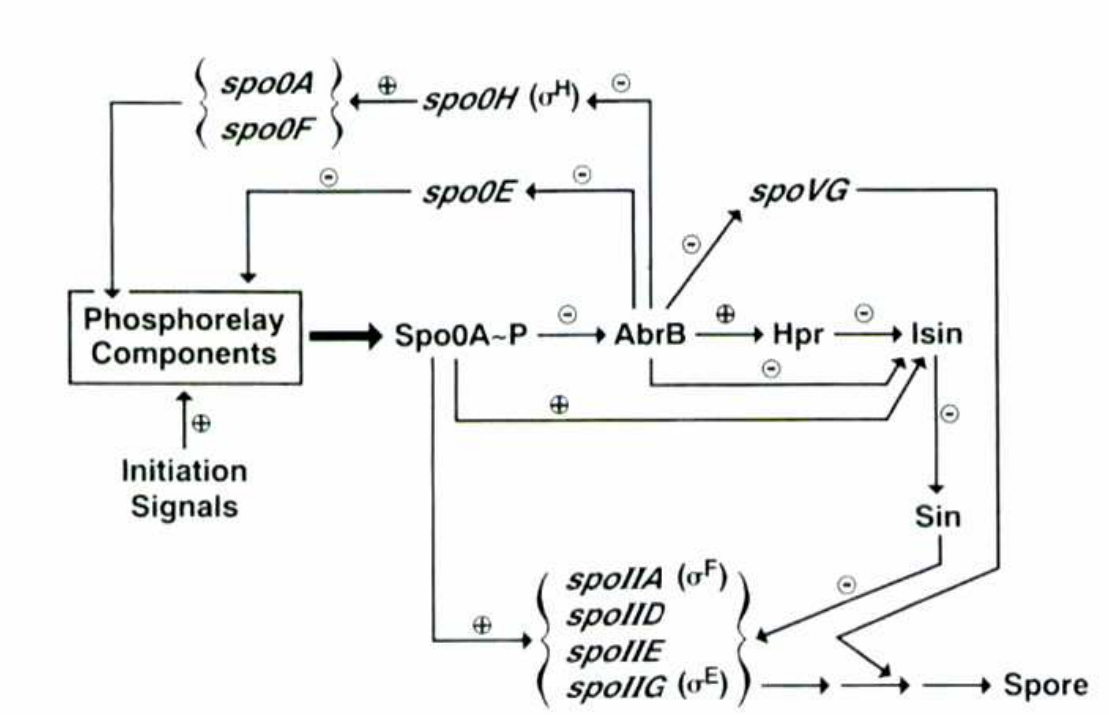

Figure 2. Scheme of the sporulation phosphorelay pathway and the Spo0A regulon according to Strauch & Hoch, 1993.

1.5 Research objective

While enterotoxin expression of *B. cereus* has been studied extensively, nothing is known about the molecular regulation of cereulide formation. For example, the potential role of the pleiotropic regulator PlcR in emetic toxin production is so far undefined. The aim of this work was to decipher the role of the master regulators PlcR, Spo0A, AbrB, σ^H, CodY and CcpA in pathogenicity of emetic *B. cereus*. Mutant strains were constructed and characterized with respect to their phenotype, cytotoxicity and *ces* gene expression in order to gain initial insights into the regulatory mechanism influencing cereulide synthesis. In addition, the effect of certain extrinsic parameters on toxin production, such as media supplementation and growth parameters, was investigated. The second part of this work dealt with the functional characterization of the megaplasmid pBCE and especially of the *ce*s operon, which encodes the cereulide peptide synthetase. Mutagenesis and *in silico* analysis of *cesH, cesC* and *cesD* were performed to determine their function in respect of cereulide synthesis. Moreover, the PPTase *cesP* was functionally analysed to clarify its putative role in the activation of the cereulide NRPS.

2 MATERIAL AND METHODS

2.1 Bacterial strains

The emetic reference strain *B. cereus* F4810/72, originally isolated from vomit by the Public Health Laboratory Service (London, UK), was chosen as model organism to create mutants and study cereulide production. The non-emetic *B. cereus* type strain ATCC14579 and the emetic-like strain *B. cereus* NVH1519/00 were used as example for cereulide negative strains. In addition, the recently described emetic *B. weihenstephanensis* strain MC67 (Thorsen *et al.*, 2006) was included in *ces* promoter studies. *E. coli* strains used for subcloning were TOP10 and the non-methylating strain INV110. *E. coli* BL21 was used for protein overexpression and *E. coli* JM83/pRK24 served as the donor strain in conjugation experiments. Details of bacterial strains used in this study are provided in table 1.

Table 1. *Bacillus* sp. and *E. coli* strains used in this study.

Strain	Description	Reference or source
E. coli		
TOP10	general cloning strain	Invitrogen
INV110	non-methylating cloning strain	Invitrogen
JM83/pRK24	donor strain for conjugation; Amp^r	Trieu-Cuot *et al.*, 1987
BL21	protein overexpression strain	Novagen
B. cereus		
ATCC14579	*B. cereus* type strain (non-emetic)	
NVH1519/00	emetic-like strain	Ehling-Schulz *et al.*, 2005a
F4810/72 (AH187)	emetic reference strain	Turnbull *et al.*, 1979
B. weihenstephanensis		
MC67	emetic strain	Thorsen *et al.*, 2006

2.2 Growth conditions

Bacterial strains were cultured on plate count agar (PC: 5.0 g tryptone, 2.5 g yeast extract, 1.0 g D-glucose and 15 g agar per litre) or Luria-Bertani agar (LB: 10 g tryptone, 10 g NaCl, 5 g yeast extract and 15 g agar per litre) for 14-16 h at 30℃ or 37℃ for *Bacillus* and *E. coli,* respectively. In addition, *B. cereus* mutant strains were grown on selective MYP agar (mannitol egg yolk polymyxin agar; Oxoid) to determine colony morphology and growth after 24 h at 30℃. For cultivation in liquid media a preculture was prepared by inoculating one cfu in 3 ml LB broth followed by overnight incubation with rotary shaking (150 rpm) at either 30℃ or 37℃ for *Bacillus* and *E. coli,* respectively. Main cultures were inoculated with 10^3 cfu/ml from the preculture and grown with rotary shaking (150 rpm) in 500 ml baffled flasks containing 100 ml LB media. Appropriate antibiotics were applied as necessary in following concentrations: 100 µg/ml spectinomycin, 3-10 µg/ml erythromycin, 5 µg/ml chloramphenicol and 100 µg/ml polymyxin B for *B. cereus;* 100 µg/ml ampicillin, 100 µg/ml spectinomycin, 50 µg/ml kanamycin and 300 µg/ml erythromycin for *E. coli*.

Growth of liquid cultures was monitored by measuring the optical density at 600nm (OD_{600nm}) using a UV/Vis spectrophotometer (Perkin-Elmer, USA). Therefor culture samples were diluted 1:10 once the OD_{600nm} values exceeded 1. Cell morphology and spore formation was observed throughout growth by phase contrast microscopy (Olympus).

2.3 DNA isolation

Genomic DNA was isolated from overnight cultures with the Puregene Yeast and Bacteria kit (Gentra, USA) according to the manufacturer´s protocol. When DNA of high quality and/or large quantity was needed, a standard phenol/chloroform extraction protocol (Ausubel *et al.*, 1997) was used with slight modifications. The incubation time for proteinase K digestion was extended to 3 h at 37℃ and for the CTAB/NaCl treatment to 30 min at 65℃. Isolated DNA was additionally digested with 0.1 mg/ml RNase A (30 min at 37℃) to remove remaining RNA. After another phenol/chloroform extraction step, DNA was precipitated with 3 M sodium acetate

and icecold ethanol at -20℃ for at least 30 min. DNA was pelleted, washed once with 70% ethanol and dissolved in ddH_2O.

For plasmid isolation from *E. coli* strains, the GeneElute™ Plasmid Miniprep kit (Sigma-Aldrich) or the Pure-Link™ HiPure Plasmid Midiprep kit (Invitrogen) was applied, depending on the plasmid amount needed. DNA concentrations of chromosomal DNA, plasmid preparation or PCR products were analysed by measurement of the absorbance at 260nm and 280nm using a ND-1000 spectrophotometer (NanoDrop).

2.4 RNA isolation

For RNA extraction 1 ml samples were taken from *B. cereus* cultures in different growth phases, cells were harvested (13200 rpm, 1 min) and immediately frozen in liquid nitrogen. Cells were disrupted with 0.1 mm zirconium-silica beads in a Ribolyser (Hybaid, UK) and total RNA was isolated using 1 ml TRIzol reagent (Invitrogen) according to the manufacturer`s instructions. Residual DNA was removed from 5 µg RNA with 10U RQ1 DNase (Promega) treatment at 37℃ for 45 min. After chloroform extraction and precipitation with sodium acetate and ethanol, the RNA pellet was washed twice with 70% ethanol and resuspended in DEPC ddH_2O. RNA concentration and purity were determined by the absorbance at 260/280nm and agarose gel electrophoresis. Complete DNA removal was checked by standard PCR with 16S rDNA universal primers (Martineau *et al.*, 1996), using the extracted RNA as template.

2.5 Reverse transcription (RT-PCR)

cDNA synthesis was performed using 100 ng total RNA, 2 pmol gene specific reverse primer, 0.5 mM of each dNTP, 10 mM DTT, 100U SuperScript II and 20U RNAase-OUT (all Invitrogen). The mixture including only RNA, dNTP and the primer was first heated for one minute each at 75℃, 70℃, 65℃, 60℃ , 55℃, 50℃ and 45℃, before adding the enzymes and incubating the reaction mix at 42℃ for 1 h. Subsequent PCR with the RT reaction as template and forward plus reverse primers confirmed the successful cDNA synthesis.

2.6 Standard PCR

Standard PCR was performed in 50 µl reaction volume including 1.5 mM MgCl, 0.4 mM of each dNTP, 50 pmol of forward and reverse primer, 1 µl of template DNA and 0.5U GoTaq Flexi DNA Polymerase (Promega) in 5x reaction buffer. The PCR reaction started with a denaturation step at 95°C for 2 min, followed by 30 amplification cycles (95°C for 30 sec; primer annealing temperature for 30 sec; 72°C depending on elongation time) and ended with a final elongation step at 72°C for 2 min. Longer fragments (>2 kb) were amplified using the Expand High Fidelity PCR System (Roche) following the manufacturer's instructions. If blunt ended amplicons or proofreading activity was desired, *Pfu* DNA Polymerase (Promega) was used. For colony PCR cell material of bacterial clones was scraped from agar plates into 50 µl ddH_2O. Samples were boiled for 10 min at 100°C and centrifuged (5 min at 13.200 rpm) to remove cell debris. The PCR was performed with 2 µl of the supernatant as template.

2.7 Quantitative real time PCR (qPCR)

Quantitative real time PCR was performed in 25 µl reaction volume containing cDNA (equivalent to 10 ng RNA) as template and 2 pmol of each primer in 1x qPCR Mastermix with SYBR Green I (ABgene). PCR was run on the SmartCycler II (Cepheid) using the following cycling conditions: polymerase activation at 95°C for 15 min followed by 40 cycles of amplification (95°C for 30 sec; annealing temperature (Tm) for 30 sec; 72°C for 45 sec). Specificity of the reactions was affirmed by the subsequent melt curve analysis of the amplicons, for which the temperature was raised from Tm to 95°C with a ramp rate of 0.2°C/sec.

All oligonucleotides used for RT-qPCR are listed in table 2. To test newly designed primers, standard curves were generated using decimal dilutions of cDNA as template for qPCR. The reaction efficiency (E) was calculated according to Pfaffl from the standard curve with $E = 10^{-1/slope}$ (Pfaffl, 2001). Furthermore, Ct (cycle at which fluorescence reaches the threshold level) values and melting curves of new products were carefully examined to ensure correct amplification.

Table 2. Oligonucleotides developed for RT-qPCR

Primer name	Target gene	Sequence (5'-3')	Reference
plcR_for	*plcR*	GTTATCCGAGAACATATGTCATC	Fricker *et al.*, 2008
plcR_rev	*plcR*	CTTTTTCAGCTCATTCCATACTC	Fricker *et al.*, 2008
cesA_for	*cesA*	GATTACGTTCGATTATTTGAAG	Dommel, 2008
cesA_rev	*cesA*	CGTAGTGGCAATTTCGCAT	Dommel, 2008
cesP_for	*cesP*	GGTTATGCATCTTGTATACCG	Dommel, 2008
cesP_rev	*cesP*	GATGAAGTGGAGATGATATAGAC	Dommel, 2008
spo_F_RT	*spo0A*	AGCGTTTGGACAAGAAGATG	This study
spo_R_RT	*spo0A*	TATGAGCAGGCACACCAAT	This study
abrB_F_RT	*abrB*	TCGTGTAGTAATTCCGATTGAA	This study
abrB_R_RT	*abrB*	TGAAGCTCGTTTAAGATTTGC	This study
pBCE_abrB_for	*abrB*-like[a]	TTAGGGCGAATTGTTCTTCC	This study
pBCE_abrB_rev	*abrB*-like[a]	TAAAAGTTCCGCCCCTTCTG	This study
ppt	*ppt*[b]	CTCGTTTTATAATCGGTTGTGTAA	This study
ppt	*ppt*[b]	CAGGTGCAGACTTTGTAAATGC	This study
ABC_F1	*berA*-like[c]	AGAAGGGGAAGTATTCGGTTAC	This study
ABC_R1	*berA*-like[c]	CTCTAATCCGTTCATTCCTTCA	This study
16SA1	*rrn*	GGAGGAAGGTGGGGATGACG	Martineau *et al.*, 1996
16SA2	*rrn*	ATGGTGTGACGGGCGGTGTG	Martineau *et al.*, 1996

[a] *abrB*-like gene located on pBCE; locus tag: BcAH187_pCER270_0167
[b] 4'-phosphopantetheinyl transferase gene; locus tag: BCAH187_A2475
[c] ABC transporter gene homologous to *berA* of *B. thuringiensis*; locus tag: BCAH187_A3620

For determination of the relative expression of target genes in different *B. cereus* strains, Pfaffl`s REST method (Pfaffl, 2001) was applied, using the difference in Ct values of the sample and a calibrator for the target gene and the reference gene *rrn* (16S rDNA). Ct values of the wild type strain *B. cereus* F4810/72 at OD_{600nm} of 1 (*ces, ppt*), 20 (*plcR*) or 10 (*abrB, spo0A*) was set as the calibrator for each respective gene.

2.8 DNA Sequencing

PCR amplicons and isolated plasmids were sequenced by 4base lab (Reutlingen, Germany). PCR products were either sequenced directly after purification or subcloned into the pCR2.1 vector using the TOPO TA cloning kit (Invitrogen) prior sequencing.

2.9 Enzymatic modification of DNA

In general, 0.1-1 µg DNA was digested with 1-2 units of the restriction enzyme (Fermentas) in a total volume of 20-40 µl under enzyme specific reaction conditions. For restriction of PCR products, amplicons were first purified via the Qiaquick PCR Purification kit (Qiagen) and then restricted with the appropriate restriction enzyme for 1-3 h before being purified again. To avoid vector re-ligation, restricted plasmid DNA was subsequently dephosphorylated with 2U of Shrimp Alkaline Phosphatase (Fermentas) at 37℃ for 30 min prior to loading the sample on a 1% agarose gel and extracting it using the Qiaquick Gel Extraction kit (Qiagen). If blunt end DNA was required, digested DNA was incubated with 0.1 mM dNTP mix and 1U T4 DNA Polymerase (Fermentas) for 5 min at 20℃ before being purified. Ligation of digested products was carried out with a molar ratio of vector and insert from 1:1 to 1:5 (up to 2 µg total DNA) in a 30 µl volume of 10x ligation buffer with 3U T4 DNA ligase (Roche) at 16℃ overnight.

2.10 Transformation of DNA

Preparation and heat shock transformation of calcium chloride chemically competent *E. coli* strains was done according to a standard protocol (Sambrook & Russell, 2001). TOP 10 cells were used for the initial transformation of ligation reactions. To increase the transformation efficiency in *B. cereus*, only plasmids isolated from the non-methylating INV 110 strain were used for electroporation of *B. cereus*. For the preparation of electro-competent *B. cereus,* cells were grown until an OD_{600nm} of 0.5 in LB media supplemented with 2% glycine. After harvest (3500 g, 4℃, 10 min) cells were sequentially washed in ice cold 2.5%, 5% and 10% glycerol before being resuspended in 10% glycerol and frozen in liquid nitrogen.

For electroporation 1 µg plasmid DNA was added to 100 µl competent cells and pulsed (2.0 kV, 25 µF, 200 Ω, 4.6-4.8 ms) in a 0.4 cm cuvette using the BioRad Gene Pulser. Cells were then resuspendend in LB and incubated for 2 h at 30℃ with shaking. Recovered cells were spread on LB agar plates with appropriate antibiotics and colonies were visible after 24-48 h at 30℃.

2.11 Heterogramic conjugation

Besides electroporation, conjugation presents an effective approach to transfer recombinant plasmids from *E. coli* to *B. cereus*. Therefor the appropriate construct was cloned into the conjugative suicide vector pAT113 (Trieu-Cuot *et al.*, 1991) and transformed to *E. coli*JM83/pRK24, carrying the IncP plasmid pRK24 (Thomas & Smith, 1987) required for DNA mobilization. For mating 50 ml *E. coli* culture and 5 ml *B. cereus* culture were grown in LB until OD_{600nm} 0.5. *E. coli* cells were harvested, washed once to remove antibiotics and then mixed with the *B. cereus* culture. The bacterial mixture was pelleted, carefully resuspended in 1 ml LB and loaded onto two Millipore HA 0.45 µm filters placed on a LB agar plate without antibiotics. After overnight incubation at 37℃, bacteria were scraped fro m the filters and dissolved in 3 ml media. Cells were plated on LB agar containing polymyxin B to eliminate *E. coli* and additional antibiotics to select *B. cereus* transconjugants, which were grown at 30℃ overnight.

2.12 Mutagenesis of *B. cereus*

Since the genome of *B. cereus* F4810/72 (NZ AAUF00000000) is so far only sequenced without annotation, target genes were searched and identified using the annotated sequence data of the strongly related strain ATCC10987 (NC003909). Sequence alignment of all studied genes revealed a high level of homology (>95% similarity), except for the *ces* genes, which are absent in *B. cereus* ATCC10987. All generated mutant strains are summarized in table 3; details of vectors and oligonucleotides used for mutagenesis are listed in the Appendix (7.1 and 7.2).

Table 3. Genetically modified bacterial strains created in this study.

Strain	Description	Reference
E. coli		
BL21/abrB	BL21 harbouring pET28/abrB for AbrB overexpression; Kan^r	This study
BL21/abrB*	BL21 harbouring pET28/abrB* for AbrB overexpression; Kan^r	This study

Strain	Description	Reference
B. cereus		
F48ΔpBCEI	plasmid cured strain of F4810/72; sporulating	This study
F48ΔpBCEII	plasmid cured strain of F4810/72; non sporulating	This study
F48Δces	*cesP* deletion mutant of F4810/72 with polar effect on the whole *ces* locus => *ces* inactivation ; Spc^r	This study
F48ΔcesP	*cesP* deletion mutant of F4810/72; Spc^r	This study
F48ΔcesCD	*cesCD* deletion mutant of F4810/72; Spc^r	This study
F48ΔplcR	*plcR* deletion mutant of F4810/72; Spc^r	This study
F48Δspo0A	*spo0A* deletion mutant of F4810/72; Spc^r	This study
F48ΔabrB	*abrB* deletion mutant of F4810/72; Spc^r	This study
F48ΔabrB/Δspo0A	*abrB* and *spo0A* deletion mutant of F4810/72; Spc^r Cm^r	This study
F48comH	F48Δspo0A complemented with pAD/spo0A/PσH; Amp^r Cm^r Spc^r	This study
F48comAH	F48Δspo0A complemented with pAD/spo0A/PσAσH; Amp^r Cm^r Spc^r	This study
F48comCD	F48ΔcesCD complemented with pAD/cesCD/Pces; Amp^r Cm^r Spc^r	This study
F48gfp/PcspA	F4810/72 harbouring pAD/PcspA; Amp^r Cm^r	Dommel, 2008
F48abrB/PcspA	F4810/72 harbouring pAD/abrB/PcspA; Amp^r Cm^r	This study
F48abrB*/PcspA	F4810/72 harbouring pAD/abrB*/PcspA; Amp^r Cm^r	This study
F48INcesH	Insertion mutant with disrupted *cesH*; Amp^r Erm^r	This study
F48INcesC	Insertion mutant with disrupted *cesC,* Amp^r Erm^r	This study
F48INcesD	Insertion mutant with disrupted *cesD*; Amp^r Erm^r	This study
F48INppt	Insertion mutant with disrupted *ppt*; Amp^r Erm^r	This study
F48ΔcesP/INppt	*cesP* knockout mutant with disrupted *ppt*; Amp^r Erm^r Spc^r	This study
F48INsigH	Insertion mutant with disrupted *sigH*; Amp^r Erm^r	This study

Strain	Description	Reference
B. cereus		
F48INcodY	Insertion mutant with disrupted *codY*; Amp^r Erm^r	This study
F48INccpA	Insertion mutant with disrupted *ccpA*; Amp^r Erm^r	This study
F48lux/Pces	F4810/72 harbouring pXen/Pces; Amp^r Cm^r	Dommel, 2008
F48Δspo0Alux/Pces	F48Δspo0A harbouring pXen/Pces; Amp^r Cm^r Spc^r	This study
F48ΔabrBlux/Pces	F48ΔabrB harbouring pXen/Pces; Amp^r Cm^r Spc^r	This study
F48ΔabrB/Δspo0Alux/ Pces	F48ΔabrB/Δspo0A harbouring pXen/Pces/erm; Amp^r Cm^r Spc^r Erm^r	This study

2.12.1 Construction of *B. cereus* deletion mutants

The cloning vector TOPO pCR2.1 was used as basis to create constructs that consist of a spectinomycin resistance cassette flanked by ~1.2 kb *B. cereus* DNA fragments presenting the upstream and downstream located sequences of the gene to be deleted. These flanking regions were amplified by PCR using primers with introduced restriction enzyme recognition sites (see Appendix 7.2). PCR products were then digested and together with the *spc* resistance cassette from pUC1318Spc successively ligated into the multiple cloning site of the TOPO vector. For the *cesP* construct the non-polar *spc* cassette from pUCspcH+2 was used to avoid polar effects on the downstream located *ces* operon. Correctness and orientation of inserts were checked by PCR, restriction analysis and sequencing. Constructs were then excised from TOPO and inserted into the multiple cloning site of the integrative vector pAT113, giving rise to pAT113ΔGOI/spc. This plasmid was transformed into *E. coli* JM83/pRK24 and the resulting strain was used for transconjugal transfer into *B. cereus* F4810/72, as described above. Transconjugants were screened for spectinomycin resistance and erythromycin sensitivity. PCR and RT-qPCR confirmed gene deletion and integration of the resistance cassette resulting from a double crossover recombination event. The deletion mutants of *plcR*, *spo0A*, *abrB, cesP* and *cesCD* were designated *B. cereus* F48ΔplcR, F48Δspo0A, F48ΔabrB, F48ΔcesP and F48ΔcesCD, respectively. For construction of the double mutant concerning *abrB*

and *spo0A*, the spectinomycin cassette of pAT113Δspo0A/spc was replaced by a chloramphenicol resistance cassette, which was gained from the pAD123 vector using the oligonucleotides CAM-F and CAM-R. The new construct pAT113Δspo0A/cm was then transformed into F48ΔabrB by conjugation, yielding the double mutant F48ΔabrB/Δspo0A.

2.12.2 Complementation of deletion mutants

For complementation of the *spo0A* null mutant, two different plasmids were constructed, one with *spo0A* and its σ^H-dependent promoter and one with spo0A plus its two promoters ($P\sigma^A$ and $P\sigma^H$). The *spo0A* gene plus its 121 bp upstream region and *spo0A* plus its 513 bp upstream region were PCR amplified with Pfu-polymerase from genomic DNA of *B. cereus* F4810/72 using the primer pairs spo0A-F-kurz/spo0A-rev-Hind and spo0A-for-Eco2/spo0A-rev-Hind. After restriction digest, PCR products were cloned into the *EcoRI-HindIII* site of the shuttle vector pAD123, releasing *gfp* and yielding pAD/spo0A/$P\sigma^H$ and pAD/spo0A/$P\sigma^A\sigma^H$. These two plasmids were introduced into the *B. cereus spo0A* null mutant by electroporation. PCR analyses with *spo0A*-specific primers confirmed the presence of the plasmid in the recombinant strains, named *B. cereus* F48comH and F48comAH. For complementation of the *cesCD* null mutant the shuttle vector pAD/Pces, containing the main promoter region of the *ces* gene cluster, was exerted. A 1.8 kb fragment comprising the *cesC* and *cesD* genes was PCR amplified using the oligonucleotides cesCD_F_Xba2 and cesCD_R_Pae, digested and cloned into the *XbaI-PaeI* site of pAD/Pces, releasing *gfp* and yielding pAD/cesCD/Pces. This plasmid was introduced into *B. cereus* F48ΔcesCD by electroporation, giving rise to *B. cereus* F48comCD.

2.12.3 Construction of *B. cereus* insertion mutants

Gene inactivation by plasmid integration was accomplished by using the thermosensitive shuttle vector pMAD (Arnaud *et al.*, 2004). An internal fragment (~300 bp) of the appropriate gene was amplified using the primers listed in the Appendix 7.2. The digested PCR product was ligated into the multiple cloning site of pMAD, which was then transformed into *B. cereus* F4810/72 by electroporation. Transformants were obtained after 2 d at 30℃ on LB plates with erythromycin and

X-Gal. Positive blue colonies were used to inoculate a LB culture, which was incubated at 40°C over several passages to select clones with integrated vector. After plating dilutions of this culture on LB agar with erythromycin, plasmid insertion and gene disruption of grown colonies was verified by PCR. For further experiments the resulting strains (*B. cereus* F48INcesH, F48INcesC, F48INcesD, F48INppt, F48INsigH, F48INcodY and F48INccpA) were only grown at high temperatures (37°C - 40°C) to avoid the loss of the integrated plasmid.

2.12.4 Construction of *B. cereus* strains overexpressing AbrB and AbrB*

The shuttle vector pAD/PcspA, harbouring the cold shock inducible promoter of *cspA*, was used for overexpression of the target proteins AbrB and AbrB*. The promoterless *abrB* and *abrB** genes were amplified by PCR using the primers abrB_SacI_F/abrB_R_Hind2 and abrB-pBCE_Sac/abrB-pBCE_Hind, respectively. The digested products were ligated between the *SacI* and *HindIII* site of pAD/PcspA, giving pAD/abrB/PcspA and pAD/abrB*/PcspA. Each plasmid was electroporated into *B. cereus* F4810/72, resulting in *B. cereus* F48abrB/PcspA and F48abrB*/PcspA. The strains were incubated in LB media at 15°C (150 rpm) for 4 d to induce overexpression of AbrB and AbrB*.

2.12.5 Plasmid curing

B. cereus F4810/72 was cultured and continuously passaged for five weeks at 42°C to promote the loss of the megaplasmid pBCE. At each passage 50 µl culture was inoculated into 5 ml of fresh LB medium and incubated for further 24 h. After five weeks dilutions of the culture were plated onto LB and incubated overnight at 30°C. Grown colonies were screened for the presence of plasmid DNA by PCR with pBCE-specific primers. Cured strains were termed F48ΔpBCEI or F48ΔpBCEII, depending on their sporulation capability.

2.13 *Ces*-promoter fusions and luciferase assay

To determine the promoter activity of the *ces* operon, the vector pXen/Pces (Dommel, 2008), which contains a *lux* fusion between the *ces* promoter region and the luciferase genes *luxABCDE*, was exerted. The plasmid was introduced into *B.*

cereus F4810/72, F48Δspo0A and F48ΔabrB by electroporation, giving rise to F48lux/Pces, F48Δspo0Alux/Pces and F48ΔabrBlux/Pces, respectively. Transformation of the double mutant F48ΔabrB/Δspo0A required another antibiotic marker for selection. Therefor the erythromycin resistance sequence, which was gained from pAT113 using the primer pair Erm-F-Nco and Erm-R-Nco, was inserted in the *NcoI* site of pXen/Pces and the resulting plasmid, pXen/Pces/erm, electroporated into the strain resulting in F48ΔabrB/Δspo0Alux/Pces. For measurement of the *ces* promoter activity in different genetic backgrounds or various growth conditions, *B. cereus* overnight cultures were diluted (1:20) and 200 µl was distributed into wells of a 96-well microtitre plate with clear bottom (µClear white; Greiner bio-one). The plate was incubated in a microtitre plate shaker with heated lid at 30℃ with 400 rpm. Optical density (585nm) and bio luminescence (490nm), indicated as relative light units (RLU), was measured for 0.1 sec each hour using a VICTOR 1420 multilabel counter (Wallac, Finland). *B. cereus* F4810/72 with a promoter-less luciferase construct (pXen1) was used as negative control.

2.14 Overexpression and purification of AbrB and AbrB*

The *abrB* gene and the *abrB** gene of *B. cereus* F4810/72 were amplified using the oligonucleotides abrB_Nco-F/abrB_Xho-R and abrB-P-Nco/abrB-P-Xho, respectively. The digested PCR products were cloned into the expression vector pET28b by fusing their C-terminal to the His-Tag coding sequence of the vector. For protein overexpression the *E. coli* strain BL21 carrying pET28/abrB or pET28/abrB* was grown in LB containing kanamycin. At OD_{600nm}0.5 IPTG was added to a final concentration of 1 mM and growth continued for 3 h at 37℃. Bacteria were harvested by centrifugation, washed once in BufferA (50 mM Tris pH 7.6, 50 mM KCl, 1 mM DTT, 0.1 mM PMSF) and resuspended in BufferB (300 mM NaCl, 50 mM sodium phosphate). Cells were disrupted by passage through a French press and cell debris removed by centrifugation (15300 rpm, 2 x 15 min, 4℃). The crude extract containing the soluble protein fraction was incubated with an equal volume of TALON metal affinity resin (Clontech) for 2 h at 15℃. The beads were then washed ten times with BufferB, followed by three washing steps with BufferB containing 7.5 mM imidazole. Finally AbrB-His_6 or AbrB*-His_6 was eluted with BufferB containing 150 mM imidazole. The protein concentration was determined according to Bradford

(RotiNanoquant) and the purity of eluted fractions was checked by standard SDS-PAGE (15% resolving gel) and Coomassie blue staining. Protein fractions were concentrated and dialyzed with BufferA using Vivaspin 500 filter units (Sartorius).

2.15 Gel mobility shift assay

To test the binding ability of AbrB to DNA, several ~350 bp DNA probes displaying various promoter regions were generated by PCR using the oligonucleotides listed in the Appendix 7.2 and purified. The binding reactions contained different amount of the AbrB protein (2-14 pmol), 1 pmol of the promoter DNA probe, 1 pmol of a negative DNA probe and 2 µl 10x Binding Buffer (50 mM Tris-HCl, 750 mM KCl, 2.5 mM EDTA, 0.5% Trition-X 100, 62.5% glycerol, 1 mM DTT) in a total volume of 20 µl. Samples were incubated at 25℃ for 30 min before adding 4 µl of DNA loading dye and loading them onto a 10% non-denaturing polyacrylamide gel. Native gels consisted of 2.66 ml 40% acrylamide, 1 ml 2% bisacrylamide, 2 ml 5x TBE buffer, 3.24 ml ddH_2O, 100µl 10% APS and 10µl TEMED. Gel electrophoresis was performed in prechilled 1x TBE buffer at 120 V for 3 h. Gels were incubated in ethidium bromide solution (0.5 µg/ml) for 5 min and DNA was visualized by UV irradiation.

2.16 Cell fractionation and cereulide extraction

For cereulide extraction from vegetative *B. cereus* cells and from culture supernatant, *B. cereus* was grown in LB at 30℃ and 150 rpm for 14 h before being harvested (2 min at 13200 rpm) in 2 ml cell culture aliquots. The supernatant, displaying the secretome extract, was filtered (0.22 µm) and stored at 4℃ until use. The cell pellet was washed once with PBS and resuspended in 1 ml PBS or 1 ml ethanol. Samples were incubated overnight with rotary shaking and centrifuged (2 x 15 min at 15000 rpm) to remove cell debris. For preparation of the cytosolic- and membrane fraction the harvested 2 ml cell pellet was dissolved in 1 ml PBS and disrupted by two passages through a chilled French Press at 140 mPa. The soluble protein extract was separated from membranes and cell debris by ultra-centrifugation at 100000 g for 1 h at 15℃. The supernatant, presenting the cytosolic fraction, was stored at 4℃ until use. The membrane pellet was resuspended in 1 ml PBS before overnight

incubation with rotary shaking. Insoluble solids were removed by centrifugation (2 x 15 min at 15000 rpm) and extracts stored at 4°C.

For hexane extraction the supernatant or PBS-sample was combined with 1 volume of hexane and incubated for 1 h with shaking. After centrifugation (15 min at 8000 rpm) the upper hexane phase was removed and the remaining aqueous phase again extracted with 1 volume of hexane. Both hexane phases were combined and evaporated. The residue was redissolved in 1 ml of 100% ethanol and incubated overnight with shaking. Insoluble solids were removed by centrifugation (2 x 15 min at 15000 rpm) and extracts stored at 4°C until use.

To test the effect of ethanol on vegetative cells, cell pellets were resuspended in 1 ml PBS buffer with different percentage of ethanol (0%, 10%, 30%, 50%, 70% and 100%) and incubated for 10 min at RT with shaking. Samples were diluted and plated on PC agar for cell count determination and then immediately centrifuged (2 x 15 min at 15000 rpm) to remove cells and gain clear supernatants for analysis in the HEp-2 bioassay.

2.17 Cereulide toxicity HEp-2 cell assay

Emetic toxin production of *B. cereus* strains was determined using a modified protocol of the HEp-2 cytotoxicity assay previously described (Finlay *et al.*, 1999). Samples of *B. cereus* cultures were taken during mid-log and stationary growth phase and were autoclaved (15 min at 120°C) to inactivate cells and heat-labile toxins. Alternatively to the autoclaved samples, ethanol extracts were prepared and tested in the HEp-2 cell assay. For the bioassay samples were two fold serially diluted in 96-well microtitre plates using Eagle minimum essential medium with Earle salts (supplemented with 1% foetal calf serum, 1% sodium pyruvate and 0.4% penicillin-streptomycin) and 2% ethanol as a solvent for cereulide. Several dilutions of valinomycin (1-500 ng/ml; Fluka) served as an internal standard. After addition of 150 µl HEp-2 cells (6 x 10^5 cells/ml) per well, the plates were incubated for 48 h at 37°C in a 5% CO_2 atmosphere. Subsequently, 100 µl supernatant of each well was discarded and 10 µl of the tetrazolium salt WST-1 (Roche) was added to detect mitochondrial activity of viable cells. After 20 min of incubation at 37°C, the

absorbance was measured in a microtitre plate reader at 450/620nm. From the resulting dose-response curve the 50% inhibitory concentration of each sample was calculated, which is presented by the reciprocal value of the sample dilution that resulted in 50% loss of mitochondrial activity. Emetic toxin titres could be deduced from the valinomycin standard curve with given concentration. For better comparison, values from one assay were usually normalized to the parental strain *B. cereus* F4810/72, whose cytotoxicity was defined as 100%.

2.18 Sample preparation for proteome analysis

B. cereus cultures were harvested in the mid-logarithmic growth phase by centrifugation (6000 rpm; 15 min; RT) and cells were washed twice with 10 mM Tris-HCl, 1 mM EDTA, 1 mM Pefabloc (pH 7.5). For preparation of the extracellular protein fraction the supernatant was rapidly filtered (0.22 µm) and proteins were precipitated with ice cold trichlor acetic acid (10% w/v) overnight at 4℃. After centrifugation (12000 rpm; 1 h; 4℃), the protein pellet was washed four times with acetone containing 0.2% DTT before being resuspended in lysis buffer (7 M urea, 2 M thiourea, 4% CHAPS, 1% DTT, 2% Pharmalyte 3-10) and stored at -80℃ until use. For preparation of the cytosolic protein fraction the harvested and washed cells were directly dissolved in lysis buffer and disrupted by three passages through a chilled French press at 140 mPa. Soluble protein extracts were separated from cell debris by repeated centrifugation at 15000 rpm for 30 min at 4℃. The supernatant was stored in aliquots at -80℃ until use. Total protein concentration of secreted and cytosolic protein fraction was determined using the 2D Quant kit (GE Healthcare).

2.19 Two-dimensional gel electrophoresis

Protein fractions were analysed by 2D electrophoresis according to Görg *et al*. (Görg *et al.*, 2004). In brief, isoelectric focusing was performed with immobilized pH gradients (IPG-strips, 18 cm, pH 4-7) using the Ettan IPGphor 3 IEF unit (GE Healthcare). The IPG-strips were rehydrated in buffer containing 8 M urea, 1% CHAPS, 0.4% DTT and 0.5% Pharmalyte overnight. Approximately 100-150 µg protein was loaded on each strip, which was focused for a total of 35-45 kVh at 20℃ (0.05 mA per IPG strip). Strips were equilibrated for 2 x 15 min in equilibration buffer

(50 mM Tris-HCl (pH 8.8), 6 M urea, 30% glycerol, 2% SDS) containing 1% DTT in the first and 4% iodoacetamide in the second washing step. The second dimension was carried out using 12.5% polyacrylamide gels in a Dalt vertical electrophoresis unit running at 15 mA per gel for 18 h. After electrophoresis proteins were visualized by silver staining or with colloidal Coomassie blue (Roti-blue, Roth). Stained gels were scanned using a calibrated flatbed scanner (HP Scanjet 4890) and computer assisted image analysis was performed with the Proteomweaver 2D software Version 4.0 (BioRad). A spot was considered to be differentially expressed if there was a threefold or more change in spot volume.

2.20 Biofilm microtitre plate assay

B. cereus overnight cultures were diluted (1:100 or 1:20) in LB-biofilm medium (10 g bacto-peptone, 5 g NaCl and 5 g yeast extract per litre) and 200 µl was distributed into wells of a 96-well microtitre plate. The plate was incubated in a microtitre plate shaker with heated lid at 30℃ with 350 rpm. After 24 h 100 µl medium was removed from each well by gentle pipetting and fresh medium was added to support biofilm formation with new nutrients. The total growth (OD_{600nm}) was measured after 48 h of incubation using a Wallac VICTOR3 multilabel counter (Perkin Elmer, Finland) before the supernatant with planktonic cells was discarded and each well was washed twice with 230 µl PBS. Subsequently biofilm cells were stained with 200 µl 0.1% crystal violet for 20 min at RT. Wells were washed again twice with ddH_2O before 200 µl 80% ethanol / 20% acetone was added to dissolve remaining crystal violet. After 20 min of incubation at 100 rpm, the absorbance was measured at 600nm to quantify biofilm formation.

3 RESULTS

3.1 Regulation of cereulide synthesis

3.1.1 Construction and phenotypic characterization of *B. cereus* deletion mutants

The transcription regulator genes *plcR*, *spo0A* and *abrB* of *B. cereus* F4810/72 were identified on the basis of sequence homology to the annotated strain *B. cereus* ATCC10987 (GenBank AccNo NC_003909). Deletion mutants were constructed by replacing the respective genes with a spectinomycin resistance cassette by heterogramic conjugation. Conventional PCR, RT-qPCR and sequencing confirmed the correct allelic exchange, which resulted from homologous recombination. Beside the single knockout strains F48ΔplcR, F48Δspo0A and F48ΔabrB, the double mutant F48ΔabrBΔspo0A was obtained. Growth kinetics in LB revealed similar growth rates for the wild type, the *plcR* and the *abrB* mutant, though the latter entered the logarithmic growth phase 2-3 hours delayed (Figure 3A). These strains also initiated sporulation synchronously in late exponential phase (data not shown). In contrast, the *spo0A* null mutant and the *abrB/spo0A* double mutant grew to a lower maximum OD_{600nm} (Figure 3B) and were unable to sporulate. However, both strains also showed distinct differences in their growth pattern. While growth of the *abrB/spo0A* mutant was strongly delayed in time and the exponential phase did not start before 12 h of incubation, this was not observed for the *spo0A* mutant. Intriguingly, the cell density of the *spo0A* mutant decreased after 18 h due to cell lysis, whereas the OD_{600nm} of the double mutant remained stable over this time period.

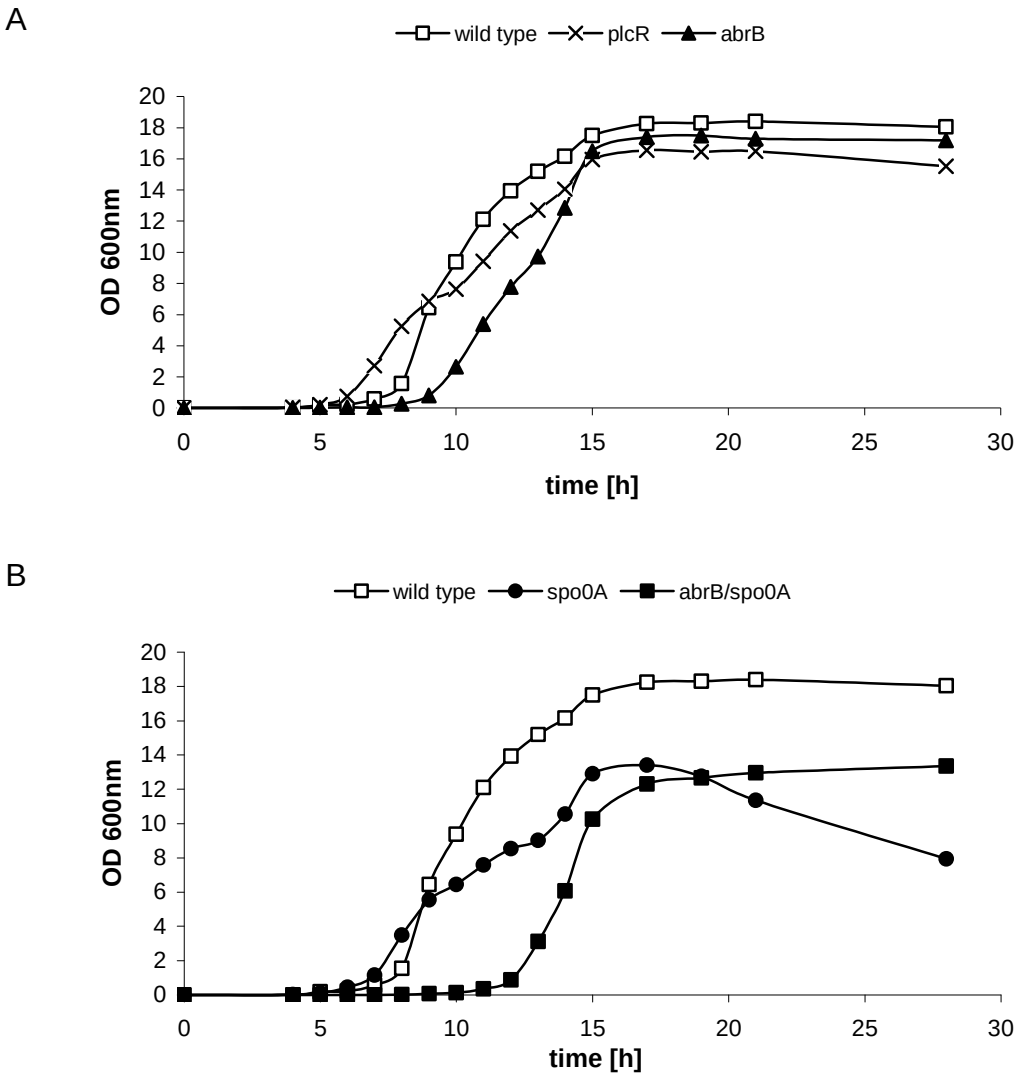

Figure 3. Growth of *B. cereus* F4810/72 wild type in comparison to its deletion mutants (A) F48ΔplcR and F48ΔabrB; (B) Δspo0A and F48ΔabrBΔspo0A. Strains were grown in LB at 30℃ and 150 rpm . Graphed curves represent mean values of two independent experiments.

All strains were grown on the selective plating media MYP (mannitol-egg-yolk-polymyxin agar, Oxoid) to define their colony morphology (Figure 4). *B. cereus* typically grows on MYP agar as a pink coloured colony, which is surrounded by a precipitation zone due to egg yolk hydrolysis. This phenotype was also seen for F48ΔabrB. In contrast, F48ΔplcR and F48Δspo0A revealed atypical colony morphologies and could therefore be easily distinguished from the *B. cereus* F4810/72 wild type. Colonies of the *plcR* null mutant were not surrounded by a precipitation zone due to the downregulated phospholipase C activity in the absence of its regulator PlcR. The *spo0A* null mutant, however, showed a characteristic precipitation zone, but colonies appeared more shiny and darker in colour than the

wild type. Interestingly, the colony morphology of the *abrB/spo0A* double mutant, which is also not able to sporulate, shows more similarity to the wild type than to the *spo0A* null mutant (Figure 4).

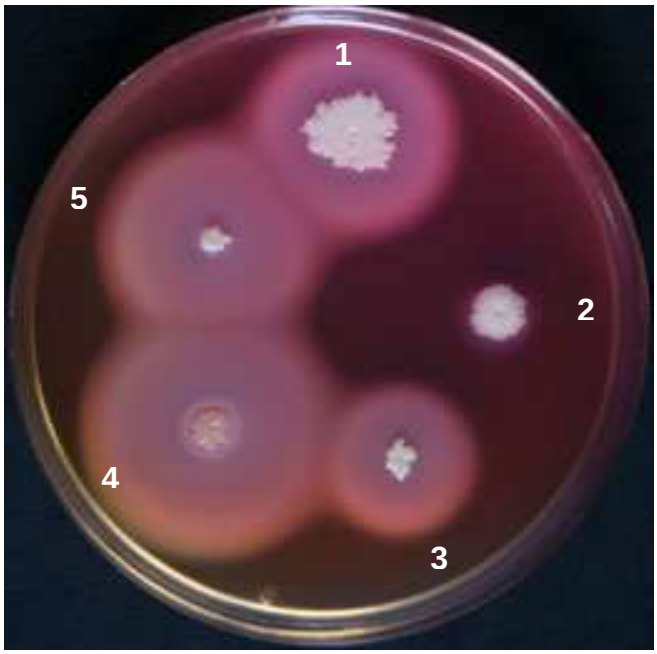

Figure 4. Colony morphology of *B. cereus* F4810/72 (1), F48ΔplcR (2), F48ΔabrB (3), F48Δspo0A (4) and F48ΔabrBΔspo0A (5) grown on MYP agar for 24 h at 30°C. Due to egg yolk hydrolysis by the phospholipase C a typical precipitation zone surrounds all strains except the *plcR* mutant, which lacks the regulator. The non sporulating *spo0A* mutant strain appears shiny and darker in colour.

3.1.2 Cytotoxicity of *B. cereus* deletion mutants

To study the potential role of the regulators on cereulide production, toxin titres of wild type and deletion mutants were determined using the HEp-2 cell bioassay. *B. cereus* cultures were grown in LB for 24 h until stationary phase, where samples were taken and heated (15 min at 120°C). The cytotoxic activity of these preparations was tested on HEp-2 cells along with valinomycin as calibrator. The results indicated that the *plcR*- and the *abrB* null mutant displayed similar toxicity as the wild type strain. In contrast, the *spo0A* null mutant revealed a cereulide deficient phenotype when tested in the HEp-2 assay (Figure 5). However, toxicity was completely restored in the *abrB/spo0A* double mutant, indicating a defined role of these two regulators in the control of cereulide synthesis.

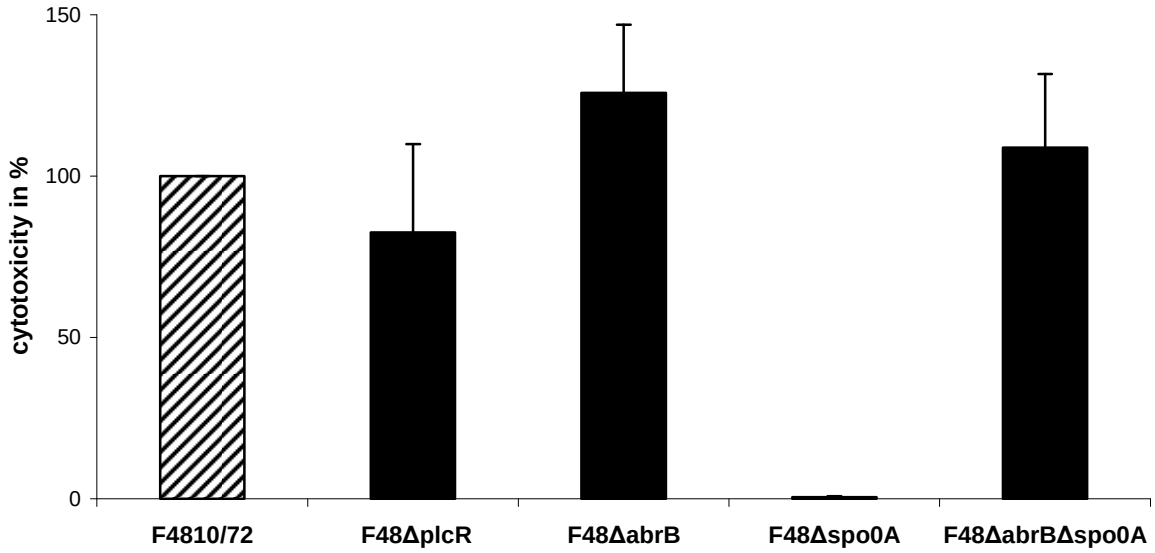

Figure 5. Cereulide production of *B. cereus* wild type and mutant strains, as determined by the HEp-2 bioassay. Cytotoxicity of autoclaved cell samples of *B. cereus* F4810/72, F48ΔplcR, F48Δspo0A, F48ΔabrB and F48ΔabrBΔspo0A, grown in LB media for 24 h at 30℃, is given . The cytotoxicity of the wild type was set to 100%. Values are means and error bars standard deviations of four independent experiments.

3.1.3 Transcriptional analysis of *cesA* by RT-qPCR

To test whether *ces* regulation occurs on transcriptional level, quantitative real time PCR of the cereulide synthetase gene *cesA* was carried out. *B. cereus* strains were grown in LB (30℃, 150 rpm) and samples for RNA isolation were taken at the mid-log growth phase (OD_{600nm}10). Relative expression of *cesA* (normalized to the 16S rDNA gene *rrn*) was determined in comparison to the transcript level of the parental strain at OD_{600nm}1, which was set as the calibrator.

Transcription levels of *cesA* in the wild type strain, the *plcR* and the *abrB* null mutant turned out to be comparable, though transcript levels of the *abrB* mutant were slightly decreased. In contrast, *cesA* transcription of the *spo0A* null mutant was severely reduced, presenting a 55 fold downregulation compared to the parental strain. However, this effect was completely suppressed in the *abrB/spo0A* double mutant, which revealed *cesA* transcript levels similar to the wild type strain (Figure 6). These data show that loss of cytotoxicity in the *spo0A* null mutant is due to the downregulation of the transcription of the *ces* genes.

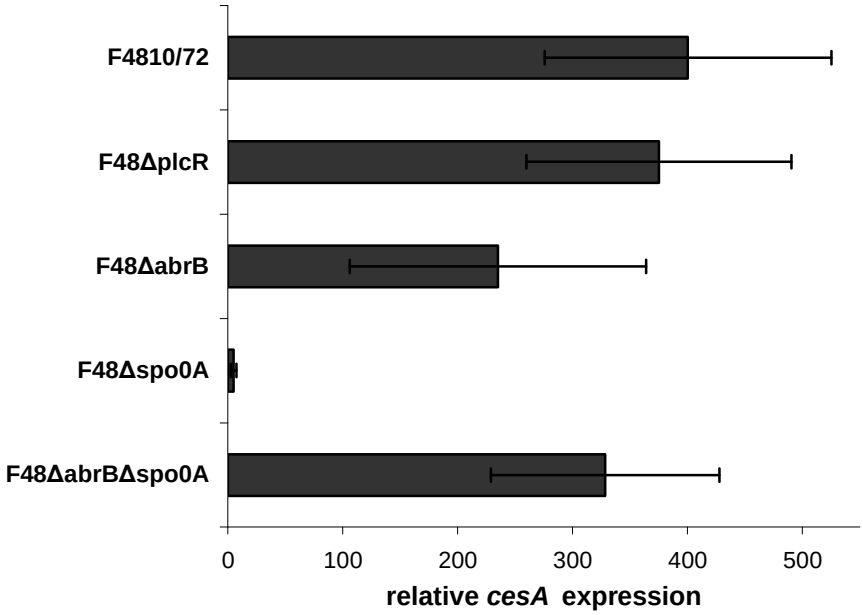

Figure 6. RT-qPCR analysis of *cesA* in *B. cereus* F4810/72 and the deletion mutants F48ΔplcR, F48Δspo0A, F48ΔabrB and F48ΔabrBΔspo0A. Strains were incubated in LB media at 30°C until the mid-log phase (OD_{600nm}10) before sampling for RNA isolation. Transcript levels represent means and error bars standard deviations of two independent data sets that were normalized to *rrn* transcript levels.

3.1.4 Spo0A complementation and AbrB overexpression

The transcription of *spo0A* occurs from two promoters, which induce *spo0A* transcription at different time points of the growth cycle. While the weak promoter $P\sigma^A$ is recognized by the sigma factor σ^A during vegetative growth, $P\sigma^H$ is strongly induced during the initial phase of sporulation (Chibazakura *et al.*, 1991; Predich *et al.*, 1992). In order to find out if the early or late *spo0A* transcription is necessary to complement the cereulide deficient phenotype of the *spo0A* null mutant, two different pAD vector constructs were tested for complementation: One containing the *spo0A* gene with its two promoter regions ($P\sigma^A$ and $P\sigma^H$) and the other with only $P\sigma^H$ upstream of *spo0A*. Plasmids were introduced into the *B. cereus spo0A* null mutant by electroporation and characterized in respect of their growth and cytotoxicity. Although both strains, *B. cereus* F48comAH and F48comH, were able to sporulate (data not shown), only F48comAH was toxic on HEp-2 cells, while the mutant with just $P\sigma^H$ revealed a very low cytotoxicity (Figure 7). Additionally, *B. cereus* F4810/72, F48Δspo0A and the two complemented strains of the *spo0A null* mutant were grown

in the presence of 2% glucose, which is known to repress $P\sigma^H$–directed transcription of *spo0A.* The cereulide titre of *B. cereus* F48comAH was again comparable to the wild type strain, whereas F48comH produced clearly less toxin. Interestingly, the amount of toxin produced by the wild type and F48comAH in the presence of glucose was significantly higher compared to the strains grown in LB without glucose (Figure 7). These data demonstrate that cereulide production is mainly affected by σA-directed *spo0A* transcription during vegetative growth.

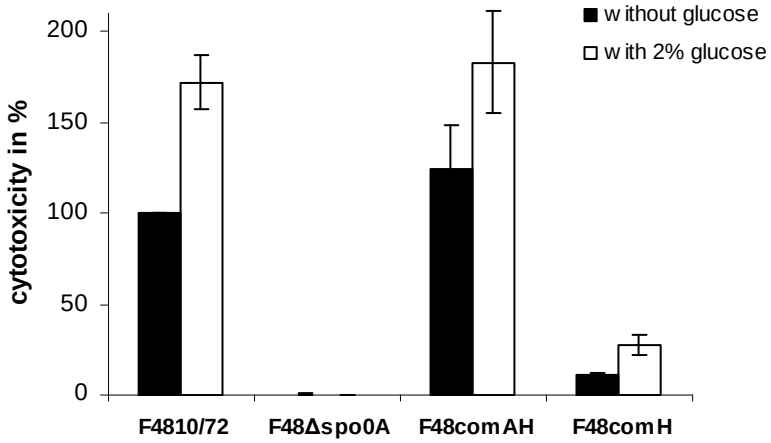

Figure 7. Cereulide production of *B. cereus* wild type, its *spo0A* null mutant and the complemented strains F48comAH and F48comH, as determined by the HEp-2 bioassay. Strains were grown in LB media and in LB media supplemented with 2% glucose for 24 h at 30℃. The cytotoxicity of the wild type in LB without glucose was set to 100%. Values are means and error bars standard deviations of three independent experiments.

However, since the *abrB/spo0A* double mutant was found to be toxic (Figure 5), it is possible that Spo0A regulates *ces* expression indirectly, for example by repressing AbrB. To test whether *abrB* of *B. cereus* F4810/72 is an early target gene of the Spo0A regulon, as it has been shown for *B. subtilis*, transcription analysis was done. RT-qPCR was performed to determine *abrB* transcript level of the parental strain and F48Δspo0A in early growth phases. In the wild type strain *abrB* transcription peaked during the transition from lag to exponential phase and decreased strongly in the further growth cycle. In contrast, the *abrB* transcript level of the *spo0A* null mutant was not repressed but remained stable throughout growth (Figure 8).

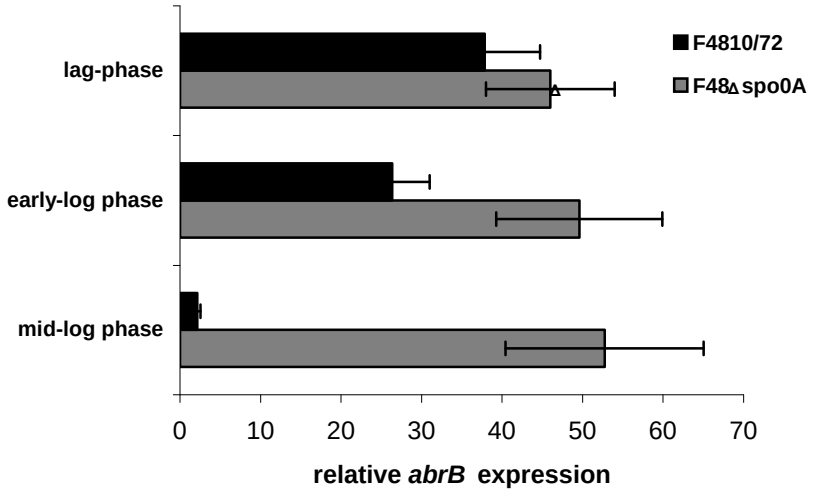

Figure 8. RT-qPCR analysis of *abrB* in *B. cereus* F4810/72 and its *spo0A* null derivative. Transcript levels were determined in early growth stages: transition from lag to logarithmic-phase (OD_{600nm}0.05), early exponential phase (OD_{600nm}0.2) and mid-exponential phase (OD_{600nm}10). Values represent means and error bars standard deviations of four different data sets that were normalized to *rrn* transcript levels.

Hence, repression of the cereulide synthetase in the *spo0A* null mutant may solely be due to the elevated AbrB level in this strain. Thus, a *B. cereus* mutant overexpressing AbrB was constructed, by cloning the *abrB* gene downstream of the cold shock inducible promoter PcspA into the pAD123 vector, which was then introduced into *B. cereus* F4810/72 by electroporation. Cells were grown in LB media for 4 days at 15℃ for protein overexpression. As a control, the wild type strain harbouring pAD/gfp/PcspA was grown under same conditions. The HEp-2 cell assay revealed that overexpression of GFP lowered cereulide expression only slightly, while AbrB overexpression resulted in a completely non toxic phenotype, suggesting that AbrB might repress cereulide synthesis (Figure 9). Interestingly, *B. cereus* F4810/72 possesses besides the chromosomal *abrB* gene, a plasmid-encoded copy (locus tag: BcAH187_pCER270_0167; here designated *abrB**), revealing 61% identity and 81% similarity on amino acid sequence level. RT-qPCR of *abrB** revealed a transcription pattern comparable to *abrB*, with high transcript levels in early growth and almost no decrease in the *spo0A* null mutant (data not shown). However, analysis of an AbrB* overexpressing strain showed a similar cytotoxic level as the wild type strain (Figure 9), implying a minor account of AbrB* in cereulide production.

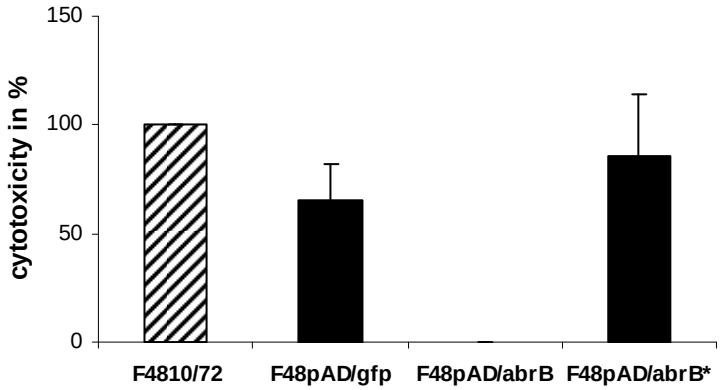

Figure 9. Cereulide production of *B. cereus* wild type and the protein overexpressing strains F48pAD/gfp, F48pAD/abrB and F48pAD/abrB*, as determined by the HEp-2 bioassay. Strains were grown in LB media for 4 d at 15℃ for induction of the *cspA* promoter. The cytotoxicity of the wild type was set to 100%. Values are means and error bars standard deviations of three independent experiments.

3.1.5 *ces* promoter studies

For further characterization of *ces* regulation by AbrB, the *ces* promoter activity was investigated in the *spo0A* and *abrB* mutant strains. Therefor the vector pXen/Pces, which contains the *ces* promoter region fused to the luciferase operon, was introduced into *B. cereus* F4810/72 wild type, F48ΔspoA, F48ΔabrB and the double mutant F48ΔabrBΔspo0A by electroporation. Strains were incubated in microtitre plates at 30℃ and bioluminescence as well as optical density was monitored throughout growth. According to its luminescence, the wild type strain showed a strictly regulated *ces* promoter activity, peaking at 15 h of incubation, which corresponds to the exponential growth phase (Figure 10). As expected, the *spo0A* null mutant displayed no *ces* promoter activity at all. In contrast, *ces* expression of the *abrB* null mutant seemed elevated at the beginning of growth, as luminescence occurred stronger and earlier in time. Also the *abrB/spo0A* double mutant revealed a higher *ces* promoter activity compared to wild type in the early growth phase, but luminescence remained rather low during the rest of the growth cycle, probably due to the poor growth rate of this strain (Figure 10).

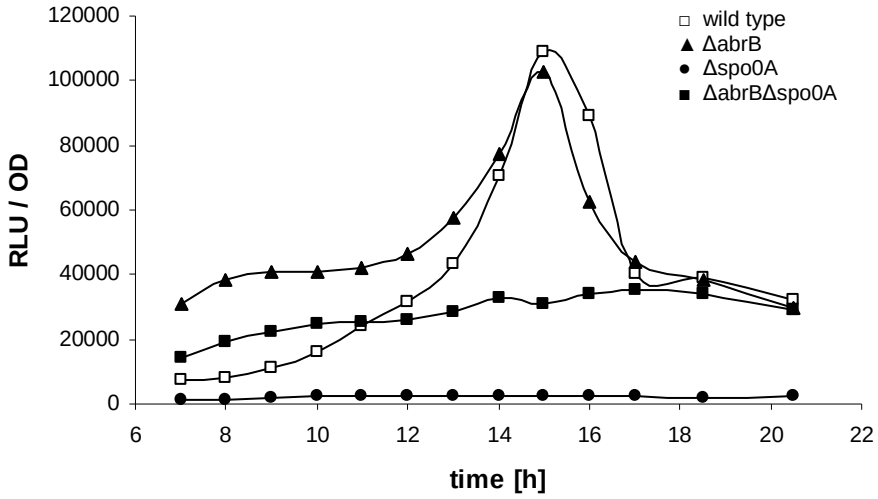

Figure 10. *ces* promoter activity, measured as bioluminescence, of the following *B. cereus* strains harbouring the *ces* promoter *lux* fusion (pXen/Pces): □ *B. cereus* F48lux/Pces; ● F48Δspo0Alux/Pces; ▲ F48ΔabrBlux/Pces; ■ F48ΔabrBΔspo0Alux/Pces. Bioluminescence intensity is indicated as relative light units (RLU) in relation to the optical density (OD_{585nm}). Curves represent mean values of two independent experiments.

3.1.6 *In vitro* binding of AbrB and AbrB*

To study the DNA binding properties of the AbrB protein and the homologous AbrB* protein a non-radioactive gel mobility shift assay was used. At first the ~11 kDa AbrB protein was overexpressed in *E. coli* BL21 and purified via its His-tag using the TALON metal affinity resin (Figure 11). Purification of AbrB* was carried out in the same manner (data not shown).

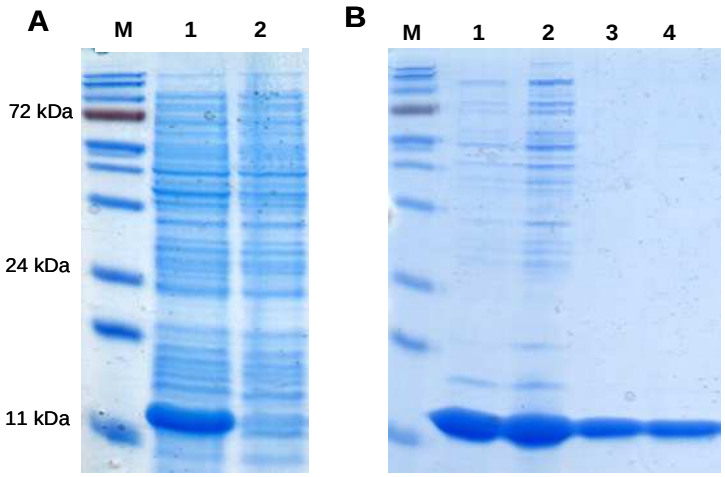

Figure 11. Overexpression and purification of AbrB-His_6. A: Protein overexpression in *E. coli* BL21 after IPTG induction (lane 1) and without induction (lane 2). B: Eluted AbrB-His_6 collected in different fractions with increasing purity (lane 1-4). M: prestained protein ladder (PageRuler; Fermentas).

The purified AbrB-His_6 and AbrB*-His_6 fusion proteins were tested for their binding activity to the main *ces* promoter region, which was identified to be located 100 bp upstream of the start codon of the *cesP* gene (Dommel, 2008). The AbrB protein was found to bind efficiently to the *cesP* promoter region, since a complete shift could already be seen with 8-10 pmol of the AbrB protein. In contrast, *in vitro* studies of the highly homologous AbrB* revealed no binding of this protein to the *ces* promoter probe (Figure 12). These results demonstrate that AbrB but not the plasmid-encoded AbrB* is able to bind to the main promoter of the cereulide synthetase gene operon and thus may act as a direct repressor of cereulide expression.

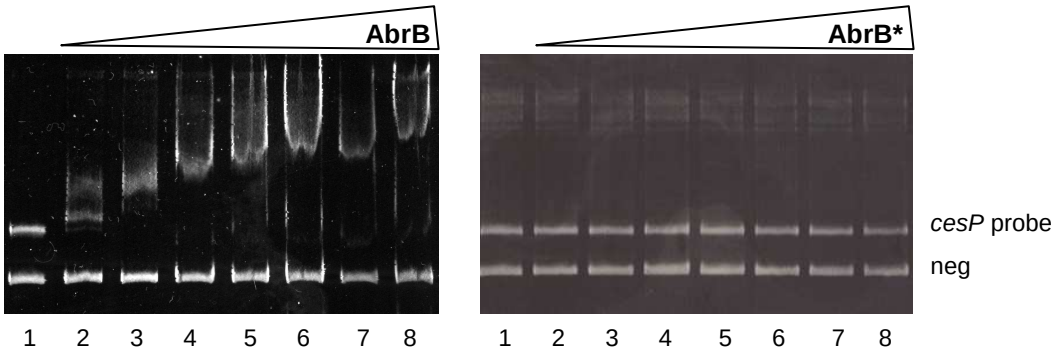

Figure 12. *In vitro* binding of AbrB and AbrB* to the *cesP* promoter region. Lanes of the gel mobility shift assays: (1) no protein; (2) 2 pmol; (3) 4 pmol; (4) 6 pmol; (5) 8 pmol; (6) 10 pmol; (7) 12 pmol; (8) 14 pmol. The different AbrB or AbrB* amounts were mixed with both 1 pmol of the *cesP* promoter probe and 1 pmol of a randomly chosen negative probe (neg).

The DNA binding ability of AbrB was not only tested with the *cesP* promoter probe, but also with other DNA probes, listed and described in table 4. Two additional probes were chosen adjacent to *cesP*, since previous studies identified besides the main *ces* promoter (P1) a second promoter (P2), which was found 256 bp upstream of the translational start (Dommel, 2008). Besides the different *cesP* probes of *B. cereus* F4810/72, the putative promoter sequences of *cesP* of the emetic *B. weihenstephanensis* strain MC67 was tested. Furthermore, the promoter regions of *abrB* and the 4'-phosphopantetheinyl transferase gene *ppt,* which encodes an enzyme homologous to CesP, were investigated by the gel shift assay.

Table 4. Characterization of DNA probes used in the AbrB-binding study

Probe name	Description	Genetic location
cesP	364 bp fragment, including P1 and P2	starting 342 bp before the start codon of *cesP*
cesP_II	375 bp fragment, including P1	starting 191 bp before the start codon of *cesP*
cesP_III	416 bp fragment, including no promoter sequence	starting 66 bp before the start codon of *cesP*
ppt	335 bp fragment, including the putative promoter sequence of *ppt*	starting 302 bp before the start codon of *ppt* (BcerAH_010100009366)
cesP_Bw	326 bp fragment, including the putative promoter sequence of *cesP* of *B. weihenstephanensis* MC67	starting 309 bp before the start codon of *cesP* of *B. weihenstephanensis* MC67
abrB	167 bp fragment, including the putative promoter sequence of *abrB*	starting 205 bp before the start codon of *abrB*
neg	327 bp inner fragment of *ppt*, including no promoter sequence	starting 142 bp after the start codon of *ppt*

The AbrB protein was found to bind strongly only to the original *cesP* probe, while almost no binding could be detected for the cesP_II and cesP_III sequences (Figure 13). This result demonstrates that AbrB binds efficiently to the upstream region of the main *ces* promoter, but not to the P1 downstream region. AbrB was also found to bind to the *cesP* probe of *B. weihenstephanensis* MC67, but to a minor degree. In contrast, no AbrB binding was obtained for the *ppt* promoter region. As expected, AbrB, which has been shown to be an auto-regulatory protein in *B. subtilis* (Strauch *et al.*, 1989a), was able to bind to its own promoter (Figure 13). Regarding *ces* regulation, these *in vitro* binding assays confirm that AbrB binds specifically to the main promoter region of the *ces* gene cluster and probably represses its expression (Figure 13).

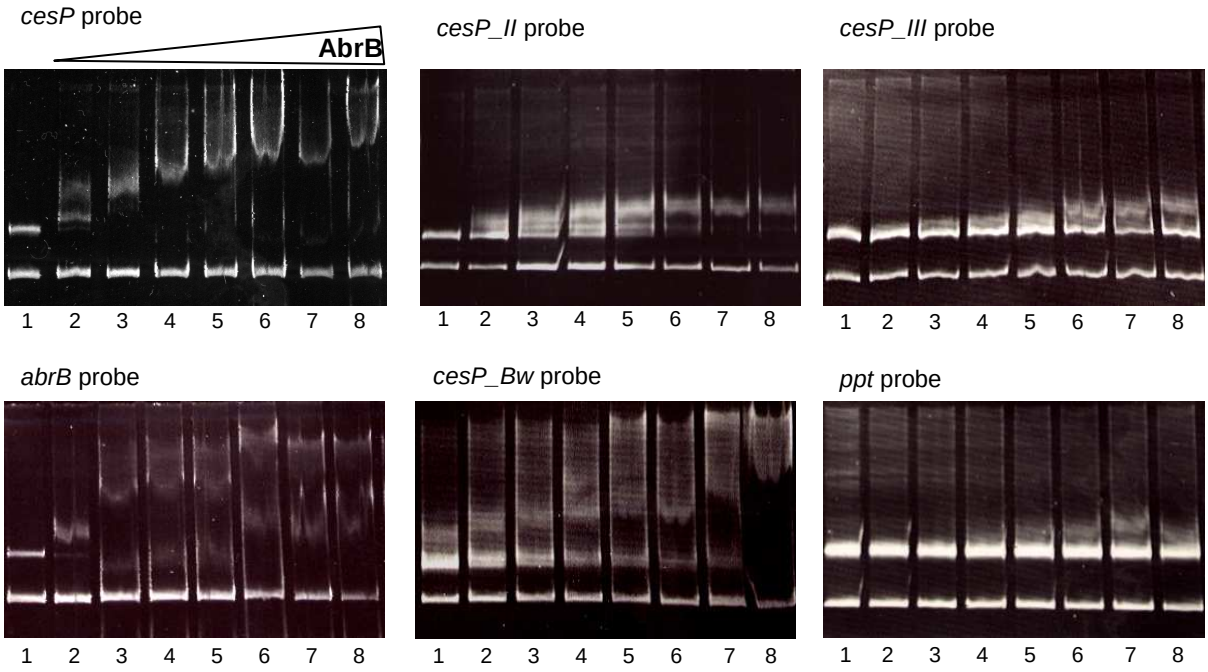

Figure 13. *In vitro* binding of AbrB to different promoter regions. Lanes of the gel mobility shift assay: (1) no AbrB protein; (2) 2 pmol; (3) 4 pmol; (4) 6 pmol; (5) 8 pmol; (6) 10 pmol; (7) 12 pmol; (8) 14 pmol of AbrB. The different AbrB amounts were mixed with both 1 pmol of the promoter probe (*cesP, cesP_II, cesP_III, cesP_Bw, abrB* or *ppt*) and 1 pmol of the negative probe (corresponds to the lower row in each gel).

3.1.7 Characterization of insertion mutants concerning the regulator genes *sigH, codY* and *ccpA*

Besides PlcR, Spo0A and AbrB, three additional regulators were chosen for investigation: the alternative sigma factor σ^H, which is essential for sporulation and a target of the AbrB repressor; the stationary phase gene regulator CodY and the carbon catabolite protein CcpA. Instead of deletion mutants, insertion mutants were constructed by inserting the pMAD vector into the target gene locus. This type of gene inactivation mutants was obtained rapidly compared to a real knock-out, but mutants were only stable at high temperature (37°C–42°C) due to the thermosensitive replication origin of the vector. Growth kinetics were performed in LB media at 37°C and revealed for all strains an increased growth rate compared to growth at 30°C. Similar growth curves were obtained for the wild type, the *ccpA* and the *sigH* mutant. An extended lag phase was observed for the *codY* insertion mutant, which entered the logarithmic phase not before 7 hours of incubation (Figure 14). Surprisingly, all three insertion mutants showed no sporulation under these

conditions, whereas the wild type sporulated efficiently in stationary phase. The sporulation deficient phenotype was expected for the mutant concerning the sporulation sigma factor σ^H, but remains unclear for the *ccpA* and *codY* mutants.

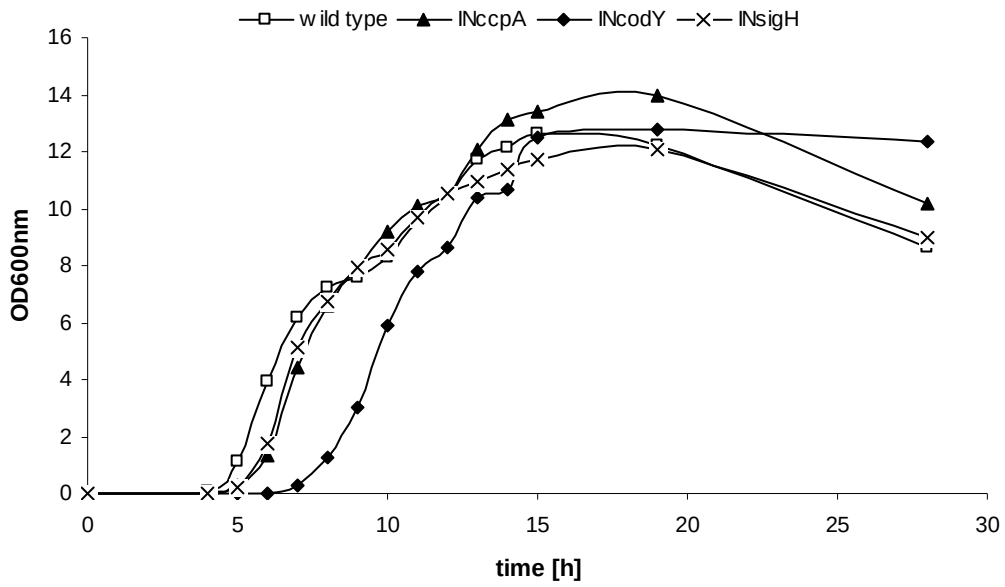

Figure 14. Growth of *B. cereus* F4810/72 wild type in comparison to the *ccpA, codY* and *sigH* insertion mutant. Strains were grown in LB at 37℃ and 150 rpm. Graphed curves represent mean values of two independent experiments.

Cytotoxicity of these strains, measured by the HEp-2 assay, revealed that both the σ^H and the CcpA insertion mutant were toxic, although slightly lesser than the wild type (Figure 15). Notably, when the CcpA mutant and the wild type were grown in LB media supplemented with 2% glucose to induce catabolite repression, no cytotoxicity was observed for both strains (data not shown). Obviously, cereulide production is repressed under these conditions (2% glucose, 37℃, 150 rpm), but in a CcpA-independent manner. In contrast to the *ccpA*- and *sigH* mutant, the *codY* insertion mutant showed a strongly toxin deficient phenotype (Figure 15). This result suggests that functional CodY may be required for cereulide synthesis under tested conditions and, thus, may present another transcription factor being involved in *ces* regulation.

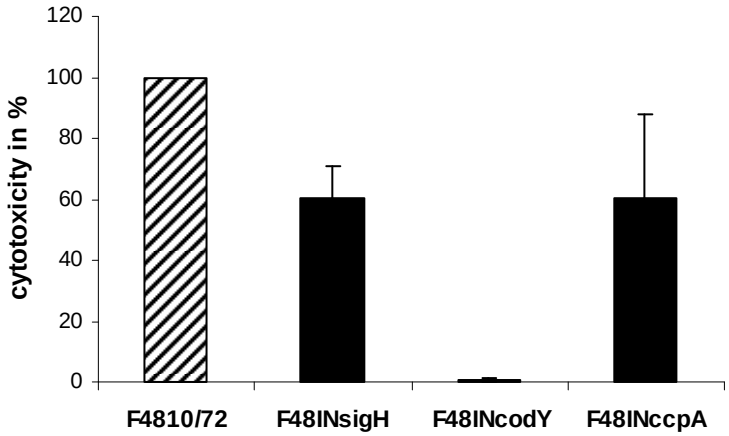

Figure 15. Cereulide production of *B. cereus* wild type and the insertion mutant strains F48INsigH, F48INcodY and F48INccpA, as determined by the HEp-2 bioassay. Strains were grown in LB media for 24 h at 37℃. The cytotoxicity of the wild type was set to 100%. Values are means and error bars standard deviations of three independent experiments.

3.1.8 Effect of glucose and other external factors on cereulide synthesis

Since previous data indicated that the addition of glucose in the culture media influenced cytotoxicity (see 3.1.4), this effect was further investigated. HEp-2 assays showed that growth of *B. cereus* F4810/72 in LB supplemented with 2% glucose resulted in significant higher cereulide toxin levels compared to growth in normal LB media. However, when culture samples were taken in the logarithmic growth phase (OD_{600nm}10) instead of the late stationary phase, the opposite effect was observed: Cells grown in the presence of glucose revealed even less cereulide than cells grown in LB media without glucose (Figure 16). This repressing effect of glucose on cereulide synthesis in the logarithmic growth phase was confirmed by previous RT-qPCR data, showing a *cesA* downregulation in the presence of glucose (Dommel, 2008). Further studies showed that the repressing and activating impact of glucose on cereulide production is independent of AbrB: The cytotoxicity levels of the *abrB* null mutant, which are in general higher than the wild type toxin titres, were affected by glucose in a similar manner as it was observed for the wild type (Figure 16).

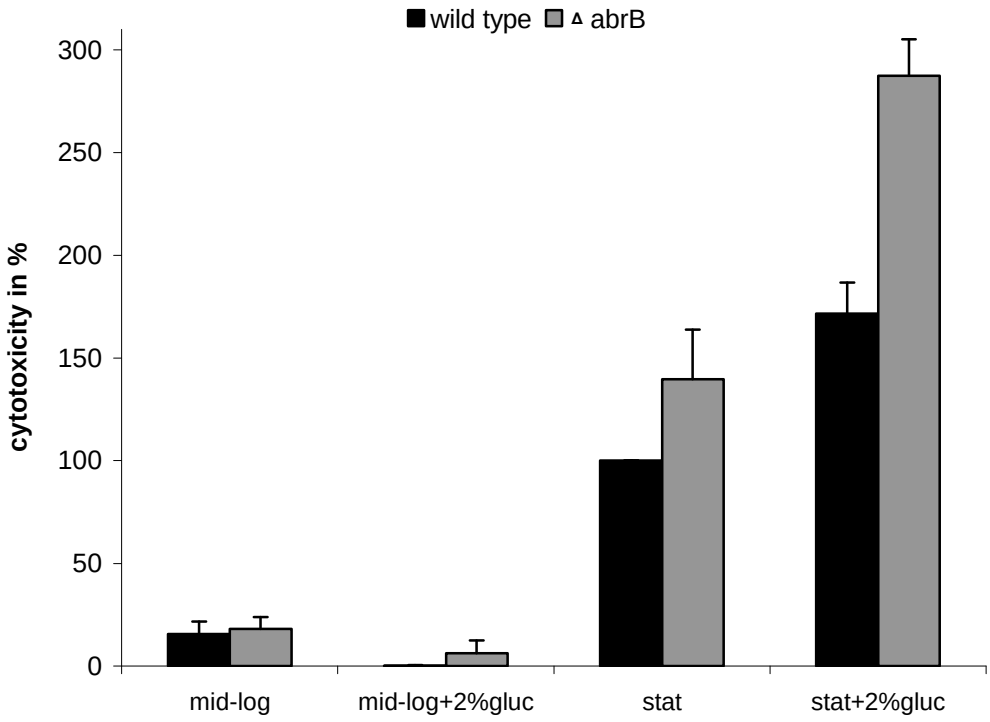

Figure 16. Cereulide production of *B. cereus* wild type and *abrB* null mutant in different growth phases and in the presence of glucose. Strains were grown in LB media and LB supplemented with 2% glucose at 30℃ and harvested in the logarithmic gr owth phase (OD_{600nm}10) as well as in stationary growth phase (after 24 h of incubation). The cytotoxicity of the wild type at 24 h was set to 100%. Values are means and error bars standard deviations of three independent experiments.

Intriguingly, when *B. cereus* F4810/72 was grown in LB media with 2% glucose at 37℃ instead of 30℃, no cytotoxicity at all was determ ined, regardless of the growth phase (data not shown). Obviously the activating effect of glucose on cereulide production is suppressed at higher growth temperature.

Besides HEp-2 assays, bioluminescence measurements were performed to determine the *ces* promoter activity of *B. cereus* grown in LB with and without glucose. Surprisingly, when grown in microtitre plates (30℃, 400 rpm), *B. cereus* displayed no *ces* promoter activity in the presence of glucose, indicating that additional growth parameters as for example oxygen supply influence cereulide synthesis. However, when cells were grown in baffled flasks (30℃, 150 rpm), luminescence was on average one log unit higher as the luminescence of the microtitre plates. Moreover, the addition of glucose resulted in a delayed but significantly higher *ces* promoter activity compared to the luminescence of *B. cereus*

grown in normal LB media (Figure 17). These glucose- and/or oxygen effects on cereulide production were also seen for the *abrB* null and the *abrB/spo0A* double mutant (data not shown), indicating their independence of AbrB regulation. Furthermore, *ces* promoter activity in the presence of glucose is consistent with HEp-2 data revealing no cereulide in logarithmic growth phase and a high toxin titre in stationary phase.

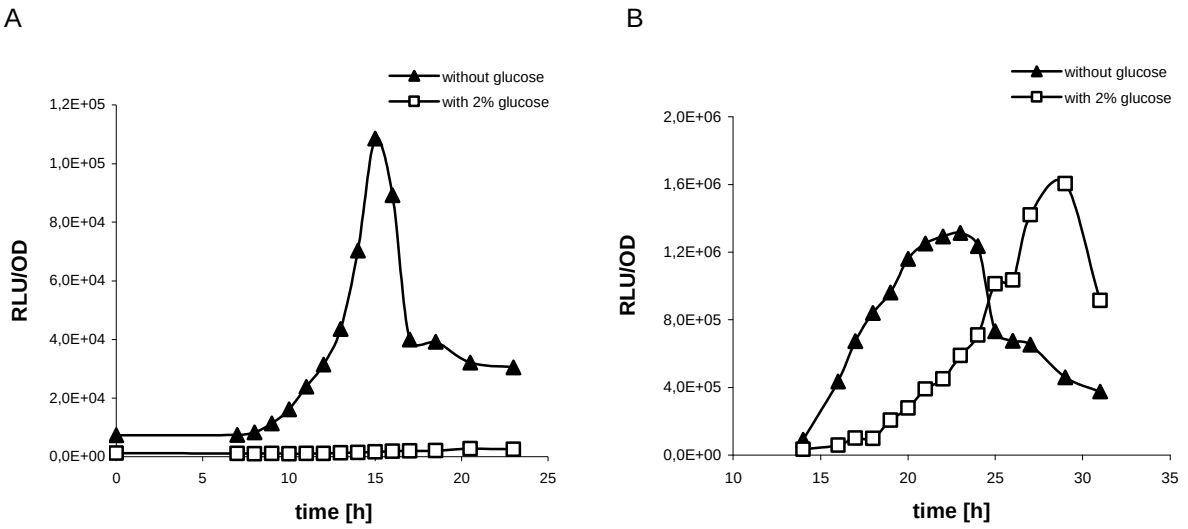

Figure 17. *ces* promoter activity of *B. cereus* F48lux/Pces grown in LB media and LB supplemented with 2% glucose and incubated in either microtitre plates or baffled flasks. (A) Bioluminescence of *B. cereus* grown in microtitre plates at 30℃ and 400 rpm. (B) Bioluminescence of *B. cereus* grown in baffled flasks at 30℃ and 150 rpm. Luminescence in tensity is indicated as relative light units (RLU) in relation to the optical density (OD_{585nm}). Curves represent mean values of two independent experiments.

Further *lux* measurements were performed to test several growth parameters possibly influencing *ces* promoter activity. It was shown that the growth rate itself is an important factor for cereulide production. The optical density of cells grown in microtitre plates had to exceed 0.7 to obtain high *ces* promoter activity. When cells only reached OD_{600nm} of 0.6, luminescence increased slowly within 20 hours of incubation and no peak was detected (data not shown). Therefore a rather high inoculum (1:20 dilution of overnight culture) and rotary shaking of at least 400 rpm were found to be necessary for proper growth and thus *ces* expression of *B. cereus* in microtitre plates.

The *lux* assay was also used to test if cereulide itself has an impact on *ces* expression. Therefor autoclaved *B. cereus* F4810/72 cell samples, which included cereulide, were added to the LB media of *B. cereus* F48lux/Pces and *ces* promoter activity was measured throughout growth. It was seen that the temporal appearance of bioluminescence differed strongly among these samples (Figure 18). While luminescence of *B. cereus* F48lux/Pces grown in LB usually peaks around 14 hours of incubation, luminescence of cells treated with autoclaved cell sample was detected earlier in growth, peaking already at 7 hours. To check if this effect was due to cereulide or to other components of the autoclaved cell sample, further samples of two cereulide-negative *B. cereus* strains were tested. The addition of autoclaved cell sample from the emetic-like strain *B. cereus* NVH1519/00 also led to an early *ces* promoter activity, indicating that this phenomenon is independent of cereulide. Moreover, when sterile-filtered supernatants of *B. cereus* F4810/72 or NVH1519/00 cultures were used instead of autoclaved cells, a similar effect on *ces* expression was obtained (data not shown). Surprisingly, treatment with the autoclaved cell sample of the non-emetic *B. cereus* type strain ATCC14579 resulted in growth inhibition of *B. cereus* F48lux/Pces and hence no *ces* promoter activity (Figure 18). However, the addition of *B. cereus* ATCC14579 supernatant did not influence growth nor luminescence (data not shown) suggesting that the inhibitory effect is caused by heat stable components closely associated with *B. cereus* ATCC14579 cells.

A

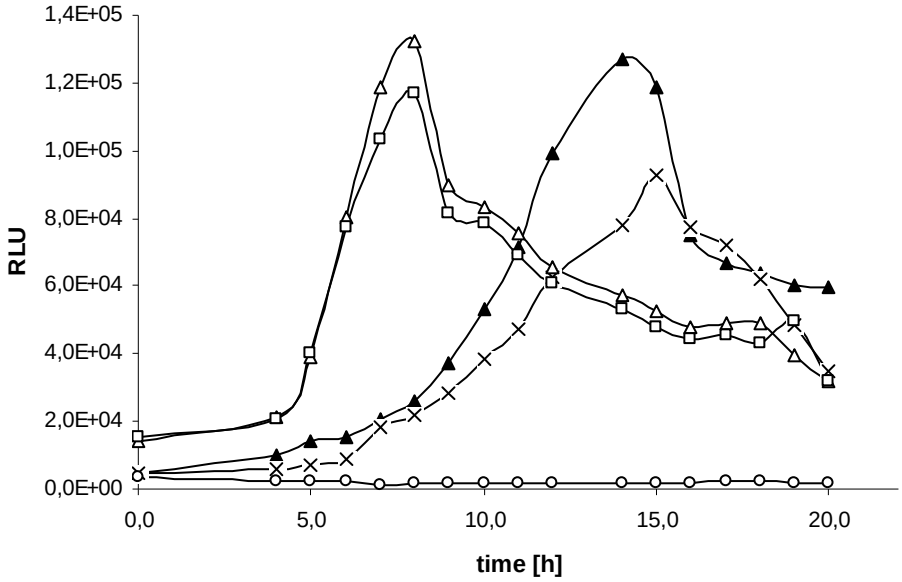

B

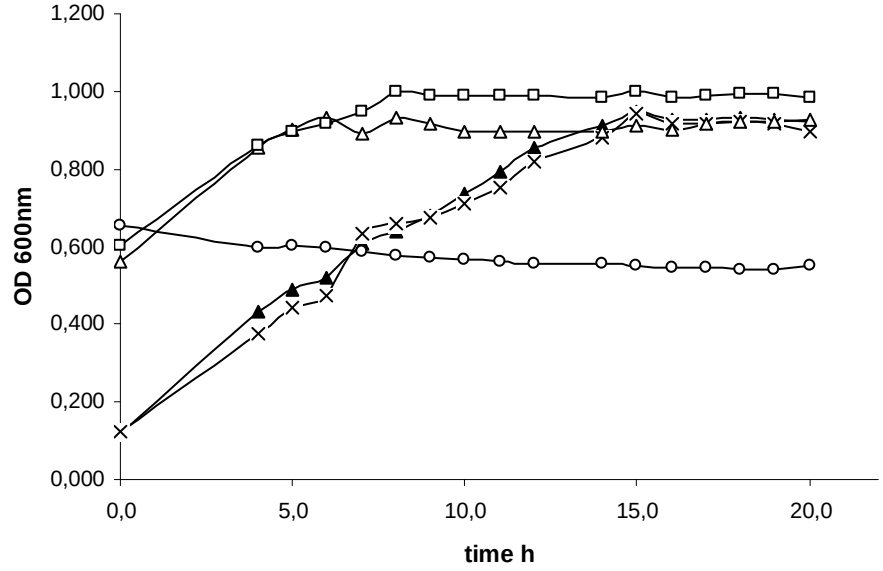

Figure 18. *ces* promoter activity (A) and growth (B) of *B. cereus* F48lux/Pces grown in LB media with 50µl additives: ▲ no additive; x additional LB; ∆ autoclaved cell sample of the emetic strain *B. cereus* F4810/72; □ autoclaved cell sample of the emetic-like strain *B. cereus* NVH1519/00; ○ autoclaved cell sample of the non-emetic strain *B. cereus* ATCC14579. *B. cereus* F48lux/Pces was grown in microtitre plates at 30℃, 500 rpm and luminescence is indicat ed as relative light units (RLU). Values are means of two to three independent experiments.

3.2 Functional analysis of *ces* locus genes

3.2.1 Role of the phosphopantetheinyl transferases CesP and Ppt on cereulide formation

The phosphopantetheinyl transferase gene c*esP* represents the first gene of the *ces* operon and lies directly downstream the main promoter of this gene cluster. Genes encoding PPTases are often found in association with peptide synthetase genes as the enzymes are crucial for the activation of NRPS. Therefore, it is possible that *cesP* is essential for cereulide synthesis. However, *in silico* analysis of the *B. cereus* F4010/72 genome revealed the presence of an additional putative 4'-phosphopantetheinyl transferase (locus tag: BCAH187_A2475; hereafter referred to as *ppt*) in the genome of *B. cereus* F4010/72. Comparison of the amino acid sequences of CesP and Ppt resulted in a rather low degree of homology (up to 26% identity and 47% similarity). Nevertheless, according to their size and sequence, both PPTases can be classified as typical members of the Sfp-like family (Figure 19).

```
Sfp             ------------MKIYGIYMDRPLSQEENERFMTFISPEKREKCRRFYHKEDAHRTLLGD 48
CesP            ---MKHIEHKNSIKIYAVELT-PITEKELSELYILISKERRLAVRKLLNQKDKIRSVIGE 56
Ppt             MIESKVVDSIPILNENDCQIWWGRISDLQSWHYNLLNDVEREKANSYHHSADRARFIIGC 60
                            ::     :     ..  .    ::.  .*   .   :. *  * ::*

Sfp             VLVRSVISRQYQLDKSDIRFS------TQEYGKPCIPDLPDAHFNISHSGRWVIGAFD-S 101
CesP            LLIRMVMHLVYR--KKNIIFA------RTREGKPYVKGEPFIHFNVSHAGDYILCAVA-S 107
Ppt             VISRLVLGKILSMSPVQVPIDRLCPVCKLQHGRPQLPEG-MPQLSVSHSGEWVVVAFTKS 119
                :: * *:         :: :         . *:* :      ::.:**:* ::: *.  *

Sfp             QPIGIDIEKTKPIS--LEIAKRFFSKTEYSDLLAKDKDEQTDYFYHLWSMKESFIKQEGK 159
CesP            HPVGVDVEKVKEIA--YEDIVHDCFTEQERQYIFQSISSPLHRFYEIWTLKESYVKCVGK 165
Ppt             APVGVDVEQMNPDVDVMKMVEGVLTDIEIAQVMKLPNEQKIEGFLTYWTRKEAVLKATGE 179
                 *:*:*:*: :      :         :  : :    ..  . *   *: **: :*  *:

Sfp             GLSLPLDSFSVRLHQDGQVSIELPDSH---SPCYIKTYEVDPGYKMAVCAAHPDFPEDIT 216
CesP            GLSIPLDSFTCVIGDG--IKVIGKDVH---EEYTCQQISIHPNYKVAVCSPQKNDKNIIL 220
Ppt             GLMIPPVDITISAPNDPPNLLVFKDRQELVENTVMRDLRPSIDYIASIAICSKEVT-EII 238
                ** :*  .::    :.    :   * :   .    :      .*  ::.    :    *

Sfp             MVSYEELL---------------------- 224
CesP            RITQEEIISYLQGILGMSPVCRLTDNLMDES 251
Ppt             QLDAVALLNYK------------------- 249
                 :    ::
```

Figure 19. Sequence alignment of the PPTase CesP with Ppt (locus tag: BCAH187_A2475) of *B. cereus* F4810/72 (26% identity, 47% similarity) and Sfp from *B. subtilis* (32% identity, 56% similarity). Conserved motifs of the "Sfp-like" PPTase group are highlighted.

Transcriptional analysis of both genes was accomplished by RT-qPCR in order to study the relative *cesP* and *ppt* gene expression in the growth cycle of *B. cereus*

F4810/72. Transcription of *cesP* and *ppt* turned out to be significantly different (Figure 20). Transcript levels of *cesP*, which belong to the polycistronic *ces* transcript, peaked in mid-log phase and decreased strongly in stationary phase. In contrast, relative *ppt* expression was very weak throughout growth and showed only a slight increase in stationary phase.

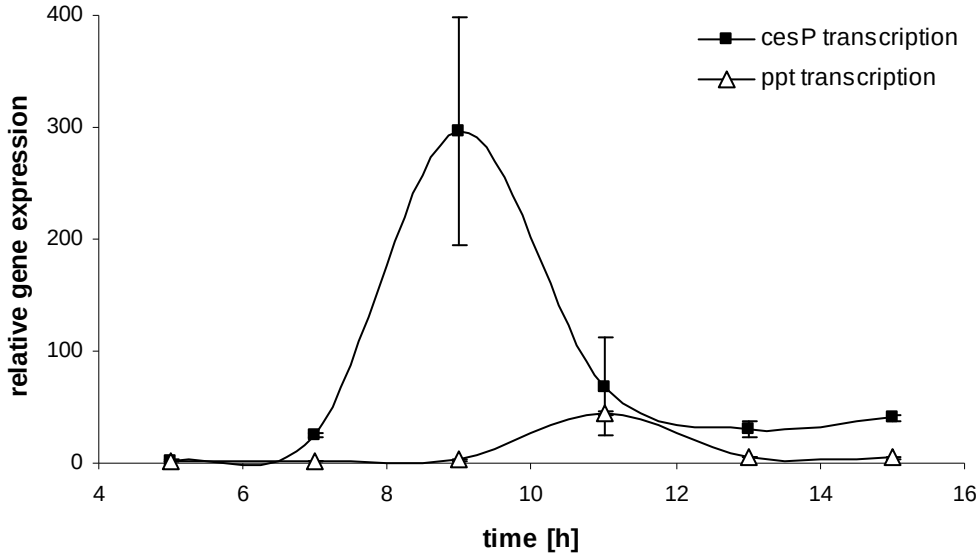

Figure 20. Relative *cesP* and *ppt* gene expression in *B. cereus* F4810/72 during growth at 30℃ in LB media. Values represent means and error bars standard deviations of two independent data sets that were normalized to *rrn* transcript levels.

To investigate the possible role of the PPTases CesP and Ppt on cereulide production, mutant strains of *B. cereus* F4010/72 were constructed. A *cesP* deletion mutant of *B. cereus* F4010/72, F48ΔcesP, was obtained by heterogramic conjugation using a non-polar spectinomycin resistance cassette, which is preceded by a translation stop codon, a ribosome-binding site and a start codon. In order to test the involvement of Ppt in cereulide synthesis, a *ppt* insertion mutant was gained. The cytotoxic potential of both mutants was determined using the HEp-2 cell bioassay. The *cesP* null mutant showed a similar toxicity level as the parental strain, indicating a CesP independent cereulide synthesis (Figure 21). As expected, also the *ppt* insertion mutant was cytotoxic towards HEp-2 cells. However, when *ppt* was disrupted in F48ΔcesP, leading to a *cesP/ppt* double mutant, a completely non toxic phenotype was displayed, suggesting a redundant effect of these two PPTases in toxin production (Figure 21).

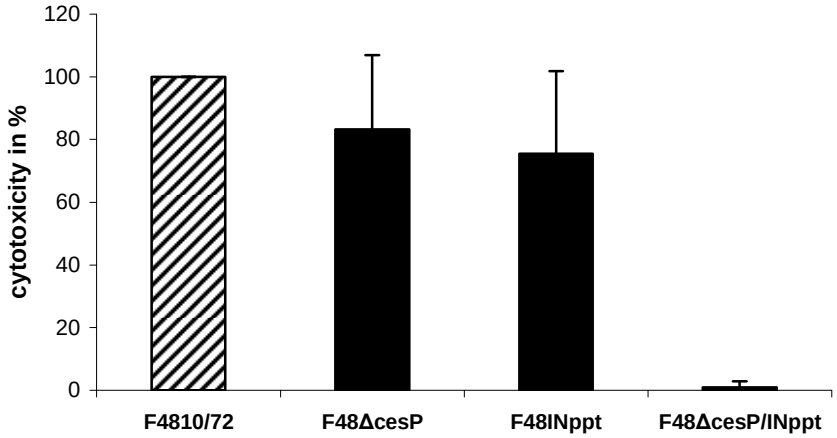

Figure 21. Cereulide production of *B. cereus* wild type and PPTase deficient strains, as determined by the HEp-2 bioassay. The strains (*cesP* knockout mutant F48ΔcesP, the *ppt* insertion mutant F48INppt and the double mutant F48ΔcesP/INppt) were grown in LB media for 24 h at 30℃ or 37℃ (for insertion mutants) before autoclaving. The cytotoxicity of the wild type was set to 100%. Values are means and error bars standard deviations of three independent experiments.

3.2.2 Cereulide production of *cesH*- and *cesCD* deficient mutants

The cereulide synthetase gene locus harbours besides the typical nonribosomal peptide synthetase genes (*cesA, cesB, cesP* and *cesT)*, genes encoding for a putative hydrolase (*cesH*) and an ABC transporter (*cesCD*) (see Figure 1). To investigate the potential impact of these adjacent genes on cereulide synthesis, appropriate gene inactivation mutants of *B. cereus* F4010/72 were constructed (F48INcesH, F48INcesC and F48INcesD) and tested towards their cytotoxicity. For CesH no direct correlation between this putative hydrolase / acetlytransferase and cereulide production was found, given that the *cesH* insertion mutant exhibited the same cytotoxicity as the wild type strain (Figure 22). Interestingly, the opposite effect was obtained for *cesC* and *cesD*, which are located at the 3' terminus of the *ces* operon and code for a putative ABC transporter protein and a permease, respectively. Both insertion mutants were entirely non toxic in the HEp-2 cell assay (Figure 22). For further studies a stable deletion mutant was constructed, lacking both *cesC* and *cesD* (F48ΔcesCD) and revealing a toxin deficient phenotype (data not shown). The toxicity of this strain could be restored to some extend by *in trans* complementation with the shuttle vector pAD123/cesCD/Pces*,* containing the

complete *cesC* and *cesD* genes under the control of the *ces* promoter (Figure 22). These results indicate that the putative ABC transporter genes *cesC* and *cesD* may be essential for cereulide formation in *B. cereus* F4872/10.

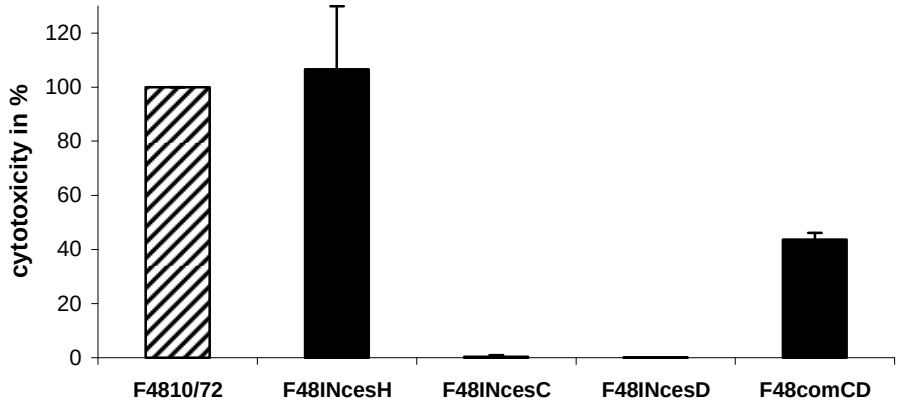

Figure 22. Cereulide production of *B. cereus* wild type and *ces* mutant strains, as determined by the HEp-2 bioassay. The strains (insertion mutants of *cesH, cesC* and *cesD* and the complemented strain F48comCD) were grown in LB media for 24 h at 30℃ or 37℃ (for insertion mutants) before autoclaving. The cytotoxicity of the wild type was set to 100%. Values are means and error bars standard deviations of three independent experiments.

3.2.3 Transcription of *cesA* in *B. cereus ces* mutant strains

To test whether the different cytotoxicity profiles of the *ces* mutants correlate with transcription levels of the structural peptide synthetase gene *cesA*, quantitative RT-PCR was carried out. *B. cereus* strains were grown in LB at 37℃ and 150 rpm until mid-log phase, in which samples for RNA isolation and reverse transcription were taken. As expected the toxic *cesH* mutant displayed a comparable *cesA* transcript level as the wild type. However, also the non toxic mutants concerning *cesP/ppt* and *cesCD* showed similar *cesA* transcription and could not be significantly distinguished from the parental strain (Figure 23). These data hint that the PPTases CesP and Ppt as well as the ABC transporter components CesC and CesD are not necessary for the transcription of the cereulide synthetase genes, but seem to play an important role in the formation of active cereulide.

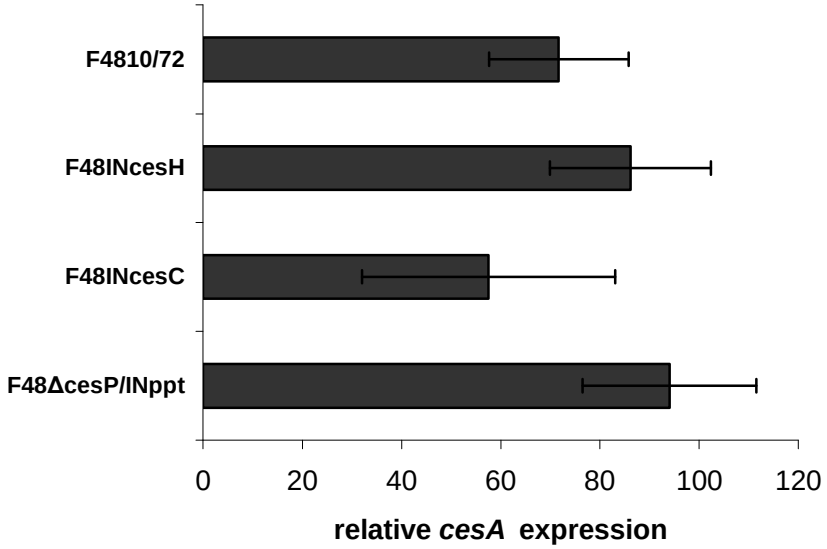

Figure 23. RT-qPCR analysis of *cesA* in *B. cereus* F4810/72 and the insertion mutants F48INcesH, F48INcesC and F48ΔcesP/ppt. Strains were incubated in LB media at 37°C until the mid-log phase (OD_{600nm}10) before sampling for RNA isolation. Values represent means and error bars standard deviations of two independent data sets that were normalized to *rrn* transcript levels.

3.2.4 *In silico* analysis of CesCD

Since the ATP-binding domain and the transmembrane domain of the cesCD transporter are encoded by separate genes, this putative transporter does not present a fused ABC system of class 1 (Dassa & Bouige, 2001), but seems to belong to the third class (ABCA subfamily), presenting mainly importers and members with diverse functions. *In silico* analysis of the amino acid sequence of CesD showed homology (33% identity and 61% similarity) to the permease components of ABC transporter present in many *B. cereus* group members. Furthermore PSORTb predicted CesD to be a membrane-spanning protein due to its six hydrophobic internal helices. For CesC no transmembrane region was found in its amino acid sequence, instead the protein possesses a conserved ATPase domain consisting of characteristic ABC modules such as the Walker A and B motifs and the linker peptide. Sequence analysis of CesC demonstrated highest similarity (up to 49% identity and 74% similarity) to ATP-binding proteins of several *Bacillus* species, which are all orthologs of the BerA transporter of *B. thuringiensis*. Other characterized proteins homologous to CesC are the ABC transporter TnrB2 of *Streptomyces longisporoflavus* and BcrA of *Bacillus licheniformis (*Figure 24). According to the

ABCISSE database (http://www1.pasteur.fr/recherche/unites/pmtg/abc/database.iphtml), which provides a phylogenetic and functional classification of ABC systems, these proteins are all member of the DRI (drug resistance and immunity) family. Therefore, it is likely that CesC also belongs to this subcategory of ABC systems. Members of this family are often associated with the transport and self resistance of peptide toxins, thus, it is possible that CesCD may play a role in the transport of cereulide.

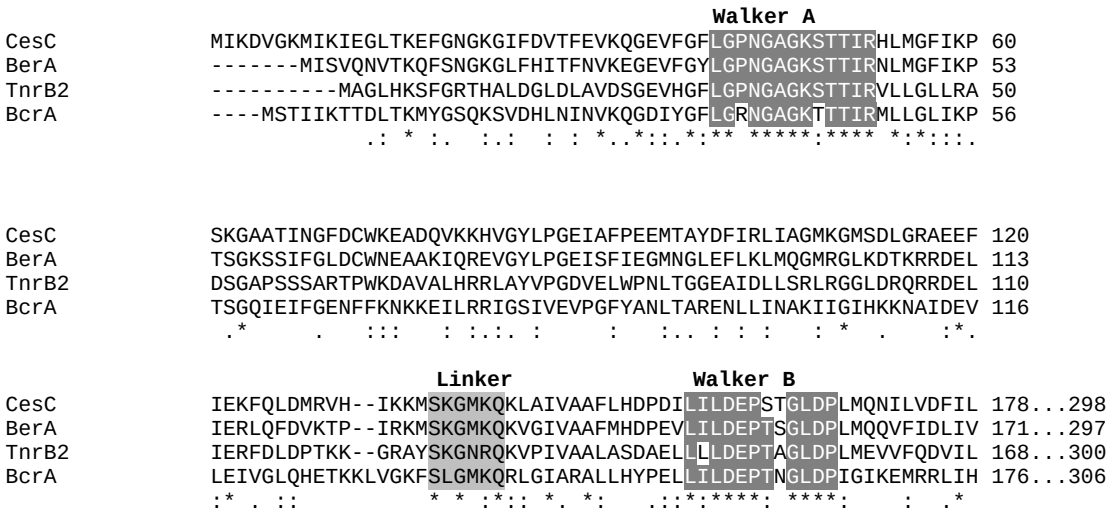

Figure 24. Alignment of the CesC amino acid sequence with the following homologous ABC transporter proteins: BerA of *B. thuringiensis* (48% identity, 74% similarity), TnrB2 of *S. longisporoflavus* (33% identity, 55% similarity) and BcrA of *B. licheniformis* (31% identity, 52% similarity). The nucleotide-binding motifs are highlighted.

3.2.5 Localization of cereulide in vegetative cells

For further investigation of the potential transport function of CesCD, the localization of cereulide was analysed. So far high toxin amounts were detected by the HEp-2 assay only in autoclaved cell culture samples, which do not provide any information about the localization of cereulide. Thus, *B. cereus* F4810/72 cells were grown for 14 h and harvested before the initiation of sporulation. Filtered culture supernatant and cell pellets, which were treated with both PBS and 100% ethanol for cereulide extraction, were tested in the HEp-2 assay. It turned out that hardly any cereulide could be detected in the secretome fraction, while high toxin amounts were present in the cell pellet extracted with ethanol (Table 5). However, the cell pellet treated with

PBS revealed no toxicity either, indicating that the hydrophobic cereulide is not extractable with aqueous solutions. Therefore, cell supernatant and PBS-sample of the cell pellet were further extracted using hexane as solvent. Obtained hexane extracts were tested on HEp-2 cells, revealing a tenfold higher toxicity level in the cell pellet fraction compared to the secretome fraction. The next step was the rough division of vegetative cells into membrane- and cytosolic fractions, which was achieved by cell lysis and ultracentrifugation. As expected, when treated with PBS both fractions revealed no toxicity in the HEp-2 assay. However, when PBS-samples were further extracted with hexane an almost fivefold higher cereulide amount could be detected in the membrane fraction in comparison to the cytosolic fraction (Table 5). These data suggest that cereulide is preferentially detectable in the proximity of the cell membrane. When the same experiments were performed with the *cesCD* deletion mutant strain almost no toxicity was measured regardless of the cell fraction (data not shown).

Table 5. Distribution of cereulide in cell fractions of *B. cereus* F4810/72. Values are means of two independent experiments.

Cell component	Extraction buffer	Cereulide titre (µg/ml)[a]
complete cells	100% ethanol	118.9 ± 29.7
complete cells	PBS	ND[b]
complete cells	hexane	25.1 ± 2.8
secretome fraction	pure supernatant	1.4 ± 0.7
secretome fraction	hexane	2.4 ± 1.7
membrane fraction after cell lysis	PBS	ND[b]
membrane fraction after cell lysis	hexane	18.3 ± 4.2
cytosolic fraction after cell lysis	PBS	ND[b]
cytosolic fraction after cell lysis	hexane	3.8 ± 2.1

[a] determined as valinomycin equivalents by the HEp-2 bioassay

[b] ND = none detected

In order to test if cereulide is located on the cell surface, further experiments, in which vegetative cells were incubated shortly in PBS buffer containing different percentage of ethanol, were conducted. Determination of cell count of each sample revealed that the cell treatment with varied ethanol amounts for 10 min hardly

influenced the cell viability (Table 6), while longer incubation is known to have a strong antibacterial effect on vegetative cells. On the other hand, HEp-2 data showed that efficient cereulide extraction was possible with buffer containing at least 50% ethanol, even if the incubation time was that short. Interestingly, when 70% ethanol was used the cereulide titre was highest, whereas the cell recovery rate was lowest, indicating that this concentration has the greatest influence on the vegetative cells. In summary, these results demonstrate that cereulide may be associated to the outer membrane or cell surface, since it is easily extracted from vegetative cells, without completely disrupting the membrane.

Table 6. Viability and cereulide extraction of vegetative *B. cereus* cells after 10 min incubation in PBS buffers with different ethanol amounts. Values are means of two independent experiments.

Extraction buffer	Cereulide titre (µg/ml)[a]	Cell count
PBS	0	2.7×10^7
10% ethanol	0	1.7×10^7
30% ethanol	0.4 ± 0.1	2.3×10^7
50% ethanol	128.9 ± 8.7	2.1×10^7
70% ethanol	169.4 ± 15.0	1.4×10^7
100% ethanol	126.2 ± 12.5	2.6×10^7

[a] determined as valinomycin equivalents by the HEp-2 bioassay

3.3 Characterization of the megaplasmid pBCE

3.3.1 Plasmid curing of *B. cereus* F4810/72

The 270 kb plasmid pBCE contains besides the seven *ces* genes 243 open reading frames, which encode mainly hypothetical proteins (Rasko *et al.*, 2007). In order to further characterize the emetic strain F4810/72 the whole megaplasmid was functionally analysed. Thus, the parental strain was cultured in LB and passaged daily for five weeks at high temperature (42℃) to promote the loss of its megaplasmid. After plating dilutions of this culture on LB agar, grown colonies were screened for the presence of plasmid DNA by PCR. Therefor different pBCE-specific oligonucleotides were used including primers against the *ces* genes (800F2/R2), against the plasmid replication protein RepX (pXO1-RepX-for/rev) and other conserved domains of pXO1-like plasmids (pCons_for/rev). Colonies which turned out to be negative for all tested plasmid PCR products were further characterized in respect to their growth and sporulation properties. The cured strains were all able to grow in LB, indicating that pBCE is not essential for vegetative cell growth. Surprisingly, growth on MYP agar revealed phenotypic differences between colonies. While some clones (designated F48ΔpBCEI) grew comparable to the wild type, others appeared darker and shiny on MYP (designated F48ΔpBCEII), similar to non sporulating mutant strains, for example F48Δspo0A (Figure 25). As observed by phase contrast microscopy, these darker clones were not able to sporulate, whereas the other colonies sporulated normally. The reason for the non sporulating phenotype remains unclear, but may be due to the loss or inactivation of additional genes or whole plasmids in this strain variant.

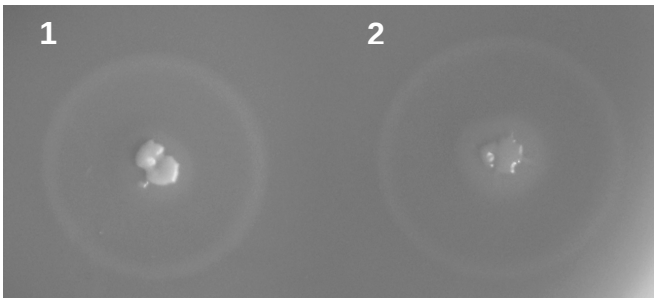

Figure 25. Colony morphology of *B. cereus* F48ΔpBCEI (1) and F48ΔpBCEII (2) grown on MYP agar for 24 h at 30℃.

3.3.2 Proteomic analysis of *B. cereus* mutants lacking pBCE

As expected the plasmid cured strain F48ΔpBCEI showed no toxicity when tested on HEp-2 cells (data not shown). For further characterization of this strain on proteomic level, two dimensional gel electrophoresis was accomplished. Cells were grown until mid-log phase and both cytosolic and secreted protein fractions were extracted. Comparison of the protein patterns from the wild type and the ΔpBCE mutant resulted in a large number of differentially expressed protein spots (Figure 26). Especially the secretome showed significant differences, mainly in the number of absent or decreased proteins in ΔpBCE. Computer assisted image analysis detected over 80 proteins to be differentially expressed in the secretome of the plasmid cured strain compared to the parental strain, whereas around 40 regulated proteins were found in the cytosolic fraction (Table 7). This result demonstrates that several proteins located on the megaplasmid pBCE may be either secreted or regulate other secreted proteins. In addition to the plasmid cured strain, a mutant containing pBCE with a disrupted *ces* gene locus (F48Δces) was investigated. 2D gel electrophoresis showed very similar protein pattern of F48Δces and the wild type (data not shown), and image analysis only revealed few proteins to be differentially expressed in these two strains (Table 7). Hence, the great influence of the megaplasmid pBCE on the secretome seems to be mainly independent of the *ces* gene cluster the plasmid harbours.

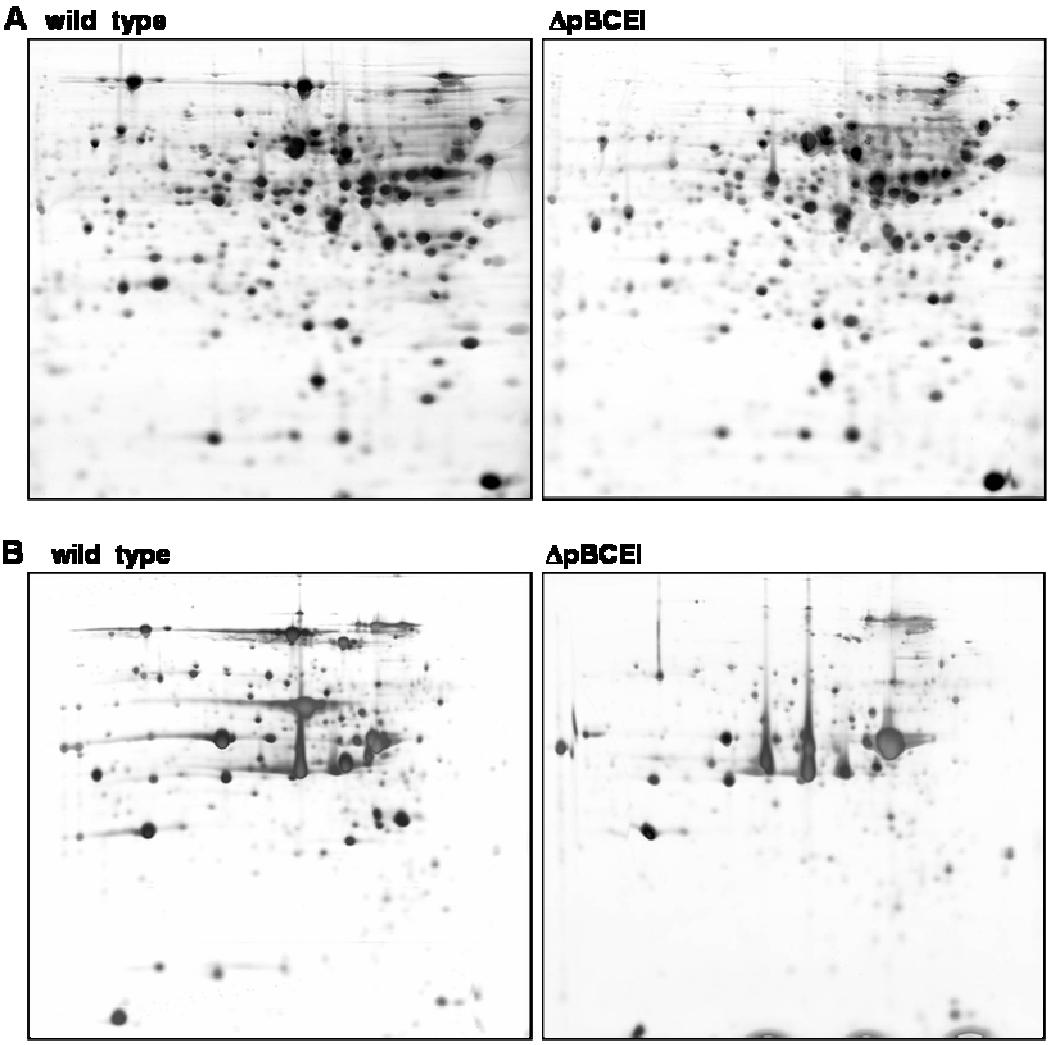

Figure 26. 2D gel electrophoresis of cytosolic (A) and secreted (B) protein fractions of *B. cereus* F4810/72 and its plasmid cured derivative F48ΔpBCEI. Electrophoresis was performed with immobilized pH gradient 4-7 in the first dimension and run on SDS-PAGE using the Dalt unit. Gels display representative protein pattern of three independent experiments.

Table 7. Number of regulated proteins of the plasmid cured strain ΔpBCEI and the Δces mutant in comparison to the wild type. Computer assisted image analysis was performed with the Proteomweaver 2D software. A spot was considered to be differentially expressed if there was a threefold or more change in spot volume.

	F48ΔpBCEI		**F48Δces**	
	cytosolic proteins	secretome	cytosolic proteins	secretome
Number of new and increased proteins	7	21	6	9
Number of absent and decreased proteins	36	60	4	7

3.3.3 Biofilm studies

Since *B. cereus* is known to produce biofilm in a very strain specific manner (Wijman *et al.*, 2007), this property was investigated for *B. cereus* F4810/72 and its plasmid cured mutants. A microtitre plate assay was established for rapid detection and quantification of biofilm production. Several growth conditions such as media, incubation time and modality were tested for optimal biofilm formation. Comparison between the media EPS (Hsueh *et al.*, 2006) and LB-biofilm (Auger *et al.*, 2006) showed that although EPS supported biofilm production of the *B. cereus* type strain ATCC14579, the emetic reference strain *B. cereus* F4810/72 formed sufficient biofilm only in the LB-based medium (data not shown). Best growth conditions for biofilm formation turned out to be incubation at 350 rpm for 48 h at 30℃ with one exchange of medium after 24 h.

Biofilm production was tested for several mutant strains of F4810/72 including the plasmid cured strains F48ΔpBCEI and F48ΔpBCEII as well as the deletion mutants of *plcR, spo0A* and *ces.* The microtitre plate assay revealed that the ability to produce biofilms varied strongly among these strains (Figure 27). While the ΔplcR mutant developed slightly more biofilm than the wild type strain, a strong decrease in biofilm formation was observed for the Δspo0A mutant. However, the biofilm defect of the *spo0A* mutant was suppressed in the *abrB/spo0A* double mutant, indicating that AbrB negatively regulates the development of a mature biofilm. The ability of the plasmid cured strains to form biofilms was also strongly affected. Especially the non sporulating strain F48ΔpBCEII showed almost no biofilm production, but also the sporulating strain F48ΔpBCEI formed significantly less biofilm than the wild type strain harbouring pBCE. These results suggest a possible role of the megaplasmid pBCE in biofilm formation. That this effect is independent of the *ces* gene locus was observed with the F48Δces mutant, which was able to form biofilms similar to the wild type strain (Figure 27).

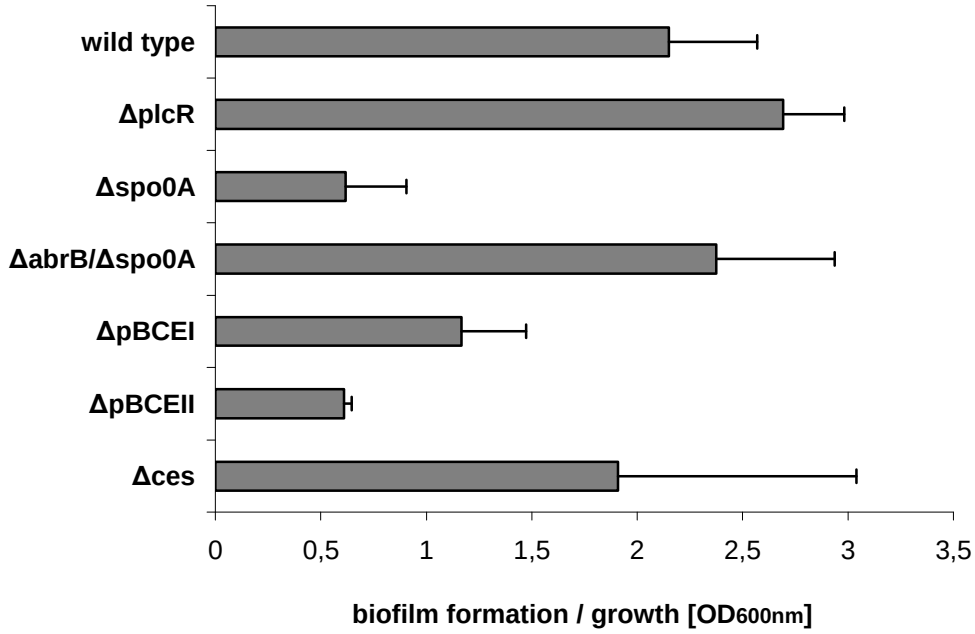

Figure 27. Biofilm formation of *B. cereus* F4810/72 and its mutant strains lacking *plcR, spo0A, abrB,* the plasmid pBCE or the *ces* locus. Cells were grown in microtitre plates for 48h at 30℃ and 350 rpm before total growth and biofilm formation was measured as $OD_{600nm.}$ The data represent means and standard deviations of each 8 wells from two independent experiments.

4 DISCUSSION

4.1 Regulation of cereulide expression in *B. cereus* is complex

4.1.1 Cereulide synthesis depends on Spo0A-AbrB regulon, but not on PlcR

The emetic toxin accumulates during the growth of *B. cereus*, reaching high levels in late stationary phase. However the transcription of the peptide synthetase genes responsible for cereulide production was shown to be strictly growth phase dependent (Dommel, 2008), suggesting the involvement of regulatory processes in cereulide expression. To investigate this hypothesis key transcription factors, such as the *B. cereus* specific virulence gene regulator PlcR and the global sporulation regulator Spo0A, were tested with respect to cereulide expression. Data presented in this work demonstrate that the pleiotropic regulator PlcR does not affect cereulide synthesis, as the *plcR* null mutant was cytotoxic and revealed high transcript levels of the cereulide synthetase gene *cesA* (Figure 5 and Figure 6). Furthermore, no highly conserved palindromic sequence, presenting a PlcR box (Agaisse *et al.*, 1999), could be found in the promoter region of the cereulide synthetase gene operon. Hence PlcR, which has been shown to activate most of the extracellular virulence factors in *B. cereus* and *B. thuringiensis* (Agaisse *et al.*, 1999; Gohar *et al.*, 2002), is not involved in cereulide formation of emetic *B. cereus*. In contrast, the master response regulator Spo0A was shown to play an important role in the expression of the emetic toxin, as the *spo0A* null mutant resulted in a toxin deficient phenotype (Figure 5). The *spo0A* gene has two known promoters, which are recognized by the housekeeping sigma factor σ^A and the alternative sigma factor σ^H, respectively (Chibazakura *et al.*, 1991). Complementation of the *B. cereus spo0A* null mutant with *spo0A* plus its two promoters revealed that cereulide production mainly depends on σ^A-induced *spo0A* expression (Figure 7). As it was shown that the σ^A-dependent promoter of *spo0A* is expressed during vegetative growth (Chibazakura *et al.*, 1991), while the stronger σ^H-dependent promoter is induced during the initial stages of sporulation (Predich *et al.*, 1992), the regulation of cereulide expression seems to occur early in the growth cycle. However, a direct activation of *ces* expression by Spo0A is unlikely, since the promoter region of the *ces* gene cluster lacks a typical “0A box” of the type

TGTCGAA (Strauch *et al.*, 1990). One of the first functions of Spo0A is the repression of the transcription factor AbrB, which is achieved by low levels of phosphorylated Spo0A (Jiang *et al.*, 2000; Trach & Hoch, 1993). In *B. subtilis* AbrB plays an important role in controlling gene expression by acting as a repressor, preventer or even activator of many stationary phase specific genes (Strauch & Hoch, 1993). It has been shown that *abrB* transcription is highly growth phase dependent, reaching a maximum during the transition from lag-phase to exponential growth and becoming undetectable in mid-exponential phase due to repression by Spo0A~P. (O'Reilly & Devine, 1997). Results presented here indicate that AbrB of *B. cereus*, which is 85% identical to the corresponding protein of *B. subtilis*, is regulated similarly, showing a strict growth cycle dependent expression and negative regulation by Spo0A (Figure 8). Analysing cereulide synthesis, an *abrB* overexpressing strain was found to be non toxic, while *ces* expression of an *abrB* null mutant was enhanced in early exponential phase (Figure 9 and Figure 10). Furthermore, the toxin deficiency of the *spo0A* null mutant was largely suppressed by additionally deleting *abrB*. Thus, it appears that the major role of Spo0A in cereulide production is its negative regulation of *abrB*. As AbrB possesses a unique DNA-binding specificity and recognizes three-dimensional DNA structures rather than an apparent consensus sequence, it is difficult to predict its target genes (Strauch *et al.*, 1989b; Xu & Strauch, 1996). However, *in vitro* DNA-binding studies showed that AbrB binds efficiently to the *ces* promoter region (Figure 12 and Figure 13), confirming its possible role as a direct repressor of the cereulide peptide synthetase operon. Also the synthesis of other peptide antibiotics, like the nonribosomally synthesized tyrocidine from *Bacillus brevis* or the bacteriocin subtilosin from *B. subtilis*, have been reported to be regulated by AbrB in a similar manner as cereulide (Marahiel *et al.*, 1987; Zheng *et al.*, 1999).

B. cereus F4810/72 harbours besides the chromosomal *abrB* gene an *abrB*-like gene, which is located on the plasmid pBCE. This paralog was also found on the megaplasmid of *B. cereus* ATCC10987 and on pXO1 of *B. anthracis* (Rasko *et al.*, 2004; Saile & Koehler, 2002). While the pXO1 copy of *abrB* in *B. anthracis* is truncated and thus probably non-functional, this is not the case for the pBCE-encoded *abrB** of *B. cereus* F4810/72. However, the AbrB* overexpressing strain generated a similar toxicity level as the wild type and no binding of AbrB* to the *ces*

promoter region could be detected *in vitro* (Figure 9 and Figure 12), suggesting a minor role of this protein in the regulation of cereulide synthesis.

Two additional interesting findings were made by studying the effect of the Spo0A-AbrB regulon on cereulide synthesis. First, the toxic but non sporulating double mutant F48ΔabrBΔspo0A indicates that emetic toxin production, though being regulated by Spo0A, is completely independent of later sporulation processes and does not require full sporulation. Secondly, *ces* promoter studies revealed that *ces* expression is strictly growth phase dependent and decreases strongly in stationary phase even in the *abrB* null mutant (Figure 10). This suggests that there are AbrB-independent modes of control possibly linked to environmental conditions and nutrient availability as well as cell density and spore-, competence- or biofilm development that play a role in *ces* gene expression and inhibit cereulide formation in later growth phases.

4.1.2 Role of the alternative sigma factor σ^H and the regulatory factors CodY and CcpA

Besides PlcR, Spo0A and AbrB three additional transcription factors, namely σ^H, CodY and CcpA, were tested with respect to their potential effect on cereulide production. These regulators have all been mentioned in connection with virulence gene expression in *Bacillus* species before. The sporulation sigma factor σ^H, which presents a target of the AbrB repressor, plays an important role in sporulation and postexponential phase gene expression (Britton *et al.*, 2002; Weir *et al.*, 1991). Moreover, σ^H was reported to be involved in toxin expression of *B. anthracis* by activating the virulence gene regulator AtxA in an AbrB-independent manner (Hadjifrangiskou *et al.*, 2007). However, recent work of Bongiorni *et al.* did not support a direct role of σ^H in *atxA* expression (Bongiorni *et al.*, 2008). Likewise, our investigations showed no distinct correlation between σ^H and cereulide expression (Figure 15) and *in silico* analysis did not reveal a consensus sequence, which is recognized by the σ^H RNA polymerase, in the promoter region of the *ces* gene cluster. These data suggest that σ^H is not directly linked to *ces* gene regulation. Nevertheless, a slight decrease of cytotoxicity was obtained in a *sigH* insertion

mutant, which is probably due to the regulatory feedback mechanism that connects σ^H, AbrB and Spo0A.

The catabolite control protein CcpA is a well studied transcription factor of Gram-positive bacteria that regulates the efficiency of glucose metabolism by binding to specific CRE-sites of its target genes (Stulke & Hillen, 2000). Recent studies revealed that CcpA-induced catabolite repression also influences the enterotoxin expression of *B. cereus* ATCC14579 and putative CRE-sites were identified for the *hbl*- and *nhe*- operon (Ouhib *et al.*, 2006; van der Voort *et al.*, 2008). Thus, glucose sensing by CcpA was shown to provide an additional control mechanism besides PlcR to regulate enterotoxin expression of *B. cereus (van der Voort et al., 2008)*. Data presented here revealed no direct relation between CcpA and cereulide production (Figure 15). The *ccpA* insertion mutant was almost as toxic as the wild type and no specific CRE-site could be detected in the *cesP* promoter region. However, the addition of glucose, which induces CcpA-mediated catabolite repression, led to a non-toxic phenotype for both the *ccpA* mutant and the parental strain (data not shown). This suggests that under these growth conditions (2% glucose, 37℃, 150 rpm) glucose might cause the repression of cereulide synthesis indirectly and independently of CcpA.

In contrast to σ^H and CcpA, the transcription factor CodY seems to be involved in cereulide production, since the *codY* insertion mutant displayed an almost non-toxic phenotype (Figure 15). The global regulator CodY is a metabolite-sensing protein that generally acts as a repressor of early stationary phase genes (Ratnayake-Lecamwasam *et al.*, 2001). In *B. subtilis* CodY was shown to control over 100 genes, the products of which are mainly involved in the adaptation of the cell to nutrient limitation and metabolic stress (Molle *et al.*, 2003b). In addition, virulence gene expression was found to be repressed by CodY in several pathogenic Gram-positive bacteria, for example *Clostridium difficile* and *Staphylococcus aureus* (Dineen *et al.*, 2007; Majerczyk *et al.*, 2008). Another direct target of CodY is the *ilvB* operon, which encodes enzymes for the biosynthesis of branched-chain amino acids (Shivers & Sonenshein, 2004). As these amino acids are most likely important precursors of the cereulide peptide, it is surprising that CodY seems to have an activating effect on cereulide synthesis. However, recent studies in *Listeria monocytogenes* and

B. anthracis suggest that CodY influences toxin gene expression in a complex manner and may also act as a positive regulator besides being a repressor (Bennett *et al.*, 2007; Sonenshein, 2007). For instance, in *B. anthracis* CodY was found to bind to the *atxA* promoter region and seems to be essential for the synthesis of toxin proteins (Fouet & Mock, 2006). Preliminary experiments of this work indicate that CodY may present an additional regulator of *B. cereus* F4810/72 that directly or indirectly influences the production of cereulide. However, further studies will be necessary to elucidate the putative role of CodY in *ces* regulation using stable deletion and complementation mutants instead of the insertion mutant strains.

In *Bacillus* species several biosynthesis genes of peptide antibiotics have been identified, which are controlled by the interaction of multiple regulators. For example, the expression of surfactin and subtilisin in *B. subtilis* is controlled by several regulatory mechanisms involving diverse factors such as AbrB, DegU, ComA, Hpr, Sin, CodY or Spo0A (Marahiel *et al.*, 1993; Sanchez & Olmos, 2004). Especially transition state regulators play a crucial role in post-exponential gene expression by controlling targets in a redundant manner (Strauch & Hoch, 1993). Moreover, in *B. anthracis* the virulence gene regulator AtxA has been shown to be involved in a complex regulatory network connecting plasmid and chromosome gene expression (Fouet & Mock, 2006; Perego & Hoch, 2008). Obviously, similar regulatory pathways exist in *B. cereus* and the regulation of the *ces* genes may be another example for cross-regulatory interaction of chromosomally- and plasmid-encoded genes. A preliminary scheme of the regulatory network involved in cereulide synthesis is presented in figure 28.

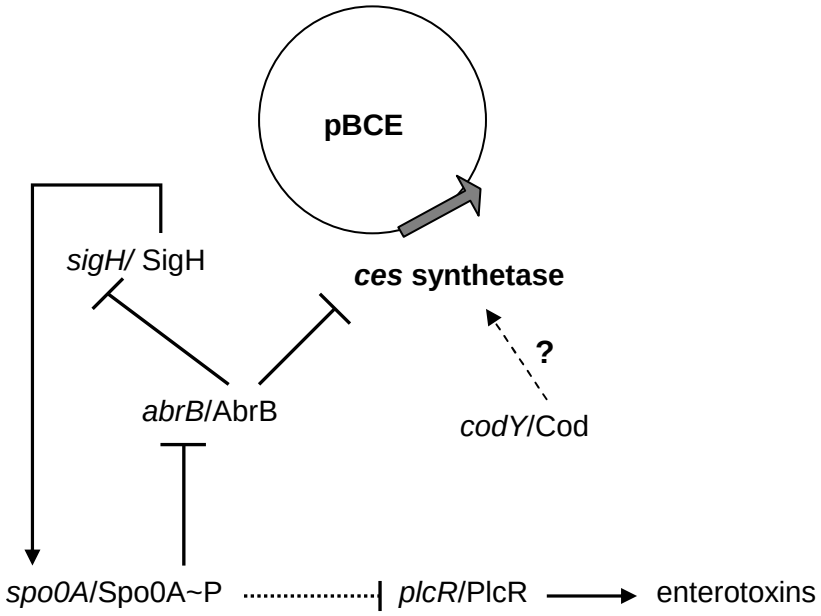

Figure 28. Tentative scheme of the regulatory network involved in cereulide synthesis.

4.1.3 Effect of glucose and other extrinsic factors influencing cereulide production

While so far nothing was reported about intrinsic regulatory factors, several environmental factors such as oxygen, pH, temperature and growth media supplements have been shown to greatly influence cereulide formation (Apetroaie-Constantin *et al.*, 2008; Dommel, 2008; Finlay *et al.*, 2000; Jaaskelainen *et al.*, 2004). Here the impact of LB media supplemented with 2% glucose on cereulide production and *ces* transcription was investigated. It is known that sporulation is blocked under these conditions due to the repression of *spo0A* transcription (Chibazakura *et al.*, 1991; Yamashita *et al.*, 1989). The addition of 2% glucose in LB media resulted in delayed, but higher cereulide production, although growth rates were identical to growth without glucose (Figure 16). The larger toxin amounts may be due to a global increase of RNA- and protein rates in the presence of glucose. Furthermore, the *ilvB* operon encoding for biosynthesis enzymes for branched-chain amino acids, which are probably essential precursors of cereulide, is known to be upregulated by CcpA in response to glucose in *B. subtilis* (Shivers & Sonenshein, 2005). However, measurement of the *ces* promoter activity with glucose excess revealed highest cereulide synthetase expression not until late stationary phase, indicating a glucose dependent repression of cereulide expression in exponential growth phase (Figure

17). These data were also confirmed by previous transcription analysis using RT-qPCR, presenting downregulated *ces* transcript levels in the exponential growth phase (Dommel, 2008). In *B. subtilis* it was shown that a regulatory network of CcpA, TCA cycle enzymes and ScoC is responsible for the glucose-induced catabolite repression of *spo0A* and other sporulation specific genes (Ireton *et al.*, 1995; Shafikhani *et al.*, 2003). Since it was observed that cereulide production depends strongly on *spo0A* transcription, toxin synthesis may be inhibited indirectly by catabolite repression in the early growth phase. As soon as the *spo0A*-repressing effect ceases, cereulide formation might be enhanced due to the positive effect of glucose on amino acid or protein synthesis. Another explanation for the higher toxin amounts in late stationary phase could be that the presence of glucose may provide a longer time period for *ces* expression due to the delay of sporulation. In comparison to other *Bacillus* strains, *B. cereus* F4810/72 starts the sporulation process very early in its growth cycle and is already fully sporulated a few hours after the entry into the stationary growth phase. This may be the reason why *ces* expression is strongly downregulated at this time point. Interestingly, in *B. anthracis* premature sporulation seems to be inhibited by mutated sensor histidine kinases and a plasmid-encoded Rap phosphatase in order to favour toxin production and multiplication in the host (Bongiorni *et al.*, 2006; Brunsing *et al.*, 2005).

Under other growth conditions the repressing effect of glucose on cereulide production was even more striking and no activation was observed. For example, when cells were grown with 2% glucose in microtitre plates, where oxygen supply is restricted, *ces* expression was nearly completely repressed (Figure 17). These glucose and/or oxygen effects were independent of AbrB regulation, as they were also seen for the *abrB* null- and *abrB/spo0A* double mutant (data not shown). Moreover, when strains were grown at 37℃ (instead of 30℃) in the presence of glucose no cytotoxicity was measured (data not shown). Consequently, additional detailed investigations are required to fully unravel the ambiguous impact of glucose on cereulide production.

Besides glucose the addition of autoclaved cell samples and culture supernatants to LB media was tested with respect to *ces* promoter activity. Premature *ces* expression was caused by autoclaved samples and supernatants from *B. cereus* F4810/72 but

also from the emetic-like strain NVH1519/00, which possesses a plasmid lacking the *ces* operon (Figure 18). Thus, the early *ces* expression can not be due to an autoregulatory effect of cereulide itself, but may be caused by other molecules present in the supernatant of 24 h cultures. In the cyanobacteria *Microcystis sp.* it was recently shown that the release of secondary metabolites, especially nonribosomal peptides from lysing cells enhanced the production of the microcystin toxins in the remaining cells (Schatz *et al.*, 2007). Since in B. *cereus* F4810/72 cereulide production is not significantly increased but only appears earlier in time, the effect may be due to rapid growth induced by metabolites of autoclaved cell samples or supernatant. Surprisingly, this phenomenon was not observed with samples of 12 h cultures (instead of 24 h) or with samples of the non-emetic *B. cereus* ATCC14579. In contrast, autoclaved samples of this strain seem to have an inhibitory effect on the growth of B. *cereus* F4810/72 and no *ces* expression could be detected (Figure 18).

4.2 Functional characterization of *ces* genes and the mega-plasmid pBCE

4.2.1 Impact of *cesH* and *cesP* on cereulide synthesis

While *cesH* encoding a putative hydrolase/ acetyltransferase is located at the 5' end of the *ces* gene cluster and is transcribed from its own promoter, the remaining genes *cesPTABCD* are co-transcribed as a 23 kb polycistronic operon (Dommel, 2008). Data presented in this work revealed no correlation between CesH and cereulide formation, as an insertion mutant was as toxic as the wild-type (Figure 22). However, the *cesH* gene is only present in cereulide positive strains and has not been detected on any pXO1-like plasmids of emetic-like *B. cereus* strains. Even the recently described emetic *B. weihenstephanensis* strain (Thorsen *et al.*, 2006) possesses a gene displaying high homology to *cesH* of *B. cereus* (Fürst, 2006). Thus, *cesH* appears to be an integral part of the *ces* gene locus with so far unknown function. According to its structure, CesH seems to belong to the vast superfamily of the α/β-hydrolase fold proteins, more precisely to the alpha/beta hydrolase subfamily

(Hotelier *et al.*, 2004). The diverse proteins of this family are frequently encountered in *Bacillus* species, for example over 20 members are present in the annotated strain *B. cereus* ATCC10987. Therefore a potential role of CesH in cereulide synthesis is difficult to unravel or predict, because many enzymes may have the ability to compensate its function.

In contrast to the wide occurrence of the α/β-hydrolase fold superfamily, only very few members of the phosphopantetheinyl transferase superfamily are present in *Bacillus* species. By posttranslational modification and thereby activation of acyl-, aryl- or peptidyl- carrier proteins, PPTases are essential enzymes for the synthesis of fatty acids, polyketides and nonribosomal peptides (Walsh *et al.*, 1997). Based on several short sequence motifs, PPTases can be classified into two major groups, the Sfp-like PPTases and the acyl carrier protein synthases (AcpS). While PPTases of the Sfp type are mostly found in association with peptide synthetases, the enzymes of the AcpS type are linked to the activation of fatty acid and polyketide synthesis. In *B. subtilis*, which comprises a large number of PPTase-dependent pathways but only two PPTases, the broad substrate specificity of Sfp was emphasized, since Sfp was able to complement even the essential function of AcpS *in vivo* (Mootz *et al.*, 2001). *In silico* analysis of the emetic reference strain *B. cereus* F4810/72 revealed the presence of at least three PPTases. Besides a typically AcpS we found a Sfp-like PPTase (here named Ppt) closely located to the *dhb* operon, which has been shown to be responsible for the nonribosomal synthesis of the siderophore bacillibactin in *B. subtilis* (May *et al.*, 2001). The plasmid-encoded *cesP* presents an additional Sfp-like PPTase and is a fixed component of the *ces* gene cluster, being co-transcribed with the *nrps* genes. Nevertheless, CesP was shown to be not essential for cereulide synthesis of *B. cereus* F4810/72, as a high toxicity level remained despite *cesP* deletion (Figure 21). Only an additionally disrupted *ppt* led to a toxic deficient phenotype, indicating that Ppt can function as a redundant CesP PPTase in cereulide formation. Comparable to Sfp of *B. subtilis*, Ppt of *B. cereus* appears to be the main Sfp-like PPTase, since most of the *B. cereus* group members were found to possess an almost identical protein. Transcriptional analysis of *ppt* revealed that it is expressed very weakly, but constitutively throughout growth, showing only a slight increase in stationary growth phase (Figure 20). Likewise, expression of *sfp* in *B. subtilis* was shown to be weak according to low promoter activity (Nakano *et al.*,

1992). In contrast, transcription of *cesP,* which is linked to the *ces* operon, is strongly growth phase dependent, peaking highly in mid-log phase (Dommel, 2008). Although the importance of the CesP PPTase itself in cereulide synthesis seems doubtful, the *cesP* promoter region has been shown to act as the main promoter of the *ces* operon, affecting strongly the transcription of the *nrps* for cereulide production.

4.2.2 Putative ABC transporter CesCD is essential for cereulide production

In contrast to *cesH* and *cesP*, gene disruption of the downstream located *cesC* and *cesD* had a massive effect on cereulide formation, resulting in completely toxin deficient phenotypes (Figure 22). CesCD codes for a putative transporter, which consists of a protein for binding and hydrolysis of ATP (CesC), whilst CesD presents a hydrophobic integral membrane protein. Although the function of CesCD is so far undefined, sequence analysis of the ATP-binding domain revealed its belonging to the DRI (drug resistance and immunity) subfamily of the superfamily of ABC transporters. Members of this subcategory of ABC systems are frequently found in prokaryotes and are mainly involved in antibiotic resistance as well as bacteriocin and lantibiotic immunity (Dassa & Bouige, 2001; Davidson *et al.*, 2008). The transporter protein BerA, which was shown to be essential for ß-Exotoxin I production in *B. thuringiensis* (Espinasse *et al.*, 2002), revealed highest sequence homology to CesC (Figure 24). Interestingly, orthologs of BerA are present in several *B. cereus* group members including the emetic *B. cereus* strain F4810/72. Transcriptional analysis of this gene by RT-PCR confirmed its expression in the wild type strain and the *cesCD* null mutant (data not shown). Consequently the BerA-like protein of *B. cereus* F4810/72 is not able to functionally compensate the CesC transporter though being 49% identical and 74% similar on sequence level. Further examples of the DRI subfamily, which are homologous to CesC, are the ABC transporter proteins TnrB2 of *S. longisporoflavus* and BcrA of *B. licheniformis*, conferring resistance to the antibiotics tetronasin and bacitracin, respectively (Linton *et al.*, 1994; Podlesek *et al.*, 1995). Although the export mechanism is so far unclear, ABC systems of the DRI family are thought to confer drug resistance by active efflux of the molecules through the membrane. Therefore, it is tempting to speculate that CesC functions in a similar way and is involved in the transport of the emetic toxin, maybe even mediating its efflux. The fact that cereulide could be extracted from the surface of vegetative cells

by short time incubation with ethanol (Table 6) confirms the hypothesis of the toxin being secreted. Surprisingly, disruption of the *cesCD* genes resulted in a complete abolition of cereulide production, though transcription of the *nrps* gene *cesA* was still intact (Figure 22 and Figure 23). These data hint that CesCD, besides having a potential transport function, plays a direct role in the cereulide biosynthesis pathway. As a putative membrane-bound protein CesCD could be involved in membrane-anchoring of the cereulide synthetase complex, which otherwise may be instable and degraded. For the lantibiotic nisin it was shown that the enzyme complex necessary for the posttranslational modification of prenisin is associated to the membrane by interaction with the transporter protein NisT (Siegers *et al.*, 1996). Several other ABC transporter linked to nonribosomal peptide synthesis have found to be essential for product assembly (Pearson *et al.*, 2004; Zhu *et al.*, 1998), suggesting that synthesis and export are tightly coupled. Further investigation of the intracellular localisation of CesCD and the cereulide peptide synthetase complex are necessary to completely decipher the involvement of the transporter protein in cereulide production.

4.2.3 Toxin plasmid pBCE influences secretome and biofilm formation

The species of the *B. cereus* group can be mainly differentiated by different plasmid-encoded features, whereas their chromosomes are similar in both gene content and order (Rasko *et al.*, 2005). While the crucial role of toxin plasmids in the pathogenesis of *B. anthracis* and *B. thuringiensis* is well known, the investigation of *B. cereus* plasmids and their function has only recently started. The cereulide biosynthesis gene cluster of emetic *B. cereus* was identified as another toxin determinant to be located on a megaplasmid (Ehling-Schulz *et al.*, 2006). Detailed sequence analysis of the entire plasmid pBCE (which was renamed pCER270) of *B. cereus* F4810/72 revealed its close relation to a 272 kb plasmid from *B. cereus* isolates linked to periodontal disease. This new group of pXO1-like plasmids share a highly conserved core region consisting of genes involved in plasmid replication and maintenance as well as sporulation and germination genes and a formaldehyde detoxification locus (Rasko *et al.*, 2007). Besides harbouring the *ces* genes, pBCE comprises 243 genes, of which the majority (146) is annotated as hypothetical and conserved hypothetical protein. In this work phenotype, proteome and biofilm formation of plasmid cured strains from *B. cereus* F4810/72 were analysed to further

characterize properties of the megaplasmid pBCE. As expected all obtained clones were non toxic due to the lack of the plasmid (data not shown). Surprisingly, the phenotypes and the ability to sporulate varied among the cured strains (Figure 25). Although three stage V sporulation genes (AC-AE) were identified on the plasmid pBCE (Rasko *et al.*, 2007), *in silico* analysis of *B. cereus* F4810/72 showed the presence of chromosomal homologues of these genes. Hence, it seems unlikely that pBCE is essential for sporulation and the sporulation deficient variant of ΔpBCE may have evolved by deletion or inactivation of additional genes or whole plasmids during the curing process.

Comparative proteomic analysis of cytosolic and extracellular protein fractions revealed a great influence of pBCE on the secretome of *B. cereus* F4810/72. Over 80 proteins were found to be differentially expressed in the secretome of the plasmid cured strain compared to the parental strain, suggesting that a high number of plasmid-borne proteins are secreted or are involved in the gene expression of other extracelluar proteins (Figure 26 and Table 7). This is in accordance with proteome analyses of *B. anthracis*, which showed significant differences between the secretomes of the virulent wild type strain and a non-toxigenic derivative lacking pXO1 and pXO2 (Lamonica *et al.*, 2005). Among these differentially expressed proteins several putative virulence factors such as proteases, sulfatases and transporters were identified, which seem to be regulated in a plasmid-dependent manner (Chitlaru *et al.*, 2006; Lamonica *et al.*, 2005). However, comparative proteome studies in *B. cereus* revealed that its secretome differs from *B. anthracis* and consists mainly of degradative enzymes and toxins controlled by the PlcR regulator (Gohar *et al.*, 2002; Gohar *et al.*, 2005). Data presented in this work indicate that not only PlcR but also the presence of the megaplasmid pBCE has a great influence on the secreted protein profile of *B. cereus* F4010/72.

Besides the analysis of the proteome, the cured strains were tested regarding their ability to produce biofilm in a microtitre assay. In comparison to the wild type biofilm formation of the strains lacking pBCE was found to be clearly reduced (Figure 27). So far production of biofilm in *B. cereus* and *B. subtilis* was only shown to be linked to chromosomal transcription factors like PlcR, CodY, Spo0A and AbrB (Hamon & Lazazzera, 2001; Hsueh *et al.*, 2006; Hsueh *et al.*, 2008). Our data also support the

involvement of these regulators in the biofilm development of *B. cereus* F4010/72, but suggests in addition a role of plasmid-encoded factors in this process. In summary, studies with the plasmid cured strains revealed that pBCE not only influences the virulence of *B. cereus* F4010/72, but has an extensive impact on the whole organism by defining phenotypic traits as well as proteomic profiles.

4.3 Conclusion and perspectives

In conclusion, this work provides a first comprehensive insight into the presumably complex regulatory networks controlling cereulide synthesis of emetic *B. cereus*. It was shown that cereulide synthesis is controlled by the key sporulation factor Spo0A, but not by the *B. cereus* specific virulence regulator PlcR. The global transition state factor AbrB was identified as one important factor repressing cereulide production in early exponential phase, presumably by direct binding to the main promoter region of the cereulide synthetase operon. Further data revealed that cereulide production is influenced by additional intrinsic factors like CodY and many extrinsic factors as for example the availability of certain nutrients. It is expected that the results presented in this work and the high similarity to the gene regulation of the anthrax toxins will facilitate the finding of further regulatory mechanisms controlling the synthesis of the emetic toxin. However, substantial continuative work will be necessary to fully decipher these regulatory networks. Besides the investigation of chromosomal-encoded transcription factors, functional analysis of the plasmid-borne regulators (so far 10 regulator genes were annotated on pBCE) and the detection of their target genes would be useful to further clarify cross-regulatory interactions between chromosomal- and plasmid-encoded genes. The extensive study of virulence gene regulation is an important step towards understanding the pathogenicity of emetic *B. cereus* and it will also contribute to explain the strain-dependent toxigenic potential of this species.

Another focus of this work was the characterization of the megaplasmid pBCE and the plasmid-borne *ces* gene cluster encoding the cereulide peptide synthetase. The importance of pBCE was emphasized as the plasmid was shown to not only determine the toxicity but to exert a more global effect on *B. cereus* F4010/72,

influencing properties like the extracellular proteomic profile or the ability to form biofilm. The identification of proteins expressed differentially in the wild type and the plasmid cured strain would provide further data that might help to define the massive impact of pBCE on the organism. Obviously, the presence of pBCE defines several traits of *B. cereus* F4810/72 and allows the discrimination of this strain from other strains or species of the *B. cereus* group. Detailed analyses of *cesH, cesP* and *cesCD,* which are adjacent to the cereulide synthetase genes, offered first functional predictions. While the putative hydrolase CesH and the 4'-phosphopantetheinyl transferase CesP turned out to be non essential for toxin production, the ABC transporter CesCD showed to be of great importance for cereulide synthesis. Data presented in this work proposes that CesCD functions as toxin exporter and membrane anchor of the peptide synthetase complex. This result may promote studies to elucidate the biological role of the emetic toxin, which is still cryptic.

5 REFERENCES

Agaisse, H., Gominet, M., Okstad, O. A., Kolsto, A. B. & Lereclus, D. (1999). PlcR is a pleiotropic regulator of extracellular virulence factor gene expression in *Bacillus thuringiensis*. *Mol Microbiol* **32**, 1043-1053.

Agata, N., Mori, M., Ohta, M., Suwan, S., Ohtani, I. & Isobe, M. (1994). A novel dodecadepsipeptide, cereulide, isolated from *Bacillus cereus* causes vacuole formation in HEp-2 cells. *FEMS Microbiol Lett* **121**, 31-34.

Agata, N., Ohta, M., Mori, M. & Isobe, M. (1995). A novel dodecadepsipeptide, cereulide, is an emetic toxin of *Bacillus cereus*. *FEMS Microbiol Lett* **129**, 17-20.

Albano, M., Hahn, J. & Dubnau, D. (1987). Expression of competence genes in *Bacillus subtilis*. *J Bacteriol* **169**, 3110-3117.

Apetroaie-Constantin, C., Shaheen, R., Andrup, L., Smidt, L., Rita, H. & Salkinoja-Salonen, M. (2008). Environment driven cereulide production by emetic strains of *Bacillus cereus*. *Int J Food Microbiol* **127**, 60-67.

Arnaud, M., Chastanet, A. & Debarbouille, M. (2004). New vector for efficient allelic replacement in naturally nontransformable, low-GC-content, gram-positive bacteria. *Appl Environ Microbiol* **70**, 6887-6891.

Aronson, A. I. & Shai, Y. (2001). Why *Bacillus thuringiensis* insecticidal toxins are so effective: unique features of their mode of action. *FEMS Microbiol Lett* **195**, 1-8.

Auger, S., Krin, E., Aymerich, S. & Gohar, M. (2006). Autoinducer 2 affects biofilm formation by Bacillus cereus. *Appl Environ Microbiol* **72**, 937-941.

Ausubel, F. M., Brent, R., Kingston, R. E., Moore, D. D., Seidman, J. G., Smith, J. A. & Struhl, K. (1997). Current Protocols In Molecular Biology. **Volume 1**.

Beecher, D. J., Schoeni, J. L. & Wong, A. C. (1995). Enterotoxic activity of hemolysin BL from *Bacillus cereus*. *Infect Immun* **63**, 4423-4428.

Bennett, H. J., Pearce, D. M., Glenn, S., Taylor, C. M., Kuhn, M., Sonenshein, A. L., Andrew, P. W. & Roberts, I. S. (2007). Characterization of *relA* and *codY* mutants of *Listeria monocytogenes*: identification of the CodY regulon and its role in virulence. *Mol Microbiol* **63**, 1453-1467.

Berry, C., O'Neil, S., Ben-Dov, E. & other authors (2002). Complete sequence and organization of pBtoxis, the toxin-coding plasmid of *Bacillus thuringiensis* subsp. *israelensis*. *Appl Environ Microbiol* **68**, 5082-5095.

Bongiorni, C., Stoessel, R., Shoemaker, D. & Perego, M. (2006). Rap phosphatase of virulence plasmid pXO1 inhibits *Bacillus anthracis* sporulation. *J Bacteriol* **188**, 487-498.

Bongiorni, C., Fukushima, T., Wilson, A. C., Chiang, C., Mansilla, M. C., Hoch, J. A. & Perego, M. (2008). Dual promoters control the expression of the *Bacillus anthracis* virulence factor AtxA. *J Bacteriol* **190**, 6483-6492.

Bourgogne, A., Drysdale, M., Hilsenbeck, S. G., Peterson, S. N. & Koehler, T. M. (2003). Global effects of virulence gene regulators in a *Bacillus anthracis* strain with both virulence plasmids. *Infect Immun* **71**, 2736-2743.

Britton, R. A., Eichenberger, P., Gonzalez-Pastor, J. E., Fawcett, P., Monson, R., Losick, R. & Grossman, A. D. (2002). Genome-wide analysis of the stationary-phase sigma factor (sigma-H) regulon of *Bacillus subtilis*. *J Bacteriol* **184**, 4881-4890.

Brunsing, R. L., La Clair, C., Tang, S., Chiang, C., Hancock, L. E., Perego, M. & Hoch, J. A. (2005). Characterization of sporulation histidine kinases of *Bacillus anthracis*. *J Bacteriol* **187**, 6972-6981.

Callegan, M. C., Kane, S. T., Cochran, D. C., Gilmore, M. S., Gominet, M. & Lereclus, D. (2003). Relationship of plcR-regulated factors to *Bacillus* endophthalmitis virulence. *Infect Immun* **71**, 3116-3124.

Chibazakura, T., Kawamura, F. & Takahashi, H. (1991). Differential regulation of *spo0A* transcription in *Bacillus subtilis*: glucose represses promoter switching at the initiation of sporulation. *J Bacteriol* **173**, 2625-2632.

Chitlaru, T., Gat, O., Gozlan, Y., Ariel, N. & Shafferman, A. (2006). Differential proteomic analysis of the *Bacillus anthracis* secretome: distinct plasmid and chromosome CO2-dependent cross talk mechanisms modulate extracellular proteolytic activities. *J Bacteriol* **188**, 3551-3571.

Dassa, E. & Bouige, P. (2001). The ABC of ABCS: a phylogenetic and functional classification of ABC systems in living organisms. *Res Microbiol* **152**, 211-229.

Davey, R. T., Jr. & Tauber, W. B. (1987). Posttraumatic endophthalmitis: the emerging role of *Bacillus cereus* infection. *Rev Infect Dis* **9**, 110-123.

Davidson, A. L., Dassa, E., Orelle, C. & Chen, J. (2008). Structure, function, and evolution of bacterial ATP-binding cassette systems. *Microbiol Mol Biol Rev* **72**, 317-364, table of contents.

Declerck, N., Bouillaut, L., Chaix, D., Rugani, N., Slamti, L., Hoh, F., Lereclus, D. & Arold, S. T. (2007). Structure of PlcR: Insights into virulence regulation and evolution of quorum sensing in Gram-positive bacteria. *Proc Natl Acad Sci U S A* **104**, 18490-18495.

Di Franco, C., Beccari, E., Santini, T., Pisaneschi, G. & Tecce, G. (2002). Colony shape as a genetic trait in the pattern-forming *Bacillus mycoides*. *BMC Microbiol* **2**, 33.

Dierick, K., Van Coillie, E., Swiecicka, I. & other authors (2005). Fatal family outbreak of *Bacillus cereus*-associated food poisoning. *J Clin Microbiol* **43**, 4277-4279.

Dineen, S. S., Villapakkam, A. C., Nordman, J. T. & Sonenshein, A. L. (2007). Repression of *Clostridium difficile* toxin gene expression by CodY. *Mol Microbiol* **66**, 206-219.

Dommel, M. K. (2008). Molecular characterization of the genetic locus responsible for cereulide toxin production in emetic *Bacillus cereus*. *PhD thesis*, Technische Universität München.

Dunn, A. K. & Handelsman, J. (1999). A vector for promoter trapping in *Bacillus cereus*. *Gene* **226**, 297-305.

Duport, C., Zigha, A., Rosenfeld, E. & Schmitt, P. (2006). Control of enterotoxin gene expression in *Bacillus cereus* F4430/73 involves the redox-sensitive ResDE signal transduction system. *J Bacteriol* **188**, 6640-6651.

Ehling-Schulz, M., Fricker, M. & Scherer, S. (2004). *Bacillus cereus*, the causative agent of an emetic type of food-borne illness. *Mol Nutr Food Res* **48**, 479-487.

Ehling-Schulz, M., Svensson, B., Guinebretiere, M. H. & other authors (2005a). Emetic toxin formation of *Bacillus cereus* is restricted to a single evolutionary lineage of closely related strains. *Microbiology* **151**, 183-197.

Ehling-Schulz, M., Vukov, N., Schulz, A., Shaheen, R., Andersson, M., Martlbauer, E. & Scherer, S. (2005b). Identification and partial characterization of the nonribosomal peptide synthetase gene responsible for cereulide production in emetic *Bacillus cereus*. *Appl Environ Microbiol* **71**, 105-113.

Ehling-Schulz, M., Fricker, M., Grallert, H., Rieck, P., Wagner, M. & Scherer, S. (2006). Cereulide synthetase gene cluster from emetic *Bacillus cereus*: structure and location on a mega virulence plasmid related to *Bacillus anthracis* toxin plasmid pXO1. *BMC Microbiol* **6**, 20.

Espinasse, S., Gohar, M., Lereclus, D. & Sanchis, V. (2002). An ABC transporter from *Bacillus thuringiensis* is essential for beta-exotoxin I production. *J Bacteriol* **184**, 5848-5854.

Fawcett, P., Eichenberger, P., Losick, R. & Youngman, P. (2000). The transcriptional profile of early to middle sporulation in *Bacillus subtilis*. *Proc Natl Acad Sci U S A* **97**, 8063-8068.

Ferrari, E., Howard, S. M. & Hoch, J. A. (1986). Effect of stage 0 sporulation mutations on subtilisin expression. *J Bacteriol* **166**, 173-179.

Finking, R. & Marahiel, M. A. (2004). Biosynthesis of nonribosomal peptides1. *Annu Rev Microbiol* **58**, 453-488.

Finlay, B. B. & Falkow, S. (1997). Common themes in microbial pathogenicity revisited. *Microbiol Mol Biol Rev* **61**, 136-169.

Finlay, W. J., Logan, N. A. & Sutherland, A. D. (1999). Semiautomated metabolic staining assay for *Bacillus cereus* emetic toxin. *Appl Environ Microbiol* **65**, 1811-1812.

Finlay, W. J., Logan, N. A. & Sutherland, A. D. (2000). *Bacillus cereus* produces most emetic toxin at lower temperatures. *Lett Appl Microbiol* **31**, 385-389.

Fouet, A. & Mock, M. (2006). Regulatory networks for virulence and persistence of *Bacillus anthracis*. *Curr Opin Microbiol* **9**, 160-166.

Francis, K. P., Joh, D., Bellinger-Kawahara, C., Hawkinson, M. J., Purchio, T. F. & Contag, P. R. (2000). Monitoring bioluminescent *Staphylococcus aureus* infections in living mice using a novel *luxABCDE* construct. *Infect Immun* **68**, 3594-3600.

Fricker, M., Reissbrodt, R. & Ehling-Schulz, M. (2008). Evaluation of standard and new chromogenic selective plating media for isolation and identification of *Bacillus cereus*. *Int J Food Microbiol* **121**, 27-34.

Fürst, R. (2006). Phenotypic and molecular characterization of unusual cereulide producing *Bacillus cereus* family members. *Master thesis*, Technische Universität München.

Gaur, A. H., Patrick, C. C., McCullers, J. A., Flynn, P. M., Pearson, T. A., Razzouk, B. I., Thompson, S. J. & Shenep, J. L. (2001). *Bacillus cereus* bacteremia and meningitis in immunocompromised children. *Clin Infect Dis* **32**, 1456-1462.

Gohar, M., Okstad, O. A., Gilois, N., Sanchis, V., Kolsto, A. B. & Lereclus, D. (2002). Two-dimensional electrophoresis analysis of the extracellular proteome of *Bacillus cereus* reveals the importance of the PlcR regulon. *Proteomics* **2**, 784-791.

Gohar, M., Gilois, N., Graveline, R., Garreau, C., Sanchis, V. & Lereclus, D. (2005). A comparative study of *Bacillus cereus, Bacillus thuringiensis* and *Bacillus anthracis* extracellular proteomes. *Proteomics* **5**, 3696-3711.

Gohar, M., Faegri, K., Perchat, S., Ravnum, S., Okstad, O. A., Gominet, M., Kolsto, A. B. & Lereclus, D. (2008). The PlcR virulence regulon of *Bacillus cereus*. *PLoS ONE* **3**, e2793.

Gordon, R. E., Haynes, W. C. & Hor-Nay, C. (1973). The Genus *Bacillus*. *Washington: US Government Printing Office*.

Görg, A., Weiss, W. & Dunn, M. J. (2004). Current two-dimensional electrophoresis technology for proteomics. *Proteomics* **4**, 3665-3685.

Granum, P. E. & Lund, T. (1997). *Bacillus cereus* and its food poisoning toxins. *FEMS Microbiol Lett* **157**, 223-228.

Hadjifrangiskou, M., Chen, Y. & Koehler, T. M. (2007). The alternative sigma factor sigmaH is required for toxin gene expression by *Bacillus anthracis*. *J Bacteriol* **189**, 1874-1883.

Hamon, M. A. & Lazazzera, B. A. (2001). The sporulation transcription factor Spo0A is required for biofilm development in *Bacillus subtilis*. *Mol Microbiol* **42**, 1199-1209.

Helgason, E., Caugant, D. A., Olsen, I. & Kolsto, A. B. (2000a). Genetic structure of population of *Bacillus cereus* and *B. thuringiensis* isolates associated with periodontitis and other human infections. *J Clin Microbiol* **38**, 1615-1622.

Helgason, E., Okstad, O. A., Caugant, D. A., Johansen, H. A., Fouet, A., Mock, M., Hegna, I. & Kolsto, A. B. (2000b). *Bacillus anthracis, Bacillus cereus,* and *Bacillus thuringiensis*--one species on the basis of genetic evidence. *Appl Environ Microbiol* **66**, 2627-2630.

Hoornstra, D., Andersson, M. A., Mikkola, R. & Salkinoja-Salonen, M. S. (2003). A new method for in vitro detection of microbially produced mitochondrial toxins. *Toxicol In Vitro* **17**, 745-751.

Hotelier, T., Renault, L., Cousin, X., Negre, V., Marchot, P. & Chatonnet, A. (2004). ESTHER, the database of the alpha/beta-hydrolase fold superfamily of proteins. *Nucleic Acids Res* **32**, D145-147.

Hsueh, Y. H., Somers, E. B., Lereclus, D. & Wong, A. C. (2006). Biofilm formation by *Bacillus cereus* is influenced by PlcR, a pleiotropic regulator. *Appl Environ Microbiol* **72**, 5089-5092.

Hsueh, Y. H., Somers, E. B. & Wong, A. C. (2008). Characterization of the *codY* gene and its influence on biofilm formation in *Bacillus cereus*. *Arch Microbiol* **189**, 557-568.

Ireton, K., Jin, S., Grossman, A. D. & Sonenshein, A. L. (1995). Krebs cycle function is required for activation of the Spo0A transcription factor in *Bacillus subtilis*. *Proc Natl Acad Sci U S A* **92**, 2845-2849.

Jaaskelainen, E. L., Haggblom, M. M., Andersson, M. A. & Salkinoja-Salonen, M. S. (2004). Atmospheric oxygen and other conditions affecting the production of cereulide by *Bacillus cereus* in food. *Int J Food Microbiol* **96**, 75-83.

Jernigan, D. B., Raghunathan, P. L., Bell, B. P. & other authors (2002). Investigation of bioterrorism-related anthrax, United States, 2001: epidemiologic findings. *Emerg Infect Dis* **8**, 1019-1028.

Jiang, M., Shao, W., Perego, M. & Hoch, J. A. (2000). Multiple histidine kinases regulate entry into stationary phase and sporulation in *Bacillus subtilis*. *Mol Microbiol* **38**, 535-542.

Kotiranta, A., Lounatmaa, K. & Haapasalo, M. (2000). Epidemiology and pathogenesis of *Bacillus cereus* infections. *Microbes Infect* **2**, 189-198.

Lambalot, R. H., Gehring, A. M., Flugel, R. S., Zuber, P., LaCelle, M., Marahiel, M. A., Reid, R., Khosla, C. & Walsh, C. T. (1996). A new enzyme superfamily - the phosphopantetheinyl transferases. *Chem Biol* **3**, 923-936.

Lamonica, J. M., Wagner, M., Eschenbrenner, M., Williams, L. E., Miller, T. L., Patra, G. & DelVecchio, V. G. (2005). Comparative secretome analyses of three *Bacillus anthracis* strains with variant plasmid contents. *Infect Immun* **73**, 3646-3658.

Lechner, S., Mayr, R., Francis, K. P., Pruss, B. M., Kaplan, T., Wiessner-Gunkel, E., Stewart, G. S. & Scherer, S. (1998). *Bacillus weihenstephanensis* sp. nov. is a new psychrotolerant species of the *Bacillus cereus* group. *Int J Syst Bacteriol* **48 Pt 4**, 1373-1382.

Lereclus, D., Agaisse, H., Grandvalet, C., Salamitou, S. & Gominet, M. (2000). Regulation of toxin and virulence gene transcription in *Bacillus thuringiensis*. *Int J Med Microbiol* **290**, 295-299.

Linton, K. J., Cooper, H. N., Hunter, I. S. & Leadlay, P. F. (1994). An ABC-transporter from *Streptomyces longisporoflavus* confers resistance to the polyether-ionophore antibiotic tetronasin. *Mol Microbiol* **11**, 777-785.

Lund, T. & Granum, P. E. (1996). Characterisation of a non-haemolytic enterotoxin complex from *Bacillus cereus* isolated after a foodborne outbreak. *FEMS Microbiol Lett* **141**, 151-156.

Lund, T., De Buyser, M. L. & Granum, P. E. (2000). A new cytotoxin from *Bacillus cereus* that may cause necrotic enteritis. *Mol Microbiol* **38**, 254-261.

Magarvey, N. A., Ehling-Schulz, M. & Walsh, C. T. (2006). Characterization of the cereulide NRPS alpha-hydroxy acid specifying modules: activation of alpha-keto acids and chiral reduction on the assembly line. *J Am Chem Soc* **128**, 10698-10699.

Mahler, H., Pasi, A., Kramer, J. M., Schulte, P., Scoging, A. C., Bar, W. & Krahenbuhl, S. (1997). Fulminant liver failure in association with the emetic toxin of *Bacillus cereus*. *N Engl J Med* **336**, 1142-1148.

Majerczyk, C. D., Sadykov, M. R., Luong, T. T., Lee, C., Somerville, G. A. & Sonenshein, A. L. (2008). *Staphylococcus aureus* CodY negatively regulates virulence gene expression. *J Bacteriol* **190,** 2257-2265.

Marahiel, M. A., Zuber, P., Czekay, G. & Losick, R. (1987). Identification of the promoter for a peptide antibiotic biosynthesis gene from *Bacillus brevis* and its regulation in *Bacillus subtilis*. *J Bacteriol* **169**, 2215-2222.

Marahiel, M. A., Nakano, M. M. & Zuber, P. (1993). Regulation of peptide antibiotic production in *Bacillus*. *Mol Microbiol* **7**, 631-636.

Martineau, F., Picard, F. J., Roy, P. H., Ouellette, M. & Bergeron, M. G. (1996). Species-specific and ubiquitous DNA-based assays for rapid identification of *Staphylococcus epidermidis*. *J Clin Microbiol* **34**, 2888-2893.

May, J. J., Wendrich, T. M. & Marahiel, M. A. (2001). The *dhb* operon of *Bacillus subtilis* encodes the biosynthetic template for the catecholic siderophore 2,3-dihydroxybenzoate-glycine-threonine trimeric ester bacillibactin. *J Biol Chem* **276**, 7209-7217.

Mesnage, S., Tosi-Couture, E., Mock, M., Gounon, P. & Fouet, A. (1997). Molecular characterization of the *Bacillus anthracis* main S-layer component: evidence that it is the major cell-associated antigen. *Mol Microbiol* **23**, 1147-1155.

Mesnage, S., Fontaine, T., Mignot, T., Delepierre, M., Mock, M. & Fouet, A. (2000). Bacterial SLH domain proteins are non-covalently anchored to the cell surface via a conserved mechanism involving wall polysaccharide pyruvylation. *Embo J* **19**, 4473-4484.

Mignot, T., Mock, M., Robichon, D., Landier, A., Lereclus, D. & Fouet, A. (2001). The incompatibility between the PlcR- and AtxA-controlled regulons may have selected a nonsense mutation in *Bacillus anthracis*. *Mol Microbiol* **42**, 1189-1198.

Mikkola, R., Saris, N. E., Grigoriev, P. A., Andersson, M. A. & Salkinoja-Salonen, M. S. (1999). Ionophoretic properties and mitochondrial effects of cereulide: the emetic toxin of *B. cereus*. *Eur J Biochem* **263**, 112-117.

Mock, M. & Fouet, A. (2001). Anthrax. *Annu Rev Microbiol* **55**, 647-671.

Molle, V., Fujita, M., Jensen, S. T., Eichenberger, P., Gonzalez-Pastor, J. E., Liu, J. S. & Losick, R. (2003a). The Spo0A regulon of *Bacillus subtilis*. *Mol Microbiol* **50**, 1683-1701.

Molle, V., Nakaura, Y., Shivers, R. P., Yamaguchi, H., Losick, R., Fujita, Y. & Sonenshein, A. L. (2003b). Additional targets of the *Bacillus subtilis* global regulator CodY identified by chromatin immunoprecipitation and genome-wide transcript analysis. *J Bacteriol* **185**, 1911-1922.

Mootz, H. D., Finking, R. & Marahiel, M. A. (2001). 4'-phosphopantetheine transfer in primary and secondary metabolism of *Bacillus subtilis*. *J Biol Chem* **276**, 37289-37298.

Nakamura, L. K. (1998). *Bacillus pseudomycoides* sp. nov. *Int J Syst Bacteriol* **48 Pt 3**, 1031-1035.

Nakano, M. M., Corbell, N., Besson, J. & Zuber, P. (1992). Isolation and characterization of *sfp*: a gene that functions in the production of the lipopeptide biosurfactant, surfactin, in *Bacillus subtilis*. *Mol Gen Genet* **232**, 313-321.

O'Reilly, M. & Devine, K. M. (1997). Expression of AbrB, a transition state regulator from *Bacillus subtilis*, is growth phase dependent in a manner resembling that of Fis, the nucleoid binding protein from *Escherichia coli. J Bacteriol* **179**, 522-529.

Ouhib, O., Clavel, T. & Schmitt, P. (2006). The production of *Bacillus cereus* enterotoxins is influenced by carbohydrate and growth rate. *Curr Microbiol* **53**, 222-226.

Paananen, A., Mikkola, R., Sareneva, T., Matikainen, S., Hess, M., Andersson, M., Julkunen, I., Salkinoja-Salonen, M. S. & Timonen, T. (2002). Inhibition of human natural killer cell activity by cereulide, an emetic toxin from *Bacillus cereus*. *Clin Exp Immunol* **129**, 420-428.

Pearson, L. A., Hisbergues, M., Borner, T., Dittmann, E. & Neilan, B. A. (2004). Inactivation of an ABC transporter gene, *mcyH*, results in loss of microcystin production in the cyanobacterium *Microcystis aeruginosa* PCC 7806. *Appl Environ Microbiol* **70**, 6370-6378.

Perego, M. & Hoch, J. A. (2008). Commingling regulatory systems following acquisition of virulence plasmids by *Bacillus anthracis*. *Trends Microbiol* **16**, 215-221.

Pfaffl, M. W. (2001). A new mathematical model for relative quantification in real-time RT-PCR. *Nucleic Acids Res* **29**, e45.

Phillips, Z. E. & Strauch, M. A. (2002). *Bacillus subtilis* sporulation and stationary phase gene expression. *Cell Mol Life Sci* **59**, 392-402.

Podlesek, Z., Comino, A., Herzog-Velikonja, B., Zgur-Bertok, D., Komel, R. & Grabnar, M. (1995). *Bacillus licheniformis* bacitracin-resistance ABC transporter: relationship to mammalian multidrug resistance. *Mol Microbiol* **16**, 969-976.

Predich, M., Nair, G. & Smith, I. (1992). *Bacillus subtilis* early sporulation genes kinA, spo0F, and spo0A are transcribed by the RNA polymerase containing sigma H. *J Bacteriol* **174**, 2771-2778.

Priest, F. G. & Alexander, B. (1988). A frequency matrix for probabilistic identification of some bacilli. *J Gen Microbiol* **134**, 3011-3018.

Rasko, D. A., Ravel, J., Okstad, O. A. & other authors (2004). The genome sequence of *Bacillus cereus* ATCC 10987 reveals metabolic adaptations and a large plasmid related to Bacillus anthracis pXO1. *Nucleic Acids Res* **32**, 977-988.

Rasko, D. A., Altherr, M. R., Han, C. S. & Ravel, J. (2005). Genomics of the *Bacillus cereus* group of organisms. *FEMS Microbiol Rev* **29**, 303-329.

Rasko, D. A., Rosovitz, M. J., Okstad, O. A., Fouts, D. E., Jiang, L., Cer, R. Z., Kolsto, A. B., Gill, S. R. & Ravel, J. (2007). Complete sequence analysis of novel plasmids from emetic and periodontal *Bacillus cereus* isolates reveals a common evolutionary history among the *B. cereus*-group plasmids, including *Bacillus anthracis* pXO1. *J Bacteriol* **189**, 52-64.

Ratnayake-Lecamwasam, M., Serror, P., Wong, K. W. & Sonenshein, A. L. (2001). *Bacillus subtilis* CodY represses early-stationary-phase genes by sensing GTP levels. *Genes Dev* **15**, 1093-1103.

Saile, E. & Koehler, T. M. (2002). Control of anthrax toxin gene expression by the transition state regulator *abrB*. *J Bacteriol* **184**, 370-380.

Salamitou, S., Ramisse, F., Brehelin, M., Bourguet, D., Gilois, N., Gominet, M., Hernandez, E. & Lereclus, D. (2000). The *plcR* regulon is involved in the opportunistic properties of *Bacillus thuringiensis* and *Bacillus cereus* in mice and insects. *Microbiology* **146 (Pt 11)**, 2825-2832.

Sambrook, J. & Russell, D. W. (2001). Molecular cloning: A Laboratory Manual, 3edn. **New York: Cold Spring Harbor Laboratory Press.**

Sanchez, A. & Olmos, J. (2004). *Bacillus subtilis* transcriptional regulators interaction. *Biotechnol Lett* **26**, 403-407.

Schatz, D., Keren, Y., Vardi, A., Sukenik, A., Carmeli, S., Borner, T., Dittmann, E. & Kaplan, A. (2007). Towards clarification of the biological role of microcystins, a family of cyanobacterial toxins. *Environ Microbiol* **9**, 965-970.

Schneider, A. & Marahiel, M. A. (1998). Genetic evidence for a role of thioesterase domains, integrated in or associated with peptide synthetases, in non-ribosomal peptide biosynthesis in *Bacillus subtilis*. *Arch Microbiol* **169**, 404-410.

Schoeni, J. L. & Wong, A. C. (2005). *Bacillus cereus* food poisoning and its toxins. *J Food Prot* **68**, 636-648.

Schwarzer, D., Mootz, H. D., Linne, U. & Marahiel, M. A. (2002). Regeneration of misprimed nonribosomal peptide synthetases by type II thioesterases. *Proc Natl Acad Sci U S A* **99**, 14083-14088.

Shafikhani, S. H., Partovi, A. A. & Leighton, T. (2003). Catabolite-induced repression of sporulation in *Bacillus subtilis*. *Curr Microbiol* **47**, 300-308.

Shinagawa, K., Ueno, Y., Hu, D., Ueda, S. & Sugii, S. (1996). Mouse lethal activity of a HEp-2 vacuolation factor, cereulide, produced by *Bacillus cereus* isolated from vomiting-type food poisoning. *J Vet Med Sci* **58**, 1027-1029.

Shivers, R. P. & Sonenshein, A. L. (2004). Activation of the *Bacillus subtilis* global regulator CodY by direct interaction with branched-chain amino acids. *Mol Microbiol* **53**, 599-611.

Shivers, R. P. & Sonenshein, A. L. (2005). *Bacillus subtilis* ilvB operon: an intersection of global regulons. *Mol Microbiol* **56**, 1549-1559.

Siegers, K., Heinzmann, S. & Entian, K. D. (1996). Biosynthesis of lantibiotic nisin. Posttranslational modification of its prepeptide occurs at a multimeric membrane-associated lanthionine synthetase complex. *J Biol Chem* **271**, 12294-12301.

Slamti, L. & Lereclus, D. (2002). A cell-cell signaling peptide activates the PlcR virulence regulon in bacteria of the *Bacillus cereus* group. *Embo J* **21**, 4550-4559.

Sonenshein, A. L. (2005). CodY, a global regulator of stationary phase and virulence in Gram-positive bacteria. *Curr Opin Microbiol* **8**, 203-207.

Sonenshein, A. L. (2007). Control of key metabolic intersections in *Bacillus subtilis*. *Nat Rev Microbiol* **5**, 917-927.

Stenfors Arnesen, L. P., Fagerlund, A. & Granum, P. E. (2008). From soil to gut: *Bacillus cereus* and its food poisoning toxins. *FEMS Microbiol Rev* **32**, 579-606.

Strauch, M., Webb, V., Spiegelman, G. & Hoch, J. A. (1990). The SpoOA protein of *Bacillus subtilis* is a repressor of the *abrB* gene. *Proc Natl Acad Sci U S A* **87**, 1801-1805.

Strauch, M. A., Perego, M., Burbulys, D. & Hoch, J. A. (1989a). The transition state transcription regulator AbrB of *Bacillus subtilis* is autoregulated during vegetative growth. *Mol Microbiol* **3**, 1203-1209.

Strauch, M. A., Spiegelman, G. B., Perego, M., Johnson, W. C., Burbulys, D. & Hoch, J. A. (1989b). The transition state transcription regulator *abrB* of *Bacillus subtilis* is a DNA binding protein. *Embo J* **8**, 1615-1621.

Strauch, M. A. & Hoch, J. A. (1993). Transition-state regulators: sentinels of *Bacillus subtilis* post-exponential gene expression. *Mol Microbiol* **7**, 337-342.

Strauch, M. A. (1995). Delineation of AbrB-binding sites on the *Bacillus subtilis spo0H, kinB, ftsAZ,* and *pbpE* promoters and use of a derived homology to identify a previously unsuspected binding site in the *bsuB1* methylase promoter. *J Bacteriol* **177**, 6999-7002.

Stulke, J. & Hillen, W. (2000). Regulation of carbon catabolism in *Bacillus* species. *Annu Rev Microbiol* **54**, 849-880.

Thomas, C. M. & Smith, C. A. (1987). Incompatibility group P plasmids: genetics, evolution, and use in genetic manipulation. *Annu Rev Microbiol* **41**, 77-101.

Thorsen, L., Hansen, B. M., Nielsen, K. F., Hendriksen, N. B., Phipps, R. K. & Budde, B. B. (2006). Characterization of emetic *Bacillus weihenstephanensis*, a new cereulide-producing bacterium. *Appl Environ Microbiol* **72**, 5118-5121.

Trach, K. A. & Hoch, J. A. (1993). Multisensory activation of the phosphorelay initiating sporulation in *Bacillus subtilis*: identification and sequence of the protein kinase of the alternate pathway. *Mol Microbiol* **8**, 69-79.

Trieu-Cuot, P., Carlier, C., Martin, P. & Courvalin, P. (1987). Plasmid transfer by conjugation from *Escherichia coli* to Gram-positive bacteria. *FEMS Microbiol Lett* **48**, 289-294.

Trieu-Cuot, P., Carlier, C., Poyart-Salmeron, C. & Courvalin, P. (1991). An integrative vector exploiting the transposition properties of Tn1545 for insertional mutagenesis and cloning of genes from gram-positive bacteria. *Gene* **106**, 21-27.

Turgay, K., Krause, M. & Marahiel, M. A. (1992). Four homologous domains in the primary structure of GrsB are related to domains in a superfamily of adenylate-forming enzymes. *Mol Microbiol* **6**, 529-546.

Turnbull, P. C., Kramer, J. M., Jorgensen, K., Gilbert, R. J. & Melling, J. (1979). Properties and production characteristics of vomiting, diarrheal, and necrotizing toxins of *Bacillus cereus*. *Am J Clin Nutr* **32**, 219-228.

van der Voort, M., Kuipers, O. P., Buist, G., de Vos, W. M. & Abee, T. (2008). Assessment of CcpA-mediated catabolite control of gene expression in *Bacillus cereus* ATCC 14579. *BMC Microbiol* **8**, 62.

Walsh, C. T., Gehring, A. M., Weinreb, P. H., Quadri, L. E. & Flugel, R. S. (1997). Post-translational modification of polyketide and nonribosomal peptide synthases. *Curr Opin Chem Biol* **1**, 309-315.

Weir, J., Predich, M., Dubnau, E., Nair, G. & Smith, I. (1991). Regulation of *spo0H,* a gene coding for the *Bacillus subtilis* sigma H factor. *J Bacteriol* **173**, 521-529.

Wijman, J. G., de Leeuw, P. P., Moezelaar, R., Zwietering, M. H. & Abee, T. (2007). Air-liquid interface biofilms of *Bacillus cereus*: formation, sporulation, and dispersion. *Appl Environ Microbiol* **73**, 1481-1488.

Xu, K. & Strauch, M. A. (1996). In vitro selection of optimal AbrB-binding sites: comparison to known in vivo sites indicates flexibility in AbrB binding and recognition of three-dimensional DNA structures. *Mol Microbiol* **19**, 145-158.

Yamashita, S., Kawamura, F., Yoshikawa, H., Takahashi, H., Kobayashi, Y. & Saito, H. (1989). Dissection of the expression signals of the *spoA* gene of *Bacillus subtilis*: glucose represses sporulation-specific expression. *J Gen Microbiol* **135**, 1335-1345.

Zheng, G., Yan, L. Z., Vederas, J. C. & Zuber, P. (1999). Genes of the *sbo-alb* locus of *Bacillus subtilis* are required for production of the antilisterial bacteriocin subtilosin. *J Bacteriol* **181**, 7346-7355.

Zhu, W., Arceneaux, J. E., Beggs, M. L., Byers, B. R., Eisenach, K. D. & Lundrigan, M. D. (1998). Exochelin genes in *Mycobacterium smegmatis*: identification of an ABC transporter and two non-ribosomal peptide synthetase genes. *Mol Microbiol* **29**, 629-639.

Zigha, A., Rosenfeld, E., Schmitt, P. & Duport, C. (2007). The redox regulator Fnr is required for fermentative growth and enterotoxin synthesis in *Bacillus cereus* F4430/73. *J Bacteriol* **189**, 2813-2824.

6 PUBLICATIONS

Original work

Lücking, G. & Ehling-Schulz, M. (2009). Functional characterization of *ces* genes associated with the cereulide synthetase gene cluster in emetic *Bacillus cereus.* in preparation.

Lücking, G., Dommel, M. K., Fouet, A., Scherer, S. & Ehling-Schulz, M. (2009). Cereulide synthesis in emetic *Bacillus cereus* is controlled by the transition state factor AbrB, but not by the virulence regulator PlcR. *Microbiology*, in press.

Serra, D. O., Lücking, G., Weiland, F., Schulz, S., Görg, A., Yantorno, O. M. & Ehling-Schulz, M. (2008). Proteome approaches combined with Fourier transform infrared spectroscopy revealed a distinctive biofilm physiology in *Bordetella pertussis. Proteomics* **8,** 4995-5010

Elmasri, H.,, Liedtke, D., Lücking, G., Volff, J.N., Gessler, M., & Winkler, C.(2004). *her7* and *hey1*, but not *lunatic fringe* show dynamic expression during somitogenesis in medaka (*Oryzias latipes*). *Gene Expr Patterns* **4**, 553-559

Abstracts & Proceedings:

Diego Serra, Genia Lücking, Florian Weiland, Stefan Schulz, Angelika Görg, Osvaldo Yantorno and Monika Ehling-Schulz. Proteome approaches combined with Fourier transform infrared spectroscopy revealed a distinctive biofilm physiology in *Bordetella pertussis*. Biofilms III: 3rd International Conference, München, Germany. (06.10. - 08.10.2008) p. 134-135.

Genia Lücking, Monica Dommel, Siegfried Scherer and Monika Ehling-Schulz. Proteome and transcription analysis of emetic *Bacillus cereus*. 10th Symposia of Food Microbiology. Stuttgart, Germany. (09.04.-11.04.2008).

Genia Lücking, Elrike Frenzel, Monica Dommel and Monika Ehling-Schulz. Analysis of cereulide synthesis in emetic *Bacillus cereus*. 1st Life-Science PhD Symposium, München, Germany (07.12.2007) B127.

Diego Serra, Genia Lücking, Siegfried Scherer, Osvaldo Yantorno, and Monika Ehling-Schulz. Phenotypic expression in *Bordetella pertussis* biofilms: Fourier transform infrared (FTIR) spectroscopic and proteomic approaches. Workshop: FTIR Spectroscopy in Microbiological and Medical Diagnostics. Berlin, Germany. (25.10.-26.10.2007).

Genia Lücking, Monica Dommel and Monika Ehling-Schulz, Proteome and transcription analysis of emetic *Bacillus cereus***.** 4th Conference on Functional Genomics of Gram-positive Microorganisms. Pisa, Italy. (24.06. – 28.06.2007) P32.

Monica Dommel, Genia Lücking, Richard Dietrich, Siegfried Scherer and Monika Ehling-Schulz. Genetic basis of cereulide synthesis in emetic *Bacillus cereus*. 9th Symposia of Food Microbiology. Seeon, Germany. (21.03.- 23.03.2007).

Genia Lücking, Monica Dommel, Siegfried Scherer and Monika Ehling-Schulz. Proteome and transcription analysis of emetic *Bacillus cereus*. 58. Tagung der Deutschen Gesellschaft für Hygiene und Mikrobiologie e.V. Würzburg, Germany. (01.10.-04.10.2006) GIP08 S. 87.

7 APPENDIX

7.1 Vectors and recombinant plasmids

Table 8. Vectors and recombinant plasmids used in this study.

Plasmid	Relevant characteristics	Reference or source
TOPO pCR 2.1	PCR cloning vector; Amp^r Kan^r	Invitrogen
pET28b	*E.coli* overexpression vector; Kan^r	Novagen
pET28/abrB	pET28b derivative carrying the *abrB* gene of *B. cereus* F4810/72 fused C-terminally to the His-tag; Kan^r	This study
pET28/abrB*	pET28b derivative carrying the *abrB** gene of *B. cereus* F4810/72 fused C-terminally to the His-tag; Kan^r	This study
pRK24	IncP plasmid for conjugation; Tra^+ Mob^+ Amp^r	Thomas & Smith, 1987
pUC1318Spc	pUC1318 carrying a Spc resistance cassette; Amp^r Spc^r	Mesnage *et al.*, 1997
pUCspcH+2	pUC19 derivative carrying a non-polar mutagenic Spc resistance cassette; Amp^r Spc^r	Mesnage *et al.*, 2000
pAT113	conjugative suicide vector for *Bacillus*; Kan^r Erm^r	Trieu-Cuot *et al.*, 1991
pAT113Δspo0A/spc	pAT113 derivative containing ~1.3 kb up- and downstream flanking regions of *spo0A* and the Spc resistance cassette; Spc^r Erm^r Kan^r	This study
pAT113Δspo0A/cm	pAT113 derivative containing ~1.3 kb up- and downstream flanking regions of *spo0A* and the Cm resistance cassette; Cm^r Erm^r Kan^r	This study
pAT113ΔplcR/spc	pAT113 derivative containing ~1.2 kb up- and downstream flanking regions of *plcR* and the Spc resistance cassette; Spc^r Erm^r Kan^r	This study
pAT113ΔabrB/spc	pAT113 derivative containing ~1.2 kb up- and downstream flanking regions of *abrB* and the Spc resistance cassette; Spc^r Erm^r Kan^r	This study
pAT113ΔcesP/spc	pAT113 derivative containing ~1 kb up- and downstream flanking regions of *cesP* and the Spc resistance cassette (polar effect on downstream located *ces* genes); Spc^r Erm^r Kan^r	This study
pAT113ΔcesP/spcH+2	pAT113 derivative containing ~1 kb up- and downstream flanking regions of *cesP* and a non-polar Spc resistance cassette; Spc^r Erm^r Kan^r	This study

pAT113ΔcesCD/spc	pAT113 derivative containing ~1.2 kb up- and downstream flanking regions of *cesCD* and the Spc resistance cassette; Spc^r Erm^r Kan^r	This study
pXen1	shuttle vector containing a promoter-less luciferase (luxABCDE) operon for Gram-positive hosts; Amp^r Cm^r	Francis *et al.*, 2000
pXen/Pces	pXen1 derivative containing the *ces* promoter region (237 bp upstream of *cesP*) fused to the Lux cassette; Amp^r Cm^r	Dommel, 2008
pXen/Pces/erm	pXen/Pces containing an additional Erm resistance cassette; Amp^r Cm^r Erm^r	This study
pMAD	thermo-sensitive shuttle vector for Gram-positive bacteria; Amp^r Erm^r	Arnaud *et al.*, 2004
pMAD/cesH	pMAD derivative containing a 293 bp inner fragment of the *cesH* gene; Amp^r Erm^r	This study
pMAD/cesC	pMAD derivative containing a 324 bp inner fragment of the *cesC* gene; Amp^r Erm^r	This study
pMAD/cesD	pMAD derivative containing a 298 bp inner fragment of the *cesD* gene; Amp^r Erm^r	This study
pMAD/ppt	pMAD derivative containing a 327 bp inner fragment of the *ppt* gene; Amp^r Erm^r	This study
pMAD/sigH	pMAD derivative containing a 261 bp inner fragment of the *sigH* gene; Amp^r Erm^r	This study
pMAD/CodY	pMAD derivative containing a 292 bp inner fragment of the *codY* gene; Amp^r Erm^r	This study
pMAD/CcpA	pMAD derivative containing a 326 bp inner fragment of the *ccpA* gene; Amp^r Erm^r	This study
pAD123	shuttle vector for Gram-positive hosts, containing a promoter-less gfpmut3a (*gfp*); Amp^r Cm^r	Dunn & Handelsman, 1999
pAD/PcspA	pAD123 derivative containing the promoter region of the cold shock protein CspA in front of *gfp*; Amp^r Cm^r	Dommel, 2008
pAD/abrB/PcspA	pAD123 derivative containing the *cspA* promoter region in front of the *abrB* gene (lacking *gfp*); Amp^r Cm^r	This study
pAD/abrB*/PcspA	pAD123 derivative containing the *cspA* promoter region in front of the *abrB*-like gene from pBCE (lacking *gfp*); Amp^r Cm^r	This study
pAD/Pces	pAD123 derivative containing the *ces* promoter region (237 bp upstream of *cesP*) in front of *gfp*; Amp^r Cm^r	Dommel, 2008

pAD/cesCD/Pces	pAD123 derivative containing the *ces* promoter region in front of the *cesCD* genes (lacking *gfp*); Amp^r Cm^r	This study
pAD/spo0A/P$\sigma^A\sigma^H$	pAD123 derivative containing *spo0A* and its two promoter regions, Pσ^A and Pσ^H (lacking *gfp*); Amp^r Cm^r	This study
pAD/spo0A/Pσ^H	pAD123 derivative containing *spo0A* and its σ^H promoter region (lacking *gfp*); Amp^r Cm^r	This study

7.2 Oligonucleotide primers

Table 9. Oligonucleotide primers used in this study.

Primer name	Sequence (5' – 3')[a]	Description
primer for deletion mutagenesis:		
cesP_up_Sac2	TTTGAGCTCTTTAGTTCCTTCATGAC	~1 kb upstream fragment of *cesP*, including 38 bp of the 5'end of *cesP*
cesP_up_Sma	TTCACCCGGGTAAATCTTTATGGAAT	
cesP_down_Sma	TCATCCCGGGTATAAAGTCGCGGTTT	~1 kb downstream fragment of *cesP*, including 153 bp of the 3'end of *cesP*
cesP_down_SacI	TCAAGAGCTCCATCAACATAGTCATA	
cesCD-up-Eco	ATTGAATTCAAATGCGTGAAGGTAGTGA	~1.1 kb upstream fragment of *cesC*, including 140 bp of the 5'end of *cesC*
cesCD-up-Sma	AATCCCGGGAAATGTCGAATTGTTGTGG	
cesCD-down-Sma	TTGCCCGGGTTGCGAATACAGAAAGCTTAG	~1.2 kb downstream fragment of *cesD*, including 257 bp of the 3' end of *cesD*
cesCD-down-Eco	TTTGAATTCCTCTACTGTTGGTACTAGTTG	
PlcR_up_Xho-for	GATCTCGAGGATGATATTGAAGTAATTG	~1.3 kb upstream fragment of *plcR*, including 8 bp of the 5'end of *plcR*
PlcR_up_Xba-rev	GCG TCTAGACTTACTCACCATCCCATTA	
PlcR_down_sma 4	CTTCCCGGGAGTCTGTTAACGTTAGCA	~1.1 kb downstream fragment of *plcR*, starting 101 bp after *plcR* stop codon
PlcR_down_Sac2	CCAGAGCTCATTCAAGGCGAAGAACTGTC	
AbrB_for_Eco	TAGAATTCCTCATCTTGTACAGAATACC	~1 kb upstream fragment of *abrB,* including 39 bp of the 5' end of *abrB*
AbrB_rev_Sac	CAACTTTACGAACGATACCAGGAGCTCAT	

AbrB_for_Sal	TTGTCGACATGATAGATTTGATATATAC	~1.3 kb downstream fragment of *abrB*, starting 28 bp after *abrB* stop codon
AbrB_rev_Sal	TAGTCGACTAGTAAAGCAAGGCGGGAAAG	
Spo0A-Sac-up	AGTGAGCTCAGGTGGACAATCAATTGGTG	~1.3 kb upstream fragment of *spo0A*, including 124 bp of the 5' end of *spo0A*
Spo0A-Sma-up	TCCCCCGGGTCTTGAGCAGCTACATAACTC	
Spo0A-Sma-down	GAACCCCGGGTTCATCGCAATGGTTGCGG	~1.4 kb downstream fragment of *spo0A*, including 61 bp of the 3' end of *spo0A*
Spo0A-Sac-down	TCGGAGCTCTATTTCCTCCACTCTCTATC	
spcF-neu	GAGGACGATCTGTATAATAAAG	1219 bp fragment including the spectinomycin resistance cassette
spcR-neu	CGTGAATATCGTGTTCTTTTC	
Am-spc2	ACTCCCGGGGAGGAAATAATAAATGAGCAA TTTGATTAACGG	~850 bp fragment including the non-polar spectinomycin resistance cassette
spc-H+2	TTTACCCGGGTTCATTTATATTTTCCTCCTTA GCCTAATTGAGAG	
CAM_F	TCTCCCGGGTATCAAGATAAGAAAG	940 bp fragment including the chloramphenicol resistance sequence
CAM_R	ACACCCGGGATTATCTCATATTATA	
Erm-F-Nco	AAACCATGGAGTGTGTTGATAGTG	1110 bp fragment including the erythromycin resistance sequence
Erm-R-Nco	TCTCCATGGCCTTTAGTAACGT	

primer for gene complementation:

cesCD_F_Xba2	TGGTCTAGAAGCATATTTAGAGTTG	1.8 kb fragment containing the genes *cesC* and *cesD*
cesCD_R_Pae	TTTGCATGCTATTTAAACATCTTAT	
spo0A-for-Eco2	TTGAATTCGTGAGTACAGTACCGCAA	*spo0A* gene plus 513 bp upstream, including two promoter, $P\sigma^A$ and $P\sigma^H$
spo0A-rev-Hind	TAAAGCTTCTATTCTCAGCTAGCCTT	
spo0A-F-kurz	TGGAATTCGTTGCGAAAAGGA	*spo0A* gene plus 121 bp upstream region, including the σ^H–promoter
spo0A-rev-Hind	TAAAGCTTCTATTCTCAGCTAGCCTT	

primer for insertion mutagenesis:

cesH_F_Hind2	TCAAAGCTTAGTTCTTGACCTAC	293 bp inner fragment of cesH
cesH_R_Eco2	TTTGAATTCCCAGTGGTAATGCC	
cesC_F_Eco	ATTGAATTCGTTTAATTGCTGG	324 bp inner fragment of *cesC*
cesC_R_Bam	TAAGGATCCAAATGGTATCTGC	
cesD_Eco_F	TAGGAATTCAAGGGAATATGGC	298 bp inner fragment of *cesD*
cesD_Bam_R	TTCGGATCCAATGTGTGCTTTC	
PPT_F_Eco2	TCAGAATTCGGCAGATCGTGCTCG	327 bp inner fragment of *ppt* (locus BcerAH_010100009366)
PPT_R_Bam2	TTAGGATCCTTCATAACTTGCGC	
sigH-for-Eco	AAGAATTCGTGATTATAAGGAGGACAAG	261 bp inner fragment of *sigH*
sigH-rev-Bam	TTGGATCCTATGTCTGTATATTCTTCC	
CodY-EcoII	GAGAATTCGCGTATGAAACAAATG	292 bp inner fragment of *codY*
CodY-rev-Bam	AAGGATCCATACCTACAACAGTTGAG	
CcpA-Eco-for	CAGGAATTCACATTGAAGAATTTAA	326 bp inner fragment of *ccpA*
CcpA-Bam-rev	AAGGATCCAGAGCTTTTCGAAT	

primer for AbrB and AbrB* overexpression:

abrB_SacI_F	AAAGAGCTCATGAAATCTACTGGTATC	complete *abrB* gene, starting 9 bp before start codon
abrB_R_Hind2	CTCATAATTGAGAAGCTTAT	
abrB-pBCE_Sac	GAAGAGCTCATGAAATCAATAGGTG	complete *abrB** gene, starting 9 bp before start codon
abrB-pBCEHind	AAGAAGCTTGTTATTTAACCAATTG	
abrB_Nco_F	TTCCATGGTTATGAAATCTACTGGTATCGTT	complete *abrB* gene, starting 10 bp before start codon
abrB_Xho_R	AGACTCGAGTTTTGCTGTTTCGATATAATC	
abrB_P_Nco	AAACCATGGACATGAAATCAATAGGTG	complete *abrB** gene, starting 10 bp before start codon
abrB_P_Xho	ATGCTCGAGTTTAACCAATTGCTGTTG	

primer for gel motility shift assay:

cesP_F_EMSA1	CTACAAGAAAACCTGTAAAAATTAG	364 bp fragment starting 342 bp before the start codon of *cesP*
PPP1-rev2	TTTATGCTCTATGTGTTTCATTG	
cesP-F-EMSA2	CGTACCCGTATGAAATTGAAAT	375 bp fragment starting 191 bp before the start codon of *cesP*
cesP-rev1	CCATTCGTATGAGCAGTTCTCC	
PPP1-for	GTTAATAATGTATTAAGGAAAATGAATG	416 bp fragment starting 66 bp before the start codon of *cesP*
cesP-rev2	ACTTTCTCCACATCCACACCTACTG	
PPT-EMSA-for	AACAATATAACGCCGCCTTC	335 bp fragment starting 302 bp before the start codon of *ppt* (locus BcerAH_010100009366)
PPT-EMSA-rev	CGGTATAGAATCTACAACTTTACTTTC	
cesP-Bw-F	AGCGTAAATATCTAAAATCCG	326 bp fragment starting 309 bp before the start codon of *cesP* of *B. weihenstephanensis* MC67
cesP-Bw-R	TTTTTATGTTCTATGTGTTTCATTG	
AbrB_F_EMSA	GTGAAATAATAGTAGAAATTACTC	167 bp fragment starting 205 bp before the start codon of *abrB*
AbrB_R_EMSA	TCGAGTCTATTTTTAGATTCG	

primer for control PCR and sequencing:

800F2	GACAAGAGAAATTTCTACGAGCAAGTACAAT	*ces* specific primers: 635 bp inner fragment of *cesB*
800R2	GCAGCCTTCCAATTACTCCTTCTGCCACAGT	
pCons_for	GGTCTTAGCCATGAGAGTAAAAACA	conserved region of pXO1-like plasmids: 595 bp fragment of hypothetical protein
pCons_rev	TGTGATGGACCTTTGTATTAATTTGT	
pXO1-RepX.for	AGAATGATAATTTCTTCTTTGTTGG	1025 bp fragment of the plasmid replication protein RepX
pXO1-RepX.rev	TGTAAAGCATGAAACCAAGATTT	
pAD_for	CATGAGCGGATACATATTTG	sequencing and test primer for pAD123
pAD_rev	GGTACATTGAGCAACTGACTG	
pMAD_for	AATGATCGAAGTTAGGCTG	sequencing and test primer for pMAD
pMAD_rev	CGTTACACATTAACTAGACAGAT	

pMUTIN-F	TTAGGATCCTTCATAACTTGCGC	sequencing and test primer for pMUTIN
pMUTIN-R	ACAGCCCAGTCCAGACTATTCG	
pXEN_for	GTTGGGTAACGCCAGGG	sequencing and test primer for pXen
pXEN_rev	CATAGAGAGTCCTCCTCTTG	
pAT113_for	ATGACCATGATTACGCCAAGC	sequencing and test primer for pAT113
pAT113_rev	AGATCCGCGCGAGCTGTA	
pCR2_1_for	GTGAGTTAGCTCACTCATTAGGC	sequencing and test primer for TOPO pCR2.1
pCR2_1_rev	CTCTTCGCTATTACGCCAGCTG	
spcF2	GGAAGTTCAATAGTTGGAGTATATC	675 bp inner fragment of the spc resistance sequence
spcR2	CTTAACGAGTGCTTTCACCTTTG	
IGA_for	GGTTAGCTGTTCGGAAATTG	360 bp inner fragment of *cesP*
label_rev_1	CTTTCAGCGTCCAAATCTC	
Forward_Val_4	GTCTGATTTAGGTAGAGCAGAG	629 bp fragment including 565bp of *cesC* and 48 bp of *cesD*
Rev3_ABC	GCCTTTACTATGTGCTTTTAGAGATG	
spo0A_for	GAGTTATGTAGCTGCTCAAG	710 bp inner fragment of *spo0A*
spo0A_rev	GCTTATCCGCAACCATTGCG	
plcR-test1	GGTACTTATTTATTCTGACATG	384 bp inner fragment of *plcR*
plcR-test2	ACTCTTTATTATCATGTAATAC	
abrB_F_Eco	ATGAATTCGGTCGTGTAG	139 bp inner fragment of *abrB*
abrB_Hind_R	GTTACTTGGCAAGTCAAGCTTGGCTT	
cesH_for_Hind	GTAAAGCTTGAAATTCATAGCTAGG	728 bp inner fragment of *cesH*
cesH_rev_Eco	AGGAATTCCATGACCAATTTTAGGAATG	

cesD_sko_for	AAGGAGCTCTAAAAGCACATAGTAAAGGC	733 bp inner fragment of *cesD*
cesD_sko_rev	CCTGAGCTCATTAGTAGTAATAATGATG	
cesC_sko_for	TTAGAGCTCATAAAGGATGTGGGAAAG	870 bp inner fragment of *cesC*
cesC_sko_rev	TTTGAGCTCTGGCTCCATGATTTCTATG	
PPTase_F_Eco	GATAGAATTCAAAGTTGTAGAT	728 bp inner fragment of *ppt*
PPTase_R_Bam	ACTGGATCCATCTGTATGATT	
sigH_F-long	GGTAATACTGACGCTCTAGA	470 bp inner fragment of *sigH*
sigH_R-long	GAAATCTCTTGATAAGAACG	
CodY_F-long	GTCTGACACAATGTGTGAAG	463 bp inner fragment of *codY*
CodY_R-long	GTAAGATAATGAGCTGATCG	
CcpA-long-for	GCAGAACTTGCTCGTGGAAT	584 bp inner fragment of *ccpA*
CcpA-long-rev	TAATGCAAGGCGTGTATTATCG	

ACKNOWLEDGEMENTS

I would like to thank Prof. Dr. Siegfried Scherer for giving me the opportunity to perform my doctoral studies at the “Abteilung Mikrobiologie, ZIEL, TU München”. Furthermore, I sincerely thank my supervisor Prof. Dr. Monika Ehling-Schulz for all her support and constant encouragement throughout the work. Thanks to Dr. Agnes Fouet for welcoming me at the Pasteur Institut and proof-reading of my manuscript.

I very much enjoyed working with the staff and students at the ZIEL, especially with the people of the *B. cereus* group. Thanks to Martina Fricker, Monica Dommel, Simone Müller-Hellwig, Elrike Frenzel and Tobias Bauer for very helpful advice, many discussions and the pleasant working atmosphere. Special thanks to Romy Renner and Michaela Bauer for excellent technical assistance and to Johann Winkler and Swanhild Meyer for their contribution to parts of this work. As well, I thank Diego Serra for great times, it was a real pleasure working with you.

I would also like to thank my dear colleagues for their genuine interest in me and my work: Cecilia Rebuffo-Scheer, Samir Velagic, Carsten Kröger, Kristina Schauer, Meike Gabert, Nicole Büchl and Martina Fricker. Thanks for every hour that we spent together in- and outside of work.

Finally, I deeply appreciate all the support, interest and patience of my parents Phyllis and Karl, my brother Kolja and especially my almost husband Holger. Even in hard times you always made me feel good again. Thank you very much.

CURRICULUM VITAE

Genia Lücking

Born 01 June 1979, Werneck, Germany

Nationality: German

Education

2005-2008	PhD (Dr. rer. nat.) Abteilung Mikrobiologie, ZIEL, Technische Universität München Thesis: “Molecular characterization of cereulide synthesis in emetic *Bacillus cereus”* Advisor: Prof. Dr. M. Ehling-Schulz
1999-2005	Diploma in biology Lehrstuhl für Mikrobiologie, Julius-Maximilians-Universität Würzburg Diploma thesis:„Characterization of putative virulence factors in *Bordetella holmesii“*
2003	Erasmus exchange student University of Umea; Sweden